Reviews in Mineralogy & Geochemistry
Vol. 69 pp. 61-120, 2008
Copyright © Mineralogical Society of America

Thermometers and Barometers for Volcanic Systems

Keith D. Putirka

Department of Earth and Environmental Sciences
California State University, Fresno
2576 E. San Ramon Ave., MS/ST24
Fresno, California, 93740-8039, U.S.A.

kputirka@csufresno.edu

INTRODUCTION

Knowledge of temperature and pressure, however qualitative, has been central to our views of geology since at least the early 19th century. In 1822, for example, Charles Daubeny presented what may be the very first "Geological Thermometer," comparing temperatures of various geologic processes (Torrens 2006). Daubeny (1835) may even have been the first to measure the temperature of a lava flow, by laying a thermometer on the top of a flow at Vesuvius—albeit several months following the eruption, after intervening rain (his estimate was 390 °F). In any case, pressure (P) and temperature (T) estimation lie at the heart of fundamental questions: How hot is Earth, and at what rate has the planet cooled. Are volcanoes the products of thermally driven mantle plumes? Where are magmas stored, and how are they transported to the surface—and how do storage and transport relate to plate tectonics? Well-calibrated thermometers and barometers are essential tools if we are to fully appreciate the driving forces and inner workings of volcanic systems.

This chapter presents methods to estimate the P-T conditions of volcanic and other igneous processes. The coverage includes a review of existing geothermometers and geobarometers, and a presentation of approximately 30 new models, including a new plagioclase-liquid hygrometer. Our emphasis is on experimentally calibrated "thermobarometers," based on analytic expressions using P or T as dependent variables. For numerical reasons (touched on below) such expressions will always provide the most accurate means of P-T estimation, and are also most easily employed. Analytical expressions also allow error to be ascertained; in the absence of estimates of error, P-T estimates are nearly meaningless. This chapter is intended to complement the chapters by Anderson et al. (2008), who cover granitic systems, and by Blundy and Cashman (2008) and Hansteen and Klügel (2008), who consider additional methods for P estimation.

THEORETICAL ASPECTS

At the foundation of well-founded belief lies belief that is not founded
- Ludwig Wittgenstein

In the search for useful geothermometers or geobarometers, the goal is to find some chemical equilibrium where there is a significant difference between the entropy (ΔS_r) (for a thermometer) or volume (ΔV_r) (for a barometer) of products and reactants. Consider:

$$NaO_{0.5}^{liq} + AlO_{1.5}^{liq} + 2SiO_2^{liq} = NaAlSi_2O_6^{cpx} \quad (1)$$

where superscripts denote phase (liq = liquid; cpx = clinopyroxene); $NaAlSi_2O_6^{cpx}$ is the jadeite (Jd) content of clinopyroxene. To compare S and V, we use partial molar entropies (S) and

1529-6466/08/0069-0003$10.00 DOI: 10.2138/rmg.2008.69.3

Downloaded from http://pubs.geoscienceworld.org/msa/rimg/article-pdf/69/1/61/2948053/61_Putirka.pdf
by University of California Berkeley Library user
on 16 March 2024

partial molar volumes ($\overline{V}$), where $\overline{S} = S/n$ and $\overline{V} = V/n$, and n = number of moles. In Equation (1), $\Delta S_r = \overline{S}_{Jd} - \overline{S}_{NaO_{0.5}^{liq}} - S_{AlO_{1.5}^{liq}} - 2\overline{S}_{SiO_2^{liq}}$, $\Delta V_r = \overline{V}_{Jd} - \overline{V}_{NaO_{0.5}^{liq}} - \overline{V}_{AlO_{1.5}^{liq}} - 2\overline{V}_{SiO_2^{liq}}$. The equilibrium constant, K_{eq}, is:

$$K_{eq} = \frac{a_{Jd}^{cpx}}{a_{NaO_{0.5}}^{liq} \cdot a_{Al_2O_3}^{liq} \cdot \left(a_{SiO_2}^{liq}\right)^2} \tag{2}$$

where terms such as a_{Jd}^{cpx} and $a_{NaO_{0.5}}^{liq}$ represent the activities of Jd in clinopyroxene, and SiO_2 in liquid respectively. Activity is something like an 'effective concentration', and in the ideal case, is equivalent to mole fraction: $a_{Jd}^{cpx} = X_{Jd}^{cpx}$, where X_{Jd}^{cpx} is the mole fraction of Jd in a clinopyroxene solid solution. In non-ideal solutions, the two quantities can be related to one another by an activity coefficient, λ, so that $a_{Jd}^{cpx} = \lambda_{Jd}^{cpx} X_{Jd}^{cpx}$.

A "good" thermometer has a large ΔS_r and a good barometer has a large ΔV_r. But what is "good"? For metamorphic systems, Essene (1982) suggests that $\Delta S_r \geq 4.0$ J/mole·K and $\Delta V_r \geq 0.2$ J/bar; these limits perhaps also apply to igneous systems. The presence of a liquid, though, poses hurdles to the igneous petrologist. Consider the very large number of distinct equilibria used for *P-T* estimation in metamorphic systems (Spear 1993). Far fewer are available to igneous petrologists. Why? To begin with, igneous rocks carry fewer crystalline phases. And the numbers of crystalline phases is perhaps in turn limited by the presence of the liquid itself. A silicate liquid is a 'high variance' phase in that, compared to minerals, it is highly compressible and has no compositional stoichiometric constraints. Liquids can thus absorb significant changes in *P*, *T* and composition (X_i^j, the mole fraction of *i* in some phase *j*), by expanding, contracting or mixing, without resorting to the extreme measure of precipitating a new phase. Metamorphic rocks have no such luxury. Carrying nothing but crystalline phases, with sharp limits on their ability to expand, contract or mix, new phases readily nucleate in response to changing *P-T-*X_i^j. This results in sharp changes in *S* and *V* in metamorphic systems, which can be exploited to formulate geothermobarometers. By their versatility, silicate liquid-bearing systems are intrinsically less amenable to thermobarometer formulation—but all is not lost.

Perhaps the single most useful equation for petrologists is:

$$-RT \ln K_{eq} = \Delta G_r^\circ \tag{3}$$

where R is the gas constant (R = 1.9872 cal/K·mole, or 8.3144 J/dK·mole) and ΔG_r° is the Gibbs free energy change of "reaction" for a balanced equilibrium, such as Equation (1). In ΔG_r°, the superscript ° means that the Gibbs free energy is for a standard state (pure substances at 1 bar), an important distinction from ΔG_r, which is the Gibbs free energy change between products and reactants at any arbitrary *P* and *T*. At equilibrium, $\Delta G_r = 0$, by definition. But rarely is $\Delta G_r = 0$ at a standard state. So when $\Delta G_r = 0$, it is usual that $\Delta G_r^\circ \neq 0$, which means that usually $K_{eq} \neq 1$.

Despite its name, however, K_{eq} is only constant at fixed *P* and *T*. Driven by differences in ΔS_r and ΔV_r, K_{eq} can vary greatly as a function of *P* and *T*. So for example, in Equation (1), if $NaAlSi_2O_6^{cpx}$ has a smaller partial molar volume compared to the collective partial molar volumes of the reactants ($\Delta V_r > 0$), then with increased *P*, Equation (1) will shift to the right and K_{eq} will increase. Similarly, higher *T* favors whichever side of an equilibrium that has higher partial molar entropy. Equation (3) provides a quantitative footing to relate K_{eq} to *P* and *T* and is at the root of all thermometers and barometers based on 'theoretical' or thermodynamic models.

The differentiation of "empirical" and "theoretical" is not always clear. The laws of thermodynamics are rooted in fundamentally empirical expressions derived by Robert Boyle, who in 1662 determined that volume, *V*, is related to *P* by the expression: $V = C/P$, where C is a constant. In the 19th century, Jacques Charles and Joseph-Louis Gay-Lussac, further illuminated the phenomenon of thermal expansion in gases: $V = \alpha V_o T$, where α is the coefficient

Downloaded from http://pubs.geoscienceworld.org/msa/rimg/article-pdf/69/1/61/2948053/61_Putirka.pdf
by University of California Berkeley Library user
on 16 March 2024

of thermal expansion, and V_o is some reference gas volume (see Castellan 1971). These two expressions, known today as Boyle's Law and Charles' (or Gay-Lussac's) Law are combined, with Avogadro's law (that equal volumes of gases have equal numbers of molecules), to yield the ideal gas law: $PV = nRT$ (which recognizes that the constant C in Boyle's Law is proportional to n). The relevance is that the form of Equation (3) is not accidental: it derives from the ideal gas law and an assumption that activities can be represented by fugacities or partial pressures, where we integrate $(\partial G/\partial P)_T = V$ by substituting $V = nRT/P$ (see Nordstrom and Munoz 1986). In effect, our most sophisticated and complex activity models for silicate liquids and minerals are based on the assumption that they act, in the phrase of David Walker, as a "*perverted ideal gas*." In the event, practice and experience indicate that models based on $-RT\ln K_{eq} = \Delta G_r^\circ$ are more accurate than those based on more arbitrary relationships and so provide the greatest promise for extrapolation outside calibration boundaries.

To make use of $\ln K_{eq} = -\Delta G_r^\circ/RT$, we use the relationship $\Delta G_r^\circ = \Delta H_r^\circ - T\Delta S^\circ$ (where ΔH_r° and ΔS_r° are respectively the enthalpy and entropy differences for a chemical equilibrium at standard state), and the expressions $(\partial \Delta G_r/\partial P)_T = \Delta V_r$ and $(\partial \Delta G_r/\partial P)_P = \Delta S_r$. If P is constant, and the differences in heat capacities (C_p) between products and reactants are effectively equal ($\Delta C_p = 0$) (meaning that ΔH_r and ΔS_r are independent of T), then substitution yields the following:

$$\ln K_{eq} = -\Delta H_r^\circ/RT + \Delta S_r^\circ/R \tag{4}$$

If we know ΔH_r° and ΔS_r°, then we can use Equations (2) and (4) to calculate T, and we have a thermometer. If ΔH_r° and ΔS_r° are unknown, we can preserve the functional relationship between K_{eq} and T in Equation (4) and use as a regression model: $\ln K_{eq} = a/T + b$, where $a = -\Delta H_r^\circ/R$ and $b = \Delta S_r^\circ/R$; we can then derive a and b from isobaric experimental data, where composition and T are known (and an activity model is assumed). Of course, P need not be constant, and ΔH_r and ΔS_r will vary with T if $\Delta C_p \neq 0$. Products and reactants might also exhibit significant differences in compressibility (β) or thermal expansion (α) such that, over a wide enough P interval, $\Delta\beta_r \neq 0$ and $\Delta\alpha_r \neq 0$. The following regression equation accounts for such changes (see Putirka 1998):

$$\ln K_{eq} = \frac{A}{T} + B + C\ln\left[\frac{T}{T_o}\right] + D\frac{P}{T} + E\frac{P^2}{T} + FP + GP^2 \tag{5}$$

where $A = -\Delta H_r^\circ/R$, $B = \Delta S_r^\circ/R$, $C = \Delta C_p/R$, $D = -\Delta V_r^\circ/R$, $E = \Delta\beta_r \Delta V_r^\circ/2R$, $F = \Delta\alpha_r \Delta V_r^\circ/R$, and $G = \Delta\alpha_r\Delta\beta_r\Delta V_r^\circ/2R$. Equation (5) contains all the terms in Equation (4), plus additional terms that correct for the cases that P is not constant, $\Delta C_p \neq 0$, etc. More terms could be added if $\Delta\alpha_r$, $\Delta\beta_r$, and ΔC_p are not constant, though for most geological purposes Equation (5) is sufficiently complex. In Equation (5), T_o is a reference temperature; in Putirka (1998) T_o was taken as the melting point of a pure mineral, T_m, in which case reference values for ΔH_r°, ΔS_r°, etc., are for fusions of pure substances. Equation (5) is also simplified in that the reference pressure (P_o, needed to calculate the effects of a non-zero $\Delta\beta_r$ and $\Delta\alpha_r$) is taken as 1 atm, or effectively zero on a kilobar or GPa scale. If some other reference pressure is required, or if 1 bar is large compared to the pressure of interest, then the term $(P\text{-}P_o)$ replaces P in each instance in Equation (5).

REGRESSION ANALYSIS & STATISTICAL CONSIDERATIONS

The stars might lie but the numbers never do

- Mary Chapin Carpenter

Experimental data, regression analysis & statistical considerations

Although some geothermometers or geobarometers are developed using calorimetric and volumetric data, most derive from regression analysis of experimental data, where K_{eq}, P and T are all known. Partial melting experiments reported in the Library of Experimental Phase

Downloaded from http://pubs.geoscienceworld.org/msa/rimg/article-pdf/69/1/61/2948053/61_Putirka.pdf
by University of California Berkeley Library user
on 16 March 2024

Relations (LEPR) (Hirschmann et al. 2008), and elsewhere, are here used to test existing, and calibrate new thermobarometers. Regression analysis of such data yields regression coefficients that minimize error for the selected dependent variable. This approach assumes that the experiments used for regression approach equilibrium. There are several possible validity tests, but none guarantee success. One is to check whether the regression-derived coefficients compare favorably with independently determined values for quantities such as ΔH_r°, ΔS_r°, and ΔV_r°. One can also test model results for their ability to predict P or T for natural systems where P and T might be known (e.g., a lava lake). Issues of error are discussed in detail in the penultimate section of this chapter.

Regression strategies. For the calibration of new models, no data-filters are applied at the outset, but generally, experiments that yield P or T estimates that are >3σ outside standard errors of estimate (SEE) for remaining data are considered suspect and not used for calibration or testing. And if particular studies contain multiple aberrant data, such studies are excluded. Most new calibrations utilize "global" regressions, which use all available data to determine the minimum number of parameters that are required to explain observed variability. All tests make use of "leverage plots" to ensure that a given model parameter is significant and explained by more than just one or a few potentially aberrant data (see JMP Statistics and Graphics Guide). We also employ regression models where P and T appear as dependent variables—a numerical necessity if one is to maximize precision.

***Regression models*.** William of Ockham, a 14th century philosopher, suggested that "plurality must not be posited without necessity" (Ockham's razor), a recommendation supported by Bayesian analysis (Jefferys and Berger 1992). Jefferys and Berger (1992) reword this principle: "if a law has many adjustable parameters then it will be significantly preferred to the simpler law only if its predictions are considerably more accurate". To illustrate, they show how Galileo's quadratic expression (relating distance (x) and time (t) to the acceleration due to gravity (g), i.e., $x = x_o + vt + 1/2gt^2$) is highly superior to a 6th order polynomial fit to the same data. The problem is not whether additional coefficients in the 6th order equation have theoretical meaning: gravity changes with elevation; this fact could be used to develop additional terms beyond the familiar quadratic expression. But Galileo's original experiments have nowhere near the level of precision required to extract such information.

Similar issues apply to petrology. Using Equation (2) as an example, Figure 1a shows two regression models: 1) a two-parameter model where $\ln K_{eq} = aP/T + b$, and 2) a five-parameter model, where $\ln K = aP/T + b\ln(T) + c(P^2/T) + dP^2 + e$. All of the coefficients (a, b, c, d, e) have thermodynamic meaning (Eqn. 5), and the 5-parameter model describes a greater fraction (99.8%) of the variation of $\ln K_{eq}$ for the calibration data (ankaramites from Putirka et al. 1996). However, the 5-parameter model yields gross systematic error when predicting $\ln K_{eq}$ for "test" data (Fig. 1b; all remaining data in Putirka et al. 1996), with a slope and intercept through $\ln K_{eq}$ (measured) vs. $\ln K_{eq}$ (calculated) of 0.5 and 1.5 respectively. In contrast, our lowly 2-parameter

Figure 1 (*on facing page*). In (a) and (b), predicted values for $\ln K_{eq}$ based on Equation (2) are used to illustrate how model complexity, no matter how valid from theoretical considerations, can yield incorrect predictions if model parameters are not supported by data. In (a), calculated and measured values of $\ln K_{eq}$ are compared using ankaramite bulk compositions from Putirka et al. 1996). For both the 2- and 5-parameter equations, all regression coefficients have thermodynamic significance (Eqn. 5), and the 5-parameter model provides a better fit to the calibration data. However, in (b) the 5-parameter equation yields strong systematic error when used to predict $\ln K_{eq}$ for experimental data not used for regression (as illustrated by the slope and intercept of the regression line $\ln K_{eq}$(calculated) vs. $\ln K_{eq}$(measured); ideally they should be 1 and 0 respectively). In contrast, the 2-parameter model is nearly free of systematic error, and describes the 'test' data with higher precision; the 5-parameter equation is of little use beyond interpolating between calibration points, while the 2-parameter equation is a useful predictive tool. Models cannot be judged solely by their fit to calibration data, nor by their thermodynamic complexity.

Downloaded from http://pubs.geoscienceworld.org/msa/rimg/article-pdf/69/1/61/2948053/61_Putirka.pdf
by University of California Berkeley Library user
on 16 March 2024

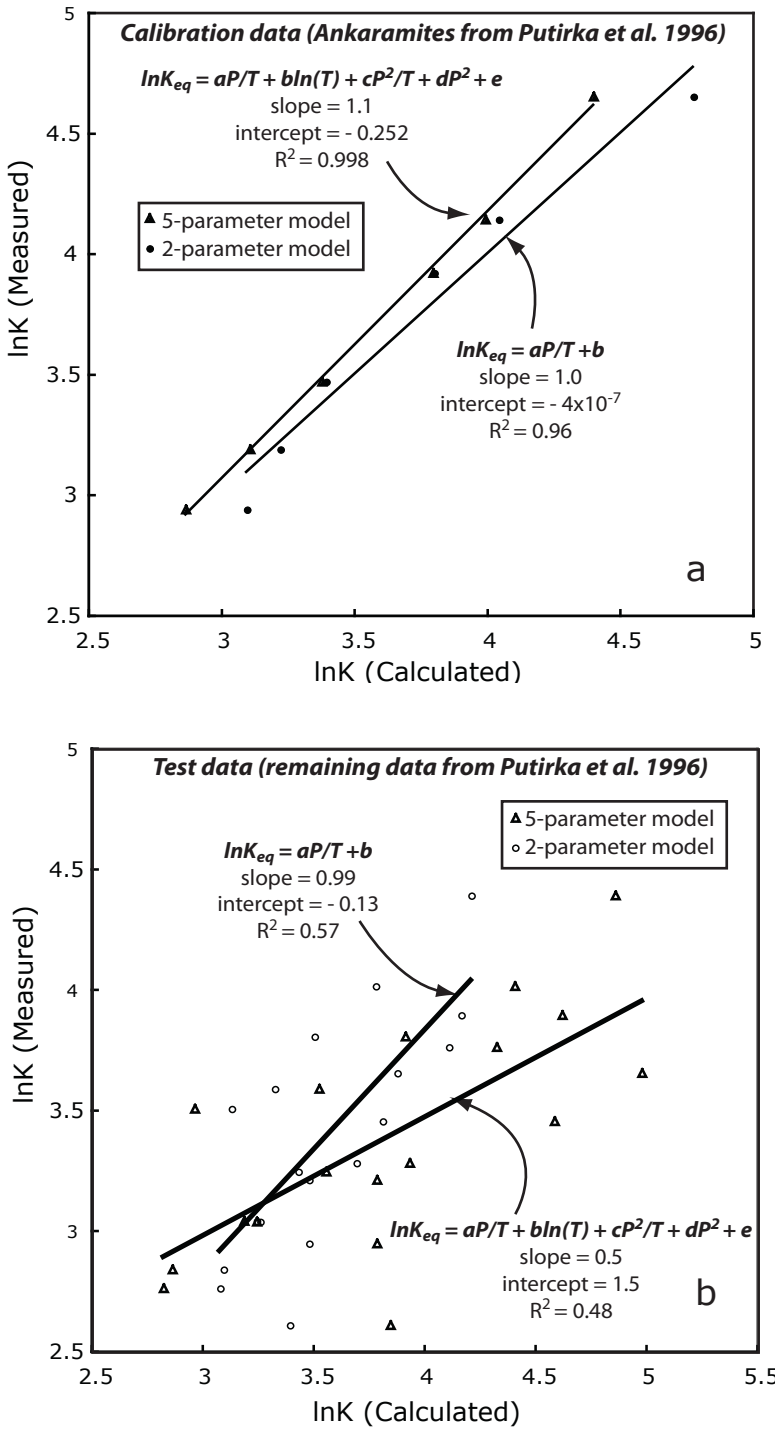

Figure 1. *caption on facing page*

Downloaded from http://pubs.geoscienceworld.org/msa/rimg/article-pdf/69/1/61/2948053/61_Putirka.pdf
by University of California Berkeley Library user
on 16 March 2024

model yields a higher correlation coefficient (R) for the test data, and is nearly absent systematic error, with slope and intercept values much closer to the ideal of one and zero respectively. Box and Draper (1987, p. 74) summarize the issue rather succinctly: "Remember that all models are wrong; the practical question is how wrong do they have to be to not be useful." In geothermobarometry, the answer is that only the first 4 terms of Equation (5) are usually needed.

Linear regression methods can be used to avoid the pitfalls noted in Figure 1 because unlike non-linear methods, validity tests are available for regression coefficients; parameters that are not supported by the data (no matter their thermodynamic significance), can be culled from a potential model. An occasional roadblock is that equations such as Equation (5) cannot always be rearranged so that P or T can be isolated as dependent variables. One solution is to perform a linear regression using some other quantity as the independent variable, and then rearrange the expression. But in multiple linear regression, error is minimized only for the dependent variable (regression analysis is not symmetric), so error will not be minimized for the variable of interest, and systematic error is assured. Equation (4), for example, will yield a very good model for predicting $\ln K_{eq}$, but will be less precise, and yield systematic error, if the same coefficients are rearranged to calculate T. *Regression models that use P or T as dependent variables will thus always be more precise and accurate* compared to models that minimize error on such quantities as $\ln K_{eq}$, Gibbs Free Energy, etc., an unavoidable consequence of numerical issues of regression analysis. If variations in P are not of concern, Equation (4) should be rearranged to yield:

$$\frac{1}{T} = a \ln K_{eq} + b \tag{6}$$

where $a = -R/\Delta H_r^\circ$ and $b = \Delta S_r^\circ/\Delta H_r^\circ$. If variations in P are important, remaining choices are to add P as an "empirical" factor,

$$\frac{1}{T} = a \ln K_{eq} + b + cP \tag{7}$$

or apply non-linear regression methods, using:

$$T = \frac{\Delta H_r^\circ + P\Delta V}{R \ln K_{eq} - \Delta S_r^\circ} = \frac{a + bP}{c \ln K_{eq} + d} \tag{8}$$

Here, $\Delta C_p = 0$, and $P_o = 0$ (i.e., 1 bar); if an additional P term is required, the term $(1/2)\, P^2 \Delta\beta_r\, \Delta V_r^\circ$ can be added to the numerator (*a, b, c*, and *d* have thermodynamic meaning as in Equation (8), but not are not identical to the coefficients in Equations (6-7)). A disadvantage to non-linear regression is that it does not yield an absolute minimum for error on the dependent variable, and there are no intrinsic validity tests for model parameters.

Activity modeling. Mixing and interaction between chemical components in an equilibrium may result in non-ideal behavior, complicating the calculation of K_{eq}. To address just such compositional dependencies, Thompson (1967) developed a polynomial model for activity coefficients, $\lambda_i = f(X_i)$. The approach uses so-called Margules parameters (W_G), which represent the energy of interaction between chemical components. Thompson's (1967) parameters can be substituted into Equation (3). For example, using the definitions for a two-parameter model (W_{G1}, and W_{G2}), describing interaction between two components, X_1 and X_2, the Margules model is: $RT\ln\lambda_1 = (2W_{G2} - W_{G1})(X_2)^2 + 2(W_{G1} - W_{G2})(X_2)^3$ and $RT\ln\lambda_1 = (2W_{G1} - W_{G2})(X_1)^2 + 2(W_{G2} - W_{G1})(X_1)^3$ (Nordstrom and Munoz 1986). Because of the extrinsic dependency of λ on T, such substitutions require non-linear regression methods for thermometers (see below). As an alternative approach, consider forsterite (Fo, Mg_2SiO_4) melting,

$$Mg_2SiO_4^{ol} = 2MgO^{liq} + SiO_4^{liq} \tag{9}$$

Downloaded from http://pubs.geoscienceworld.org/msa/rimg/article-pdf/69/1/61/2948053/61_Putirka.pdf
by University of California Berkeley Library user
on 16 March 2024

In the ideal case, $a_{\mathrm{Fo}}^{ol} = X_{\mathrm{Fo}}^{ol}$, $a_{\mathrm{MgO}}^{liq} = X_{\mathrm{MgO}}^{liq}$ and $a_{\mathrm{SiO_2}}^{liq} = X_{\mathrm{SiO_2}}^{liq}$, and so $K_{eq}^{ol\text{-}liq} = X_{\mathrm{Fo}}^{ol}/(X_{\mathrm{MgO}}^{liq}.X_{\mathrm{SiO_2}}^{liq})$. If the system is non-ideal and we know the values for $\lambda_{\mathrm{MgO}}^{liq}$, $\lambda_{\mathrm{Fo}}^{ol}$, etc., the activity coefficients can be inserted to yield $K_{eq}^{ol\text{-}liq} = \lambda_{\mathrm{Fo}}^{ol}X_{\mathrm{Fo}}^{ol}/(\lambda_{\mathrm{MgO}}^{liq}X_{\mathrm{MgO}}^{liq}.\ \lambda_{\mathrm{SiO_2}}^{liq}X_{\mathrm{SiO_2}}^{liq})$. O'Nions and Powell (1977) extract such terms to yield linear coefficients in Equations such as (4) and (8). Using Equation (9) as an example,

$$\begin{aligned}\ln K_{eq} &= \ln\left[\frac{\left(a_{\mathrm{MgO}}^{liq}\right)^2 \cdot a_{\mathrm{SiO_2}}^{liq}}{a_{Fo}^{ol}}\right] = \ln\left[\frac{\left(\lambda_{\mathrm{MgO}}^{liq}X_{\mathrm{MgO}}^{liq}\right)^2 \cdot \lambda_{\mathrm{SiO_2}}^{liq}X_{\mathrm{SiO_2}}^{liq}}{\lambda_{Fo}^{ol}X_{Fo}^{ol}}\right] \\ &= \ln\left[\frac{\left(\lambda_{\mathrm{MgO}}^{liq}\right)^2 \cdot \lambda_{\mathrm{SiO_2}}^{liq}}{\lambda_{Fo}^{ol}}\right] + \ln\left[\frac{\left(X_{\mathrm{MgO}}^{liq}\right)^2 \cdot X_{\mathrm{SiO_2}}^{liq}}{X_{Fo}^{ol}}\right] \\ &= 2\ln\left(\lambda_{\mathrm{MgO}}^{liq}\right) + 2\ln\left(X_{\mathrm{MgO}}^{liq}\right) + \ln\left(\lambda_{\mathrm{SiO_2}}^{liq}\right) + \ln\left(X_{\mathrm{SiO_2}}^{liq}\right) - \ln\left(\lambda_{Fo}^{ol}\right) - \ln\left(X_{Fo}^{ol}\right)\end{aligned} \tag{10}$$

where a term such as X_i^j refers to the mole fraction of component i in phase j. A possible regression model based on Equations (6), (9) and (10) is thus:

$$\frac{1}{T} = a\ln\left[\frac{\left(X_{\mathrm{MgO}}^{liq}\right)^2 \cdot X_{\mathrm{SiO_2}}^{liq}}{X_{Fo}^{ol}}\right] + b + c\ln\left(\lambda_{\mathrm{MgO}}^{liq}\right) + d\ln\left(\lambda_{\mathrm{SiO_2}}^{liq}\right) + e\ln\left(\lambda_{Fo}^{ol}\right) \tag{11}$$

where the coefficients a and b are as in Equation (6). For ideal mixing, the λ_i^j are all 1, and c, d, and e are zero; if λ_i^j are known, then $c = d = e = 1$. For non-ideal mixing, λ_i^j can be related to mole fractions, X_i^j, using

$$\frac{1}{T} = a\ln\left[\frac{\left(X_{\mathrm{MgO}}^{liq}\right)^2 \cdot X_{\mathrm{SiO_2}}^{liq}}{X_{Fo}^{ol}}\right] + b + c\left(X_{\mathrm{MgO}}^{liq}\right) + d\ln\left(X_{\mathrm{SiO_2}}^{liq}\right) + e\ln\left(X_{Fo}^{ol}\right) \tag{12}$$

where a and b are as in Equation (6), and c, d, and e are "empirical" regression coefficients that can be related to the activity coefficients: in the case of X_{MgO}^{liq}, we presume that there is some number c such that $\lambda_{MgO}^{liq} = \exp\left(cX_{MgO}^{liq}\right)$, where c is as in Equation (12). Stormer (1975) shows how coefficients to a polynomial expansion can be equated to Margules parameters. In any case, activity models are important here, only to the extent that they provide increased precision when estimating P or T.

IGNEOUS THERMOMETERS AND BAROMETERS

All models are wrong, some models are useful

- George Box

History and background

James Hall (1798) presented the first attempts to measure the melting temperatures of volcanic rocks. However, at the time there were few methods for determining temperatures above the boiling point of mercury, and his use of the Wedgwood pyrometer (based on the volume change in clays when heated) yielded widely ranging estimates (1029-3954 °C; see Hall's "Table of Fusibilities," where °W ≈ 130 °F). Later experiments had much better temperature control, with Joly (1891) using his "meldometer" and later experimentalists eventually employing the thermocouple (e.g., Doelter 1902; Day and Allen 1905; Shepherd et al. 1909).

Some of the earliest temperature-controlled experimental studies of melting temperatures for minerals and rocks (Joly 1891; Doelter 1902; Day and Allen 1905; Shepherd et al. 1909) were no doubt conducted in part to understand the thermal conditions of partial melting and

Downloaded from http://pubs.geoscienceworld.org/msa/rimg/article-pdf/69/1/61/2948053/61_Putirka.pdf
by University of California Berkeley Library user
on 16 March 2024

crystallization. But the first study to establish, with some accuracy, the temperature interval for the crystallization of natural basaltic magmas was conducted by Sosman and Merwin (1913). They determined that the solidus and liquidus temperatures for the Palisades Sill in New York are ≈1150 °C and 1300 °C respectively. Contributions by Bowen (1913, 1915) have outshone such work. In his 1913 paper, Bowen established with accuracy the continuous solid solution of the plagioclase feldspars, and then in 1915 applied experimental results, thermodynamic theory and phase diagrams to show that a wide range of igneous rocks can be derived from basaltic parental liquids by the process of fractional crystallization (Bowen 1915). But Sosman and Merwin's estimates were nonetheless largely correct: their estimation of the 1 atm temperature interval for basalt crystallization matched well with Perret's (1913) and Jagger's (1917) direct temperature estimates of freshly formed lava at Hawaii (est. 1050-1200 °C), and were qualitatively verified by experiments in simple systems (Bowen 1915); together, these experimental and field-based studies represent the first accurate determinations of the temperatures at which basaltic rocks form. More thorough experimental studies (e.g., Tuttle and Bowen 1958; Yoder and Tilley 1962; Green and Ringwood 1967) would later establish temperatures of partial crystallization for both granitic and basaltic systems, over a range of *P-T* conditions.

None of these early efforts, though, established a means to *estimate T or P for any particular igneous rock*. One of the first attempts to establish a true geothermometer was by Wright and Larson (1909), using the optical and morphological properties of quartz. The first analytic geothermometer, though, was proposed by Barth (1934) and presented by Barth (1951), who developed an approach that is still in use today: the two-feldspar thermometer. Barth (1951) presented a theoretical model based on the alkali-feldspar solvus, which was retracted in proof when he discovered that his theoretical solvus did not match the experimentally determined curve of Bowen and Tuttle (1950). Barth's (1951) effort was followed by a Ti-in-magnetite thermometer by Buddington et al. (1955) and Buddington and Lindsley (1964), a two-pyroxene thermometer by Davis and Boyd (1966), a thermometer based on Ni partitioning between olivine and liquid by Hakli and Wright (1967), and Barth's own recalibrations of a two-feldspar thermometer (Barth 1962, 1968). The following decade then saw a substantial increase in the methods of igneous thermobarometry, with new calibrations of a plagioclase thermometer by Kudo and Weill (1970), a new olivine thermometer by Roeder and Emslie (1970), new calibrations of the two-feldspar thermometer (e.g., Stormer 1975) and the calibration of multiple *P*- and *T*-sensitive igneous equilibria by Nicholls et al. (1971), Nicholls and Carmichael (1972) and Bacon and Carmichael (1973), among others. Since the 1970's the number of igneous thermometers and barometers has greatly expanded.

Selection criteria. Within the space of a single chapter, it is possible to review neither all the various igneous thermometers that have been calibrated, nor to detail their thermodynamic bases. Emphasis is thus placed upon cataloging those tools that can be used widely, especially for volcanic systems. The thermometers and barometers presented here are thus based on commonly found minerals, using, for the most part, elemental components that are easily determined in most laboratories.

Calculating "liquid" and mineral components, and activities

It is absolutely crucial that all components, be they minerals or liquids, are calculated in precisely the same way as originally handled for a particular thermometer or barometer. Here, component calculations that are common to many models shown below are discussed, but care should be taken to examine specific component calculation procedures when presented below.

Several Tables are presented to illustrate nearly all the calculations presented in this chapter (Tables 1-7); readers attempting to reproduce these and other numbers should note the following: Table 1 in Putirka (1997) contains small errors relative to *P* and *T* (using the models in Putirka et al. 1996); Table A2 in Putirka et al. (2007) contains small errors relative to melt fraction F, and derivative calculations. All related equations are valid as published;

Downloaded from http://pubs.geoscienceworld.org/msa/rimg/article-pdf/69/1/61/2948053/61_Putirka.pdf
by University of California Berkeley Library user
on 16 March 2024

the errors result from the use of earlier versions of certain equations, later abandoned for the published (more accurate) models (the Tables were not updated). In addition, some *P* and *T* calculations presented here require numerical solution methods (when *T* and *P* depend upon one another and both are to be calculated). Here and in other works *P-T* estimates are based on the numerical module found within "Excel – Preferences – Calculation – Iteration". This feature may have numerical instabilities, and the "Solver" or "Goal Seek" options of Excel, or other numerical methods, should perhaps be preferred.

Liquid components. In the models that follow, various calculation schemes are used to represent the chemical components of silicate phases. For the empirical "glass" thermometers, most liquid components are entered as wt%, so no special calculations are needed, except for terms such as Mg#, which are always represented on a mole fraction basis, and calculated as $Mg\#(liq) = (MgO^{liq}/40.3)/[((MgO^{liq}/40.3) + (FeO^{liq}/71.85))]$, where terms such as MgO^{liq} represent the wt% of MgO in the liquid. For all other models, liquid components are calculated either as a mole fraction or a cation fraction (Table 1), always on an anhydrous basis (even if H_2O occurs in the equation or analysis, so as to avoid estimating molecular H_2O vs. OH^-). The purpose of such calculations is to be able to compare numbers of molecules, as this is how we calculate K_{eq}. Mole and cation fractions are very similar. For a mole fraction, the wt% of each oxide is divided by its molecular weight; for example, Al_2O_3 would be divided by 101.96 and Na_2O would be divided by 61.98; this calculation yields a "mole proportion" for the oxides, which is converted to a mole fraction by renormalizing the sum of the molecular proportions so that they sum to 1.0 (see Table 1). In a chemical equilibrium, the Al content of a liquid, for example, would be written as $Al_2O_3^{liq}$, and in a K_{eq}, the mole fraction would appear as $X^{liq}_{Al_2O_3}$.

Liquid components using cation fractions. For a cation fraction, each oxide is normalized by the molecular weight of the oxide having only one cation. So Al_2O_3 is divided by the molecular weight of $AlO_{1.5}$, or 50.98; similarly, the wt% of Na_2O is divided by the weight of $NaO_{0.5}$, or 30.99. Compared to the usual mole fraction, this approach doubles the "molecular" units for oxides that contain two cations per formula unit, such as Al_2O_3, Na_2O, K_2O, Cr_2O_3, and P_2O_5; using Al_2O_3 again as an example, we effectively divide one molecular unit of Al_2O_3 into two molecular units of $AlO_{1.5}$. For oxides such as SiO_2, which already have only one cation per formula unit, the wt% of SiO_2 is divided by 60.08, as usual. These "cation proportions" are converted to a "cation fraction" by renormalizing each oxide by the sum of the cation proportions, so that the new sum is 1.0 (Table 1). In a chemical equilibrium, the Al content of a liquid would be written as $AlO_{1.5}^{liq}$, and in a K_{eq}, would appear as $X^{liq}_{AlO_{1.5}}$.

The advantage of the cation fraction is that the relative numbers of cations can be compared directly. Ratios of Fe/Mg (or equivalently, FeO/MgO) are the same whether a "mole" or cation fraction are considered; but the cation fraction allows a more straightforward comparison of, for example, Ca/Al ($CaO/AlO_{1.5}$) or Na/Al ($NaO_{0.5}/AlO_{1.5}$) ratios. With a mineral composition, cation fractions can also be multiplied by the number of cations in a mineral formula so that the sum, instead of 1, is equal to the number of cations per formula unit (e.g., 2 for olivine, 4 for pyroxene, 5 for feldpsar); this procedure yields the number of cations per formula unit.

Activity models take these calculations further, recognizing that the actual chemical species in liquids and minerals probably do not occur in the form of isolated, non-interacting oxides. Two notable approaches for calculating the activities of liquid components are the two-lattice (Bottinga and Weill 1972; Nielsen and Drake 1979) and the regular solution (Ghiorso 1987) models. Beattie (1993), however, recognized that because of numerous interactions at the molecular level, silicate liquids have many more chemical species than components, which limits what activity models can reveal about liquid properties. Beattie (1993) developed an activity model that increased the precision of his olivine-liquid thermometer, and his two-lattice model appears to be more successful than any proposed thus far. Beattie's (1993) two-lattice model yields several terms (calculated from cation fractions) that appear in the models

Downloaded from http://pubs.geoscienceworld.org/msa/rimg/article-pdf/69/1/61/2948053/61_Putirka.pdf
by University of California Berkeley Library user
on 16 March 2024

Table 1. Sample calculations for liquid components.

	SiO_2	TiO_2	Al_2O_3	FeO	MnO	MgO	CaO	Na_2O	K_2O	total
1) Weight %	47.05	0.89	16.11	7.96	0.15	12.78	11.13	2.18	0.04	98.29
2) Molecular weights	60.08	79.9	101.96	71.85	70.94	40.3	56.08	61.98	94.2	
3) Mole proportions	0.7831	0.0111	0.1580	0.1108	0.0021	0.3171	0.1985	0.0352	0.0004	1.62
	$X^{liq}_{SiO_2}$	$X^{liq}_{TiO_2}$	$X^{liq}_{Al_2O_3}$	X^{liq}_{FeO}	X^{liq}_{MnO}	X^{liq}_{MgO}	X^{liq}_{CaO}	$X^{liq}_{Na_2O}$	$X^{liq}_{K_2O}$	
4) Mole fractions	0.4845	0.0069	0.0978	0.0685	0.0013	0.1962	0.1228	0.0218	0.0003	1.00
	SiO_2	TiO_2	$AlO_{1.5}$	FeO	MnO	MgO	CaO	$NaO_{0.5}$	$KO_{0.5}$	
5) Molecular weights	60.08	79.9	50.98	71.85	70.94	40.3	56.08	30.99	47.1	
6) Cation proportions	0.7831	0.0111	0.3160	0.1108	0.0021	0.3171	0.1985	0.0703	0.0008	1.81
	$X^{liq}_{SiO_2}$	$X^{liq}_{TiO_2}$	$X^{liq}_{AlO1.5}$	X^{liq}_{FeO}	X^{liq}_{MnO}	X^{liq}_{MgO}	X^{liq}_{CaO}	$X^{liq}_{NaO_{0.5}}$	$X^{liq}_{KO_{0.5}}$	
7) Cation fractions	0.4327	0.0062	0.1746	0.0612	0.0012	0.1752	0.1096	0.0389	0.0005	1.00
			$C^{liq}_{SiO_2}$	C^{liq}_{NM}	C^{liq}_{NF}	NF				
8) Beattie (1993) components			0.4327	0.3472	0.4782	-0.7148				

The mole proportions in row 3) are equal to row 1) divided by row 2); mole fractions, row 6) are equal to row 3) divided by its total, 1.62. Cation proportions in row 6) are equal to row 1) divided by row 5); cation fractions; row 7), is row 6) divided by its total, 1.81. Beattie (1993) components are calculated from cation fractions as follows: $C^{liq}_{SiO_2} = X^{liq}_{SiO_2}$; $C^{liq}_{NM} = X^{liq}_{FeO} + X^{liq}_{MnO} + X^{liq}_{MgO} + X^{liq}_{CaO} + X^{liq}_{CoO} + X^{liq}_{NiO}$; $C^{liq}_{NF} = X^{liq}_{SiO_2} + X^{liq}_{NaO_{0.5}} + X^{liq}_{KO_{0.5}} + X^{liq}_{TiO_2}$; $NF = \frac{7}{2}\ln\left(1 - X^{liq}_{AlO_{1.5}}\right) + 7\ln\left(1 - X^{liq}_{TiO_2}\right)$, where X^j_i is the cation fraction of i in phase j. Here, the values of X^j_i are equal to the contents of row 7).

Downloaded from http://pubs.geoscienceworld.org/msa/rimg/article-pdf/69/1/61/2948053/61_Putirka.pdf
by University of California Berkeley Library user
on 16 March 2024

below (Table 1): $NF = \frac{7}{2}\ln(1 - X^{liq}_{AlO_{1.5}}) + 7\ln(1 - X^{liq}_{TiO_2})$, (where NF refers to "network formers," i.e., chemical constituents that comprise a silicate network in the liquid); the concentration of network modifying cations, $C^{liq}_{NM} = X^{liq}_{MgO} + X^{liq}_{MnO} + X^{liq}_{FeO} + X^{liq}_{CaO} + X^{liq}_{CoO} + X^{liq}_{NiO}$; the concentration of Si, $C^{liq}_{SiO_2} = X^{liq}_{SiO_2}$.

Mineral components. Mineral components are typically calculated using the numbers of "cations per formula unit," which can be derived from the "cation fractions" (just as for liquids), sometimes with consideration of charge balance constraints. The forsterite (Fo) content of olivine, for example, is often presented as Mg/(Mg+Fe), where Mg and Fe represent the number of cations per formula unit in olivine; because Fo is expressed as a ratio, it does not matter whether the formula is expressed as $(Mg,Fe)Si_{0.5}O_2$ or $(Mg,Fe)_2SiO_4$. This calculation is also numerically equivalent to $X_{MgO}{}^{ol}/(X_{MgO}{}^{ol}+X_{FeO}{}^{ol})$, where a term such as $X_{MgO}{}^{ol}$ represents the mole or cation fraction of MgO, just as is calculated for a liquid (Table 1). Similarly, the anorthite (An), albite (Ab) and orthoclase (Or) contents of plagioclase, can be represented as Ca/(Ca+N+K), Na/(Ca+Na+K) and K/(Ca+Na+K) respectively, and are numerically equivalent to $X_{CaO}{}^{pl}/(X_{CaO}{}^{pl}+X_{NaO0.5}{}^{pl}+X_{KO0.5}{}^{pl})$, $X_{NaO0.5}{}^{pl}/(X_{CaO}{}^{pl}+X_{NaO0.5}{}^{pl}+X_{KO0.5}{}^{pl})$ and $X_{KO0.5}{}^{pl}/(X_{CaO}{}^{pl}+X_{NaO0.5}{}^{pl}+X_{KO0.5}{}^{pl})$, where here, all X_i are cation fractions.

Pyroxene components can be calculated in a similar manner, but normative type methods are also employed, to handle charge-couple substitutions. In addition, instead of using a fixed number of cations, the cations in clinopyroxene are usually calculated on the basis of a fixed number of oxygen's (Table 2). The advantage here is that the number of cations can then be added together to test whether the analysis is valid. For example, if clinopyroxene cations are calculated on the basis of 6 oxygens per formula unit, then the sum of all cations should be 4. If the sum is very different from 4, then either the given composition is not (at least wholly) a pyroxene, or the analysis itself is in error. Because of the complexity of clinopyroxene compositions, component calculations are handled differently in different models; for this reason clinopyroxene components are discussed in conjunction with specific thermometers and barometers below.

Units and notation. It is now customary to report *P* in units of GPa, instead of kbar, while *T* units are commonly reported in either Kelvins (K) or degrees centigrade (°C). Because this review reproduces equations from earlier publications, and because unit conversions would in some cases require recalibration of regression coefficients, with some risk of introducing additional error, *P-T* units from original works are largely preserved; the conversions in any case are simple (10 kbar = 1 GPa; K = °C + 273.15). Additionally, since in geobarometry most pressures of interest occur within the highly convenient magnitude range of 0-10 kbar, new geobarometers are calibrated on a kbar scale, custom be damned.

For ease of calculation, all equations are presented using the same compositional notation throughout (see Tables 1-3). Terms such as $SiO_2{}^{liq}$ represent the wt% of SiO_2 (or some other oxide) in the liquid; terms such as X_i^j are either the mole or (nearly always, here) the cation fraction of *i* in phase *j*, the choice of which will be indicated as appropriate (and will be evident from oxides of Al or Na, for example, where for a mole fraction we write $X_{Al_2O_3}$ and X_{Na_2O}, and for a cation fraction we write $X_{AlO_{1.5}}$ and $X_{NaO_{1.5}}$). Terms such as NF and $C_{NM}{}^{liq}$ are calculated from cation fractions and derive from the activity model of Beattie (1993) (see Table 1). All mole and cation fractions are calculated on an anhydrous basis, from weight percent oxides that are not renormalized to 100%, even when hydrous. Compositional terms involving water are always in units of wt% H_2O.

"Glass" (or liquid) thermometers

The Helz and Thornber (1987) thermometer is simplicity itself, depending only upon the wt% of MgO in a liquid (MgO^{liq}): $T(°C) = 20.1MgO^{liq} + 1014$ °C. Their model was updated by Montierth et al. (1995; $T(°C) = 23.0MgO^{liq} + 1012$ °C), and Thornber et al. (2003). In spite of the simplicity and narrow calibration range, the Helz and Thornber (1987) and Montierth et

Downloaded from http://pubs.geoscienceworld.org/msa/rimg/article-pdf/69/1/61/2948053/61_Putirka.pdf
by University of California Berkeley Library user
on 16 March 2024

Downloaded from http://pubs.geoscienceworld.org/msa/rimg/article-pdf/69/1/61/2948053/61_Putirka.pdf
by University of California Berkeley Library user
on 16 March 2024

Table 2. Pyroxene calculations example part I. Calculation of pyroxenes on the basis of six oxygens, and orthopyroxene components.

	SiO_2	TiO_2	Al_2O_3	FeO	MnO	MgO	CaO	Na_2O	K_2O	Cr_2O_3
1) Opx wt%	55.7	0.03	1.88	13.82	0	27.7	1.47	0.44	0	0
2) Mol wt	60.08	79.9	101.96	71.85	70.94	40.3	56.08	61.98	94.2	152.0
3) mole prop	0.9271	0.0004	0.0184	0.1923	0.0000	0.6873	0.0262	0.0071	0	0
4) # of oxygens	2(0.9271)	2(0.0004)	3(0.0184)	0.1923	0.00	0.6873	0.0262	0.0071	0.00	3(0.00)
5) # of oxygens	1.8542	0.0008	0.0553	0.1923	0.0000	0.6873	0.0262	0.0071	0.0000	0.0000
6) sum of row 5	2.8233									
7) ORF	6/(oxy sum) =	2.1252								

Cations on the basis of 6 oxygens

	X^{opx}_{Si}	X^{opx}_{Ti}	X^{opx}_{Al}	X^{opx}_{Fe}	X^{opx}_{Mn}	X^{opx}_{Mg}	X^{opx}_{Ca}	X^{opx}_{Na}	X^{opx}_{K}	X^{opx}_{Cr}
8) cat/6 O	1.9703	0.0008	0.0784	0.4088	0	1.4607	0.0557	0.0302	0	0
9) cation sum	4.0048									

Orthopyroxene Components

	$X^{cpx}_{Al(IV)}$	$X^{cpx}_{Al(VI)}$	$X^{opx}_{NaAlSi_2O_6}$	$X^{opx}_{FmTiAlSiO_6}$	$X^{opx}_{CrAl_2SiO_6}$	$X^{opx}_{FmAl_2SiO_6}$	$X^{opx}_{CaFmSi_2O_6}$	$X^{opx}_{Fm_2Si_2O_6}$	total
10)	0.0297	0.0486	0.0302	0.0008	0.0000	0.0185	0.0557	0.8973	1.0024

To obtain row 8), the basis for *P-T* calculations involving pyroxenes (opx=orthopyroxene) first divide row 1) by row 2) to obtain row 3). To get row 4), multiply row 3) by the numbers of oxygens that occur in each formula unit, as indicated; results are shown in row 5). Row 6) shows the sum of row 5), and ORF, the "Oxygen Renormalization Factor", in row 7), is equal to the number of oxygens per mineral formula unit, divided by the sum shown in 6); in our case, we will calculate pyroxenes on the basis of six oxygens, yielding ORF = 2.1252. To obtain the numbers of cations on a six oxygen basis, as in row 8), multiply each entry in row 3) by the ORF and by the number of cations in each formula unit (so for SiO_2, X^{opx}_{Si} = (0.9271)(2.1252), and for Al_2O_3, X^{opx}_{Al} = (2)(0.0184)(2.1252)). Row 9) shows the sum of cations per six oxygens (per formula unit). For a "good" pyroxene analysis, this value should be, as in this case, close to the ideal value of 4, thus providing a test of the quality of a pyroxene analysis. Orthopyroxene components, in 10) are calculated from the cations in 8), using the following algorithm: $X^{opx}_{Al(IV)} = 2 - X^{opx}_{Si}$; $X^{opx}_{Al(VI)} = X^{opx}_{Al} - X^{opx}_{Al(IV)}$; $X^{opx}_{NaAlSi_2O_6} = X^{opx}_{Al(VI)}$ or X^{opx}_{Na}, whichever is less; $X^{opx}_{FmTiAlSiO_6} = X^{opx}_{Ti}$; $X^{opx}_{CrAl_2SiO_6} = X^{opx}_{Cr}$; $X^{opx}_{FmAl_2SiO_6} = X^{opx}_{Al(VI)} - X^{opx}_{NaAlSi_2O_6} - X^{opx}_{CrAl_2SiO_6}$; $X^{opx}_{CaFmSi_2O_6} = X^{opx}_{Ca}$; $X^{opx}_{Fm_2Si_2O_6} = [(X^{opx}_{Fe} + X^{opx}_{Mn} + X^{opx}_{Mg}) - X^{opx}_{FmTiAlSiO_6} - X^{opx}_{FmAl_2SiO_6} - X^{opx}_{CaFmSi_2O_6}]/2$. The sum of the opx components in row 10) should be close to 1.0.

al. (1995) thermometers work remarkably well. When predicting *T* for 1,536 olivine-saturated (± other phases) experimental data (Fig. 2), the models yield systematic error, but very high correlation coefficients (R = 0.91for both models), capturing 84% of experimental *T* variation (R^2 = 0.84). A simple linear correction to the Helz and Thornber (1987) model removes the systematic error, yielding a new model:

$$T(°C) = 26.3MgO^{liq} + 994.4\ °C \tag{13}$$

Equation (13) yields R^2 = 83 (R = 0.91) and a standard error of estimate (SEE) of ±71 °C (Fig. 2). Additional compositional terms can be added to reduce error further, yielding the following empirical expressions, one *P*-independent the other *P*-dependent,

$$T(°C) = 754 + 190.6[Mg\#] + 25.52[MgO^{liq}] + 9.585[FeO^{liq}] + 14.87[(Na_2O + K_2O)^{liq}] - 9.176[H_2O^{liq}] \tag{14}$$

$$T(°C) = 815.3 + 265.5[Mg\#^{liq}] + 15.37[MgO^{liq}] + 8.61[FeO^{liq}] + 6.646[(Na_2O + K_2O)^{liq}] + 39.16[P(GPa)] - 12.83[H_2O^{liq}] \tag{15}$$

where $Mg\#^{liq}$ is a molar ratio and the remaining terms are weight percent oxides in a liquid (or glass). In Equation (14), R^2 = 0.92 and SEE = 51 °C; in Equation (15) R^2 = 0.89 and SEE = 60 °C. Equations (13)-(15) are applicable to any volcanic rock saturated with olivine and any other collection of phases, over the following compositional and *P-T* range: *P* = 0.0001-14.4 GPa; *T* = 729-2000 °C; SiO_2 = 31.5-73.64 wt%; Na_2O+K_2O = 0-14.3 wt%; H_2O = 0-18.6 wt% (Fig. 2).

Yang et al. (1996) suggest an improvement to this type of geothermometer by requiring that additional phases be in equilibrium with the liquid, placing further constraints on compositional degrees of freedom. Their thermometer applies to liquids in equilibrium with olivine + plagioclase + clinopyroxene; a new equation similar to their equation 4 is:

$$T(°C) = -583 + 3141[X^{liq}_{SiO_2}] + 15779[X^{liq}_{Al_2O_3}] + 1338.6[X^{liq}_{MgO}] - 31440[X^{liq}_{SiO_2} \cdot X^{liq}_{Al_2O_3}] + 77.67[P(GPa)] \tag{16}$$

where terms such as $X_{MgO}{}^{liq}$ represent the mole fraction of MgO in the liquid. Equation (16) performs less well for liquids that are additionally saturated with other phases, such as spinel or other oxides, but for experiments where only liquid + olivine + plagioclase + clinopyroxene are reported, Equation (16) yields R^2 = 0.92 and SEE = ±19 °C (*n* = 73) for the calibration data and R^2 = 0.75 and SEE = 26 °C for 119 test data (Fig. 2).

Olivine-liquid equilibria

Tests for equilibrium. When using thermometers or barometers based on equilibrium constants, it is essential that equilibrium between the phases in question is approached, otherwise calculated *P-T* conditions have no meaning. Roeder and Emslie (1970) produced the first experiments designed to test whether olivine of a given forsterite (Fo) content might be in equilibrium with a liquid composition. Their landmark study of Fe-Mg partitioning between olivine and liquid showed that the equilibrium constant for the following reaction,

$$MgO^{ol} + FeO^{liq} = MgO^{liq} + FeO^{ol} \tag{17}$$

otherwise known as the Fe-Mg exchange coefficient, or $K_D(Fe\text{-}Mg)^{ol\text{-}liq} = [(X_{Fe}{}^{ol}X_{Mg}{}^{liq})/(X_{Mg}{}^{ol}X_{Fe}{}^{liq})]$ varies little with *T* or composition, and so is nearly constant at 0.30±0.03. Subsequent work has shown that $K_D(Fe\text{-}Mg)^{ol\text{-}liq}$ decreases with decreasing SiO_2 or increasing alkalis (Gee and Sack 1988), and increases with increased *P* (Herzberg and O'Hara 1998; Putirka 2005a) (Toplis (2005) calibrates all these effects). But the Roeder and Emslie (1970)

Downloaded from http://pubs.geoscienceworld.org/msa/rimg/article-pdf/69/1/61/2948053/61_Putirka.pdf
by University of California Berkeley Library user
on 16 March 2024

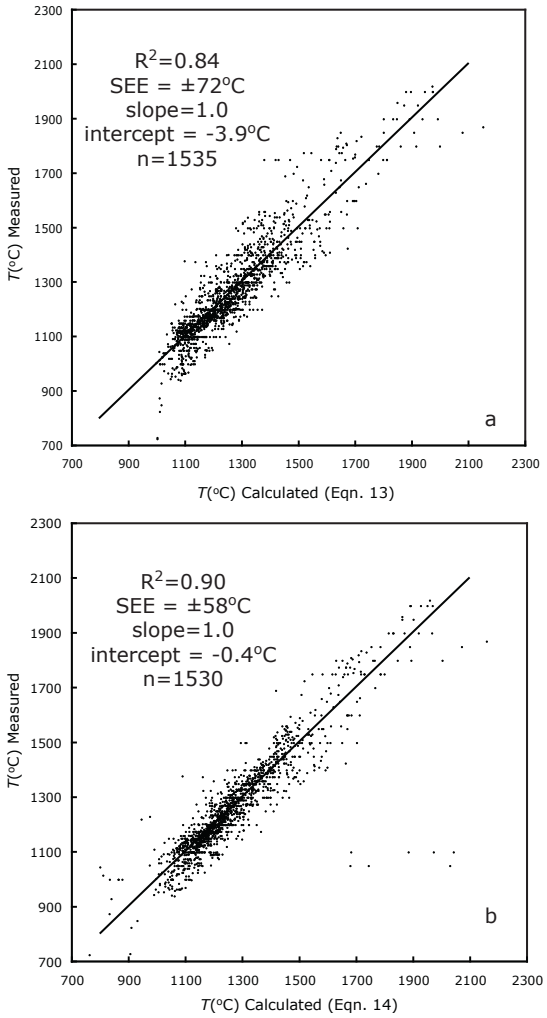

Figure 2. Calculated and measured temperatures are compared for the empirical glass geothermometers using: (a) Equation (13), (b) Equation (14), (c) Equation (15) and (d) Equation (16) from the text. In (a) – (c) all available data are used for calibration: Agee and Walker (1990), Agee and Draper (2004), Almeev et al. (2007), Arndt (1977), Baker and Eggler (1987), Baker et al. (1994), Barclay and Carmichael (2004), Bartels et al. (1991), Bender et al. (1978), Blatter and Carmichael (2001), Bulatov et al. (2002), Chen et al. (1982), Dann et al. (2001), Delano (1977), Di Carlo et al. (2006), Draper and Green (1997, 1999), Dunn and Sen (1994), Elkins and Grove (2003), Elkins et al. (2000, 2003, 2007), Falloon and Danyushevsky (2000), Falloon et al. (1997, 1999, 2001), Feig et al. (2006), Fram and Longhi (1992), Fuji and Bougault (1983), Gaetani and Grove (1998), Gee and Sack (1988), Grove and Beaty (1980), Grove and Bryan (1983), Grove et al. (1982, 1992, 1997, 2003), Grove and Juster (1989), Hesse and Grove (2003), Holbig and Grove (2008), Jurewicz et al. (1993), Juster et al. (1989), Kawamoto (1996), Kelemen et al. (1990), Kennedy et al. (1990), Kinzler and Grove (1985), Kinzler and Grove (1992a), Kinzler (1997), Kogi et al. (2005), Kogiso et al. (1998), Kogiso and Hirschmann (2001), Kushiro and Mysen (2002), Kushiro and Walter (1998), Laporte et al. (2004), Longhi (1995), Longhi (2002), Longhi and Pan (1988, 1989), Longhi et al. (1978), Maaloe (2004), Mahood and Baker (1986), McCoy and Lofgren (1999), McDade et al. (2003), Medard and Grove (2008), Medard et al. (2004), Meen (1987, 1990), Müntener et al. (2001), Mibe et al. (2005), Moore and Carmichael (1998), Morse et al. (2004), Müntener, et al. (2001), Musselwhite et al. (2006),

caption continued on facing page

Downloaded from http://pubs.geoscienceworld.org/msa/rimg/article-pdf/69/1/61/2948053/61_Putirka.pdf
by University of California Berkeley Library user
on 16 March 2024

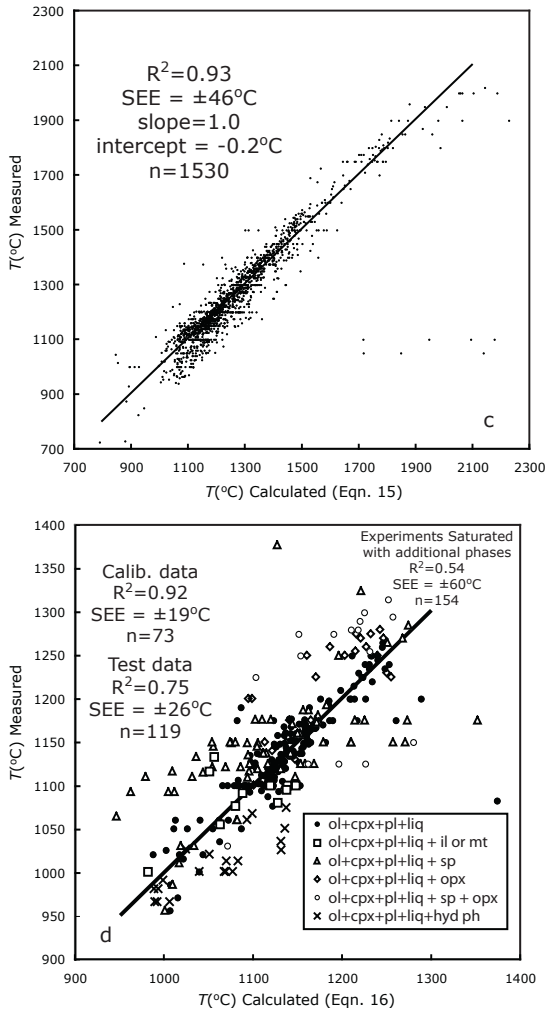

Figure 2. (continued) Parman et al. (1997), Parman and Grove (2004), Pichavant et al. (2002a,b), Pickering-Witter and Johnston (2000), Putirka (1998), Ratajeski et al. (2005), Rhodes et al. (1979b), Robinson et al. (1998), Sack et al. (1987), Salters and Longhi (1999), Scaillet and MacDonald (2003), Schwab and Johnston (2001), Scoates et al. (2006), Sisson and Grove (1993a.b), Stolper (1977), Stolper (1980), Takagi et al. (2005), Takahashi (1980), Taura et al. (1998), Thy et al. (2004), Tormey et al. (1987), Vander Auwera and Longhi (1994), Vander Auwera et al. (1998), Villiger et al. (2004), Wagner and Grove (1997, 1998), Walter (1998), Wasylenki et al. (2003), Xirouchakis et al. (2001), Yang et al. (1996). In (d) the calibration data are only the subset of experiments where liquid is in equilibrium with clinopyroxene (cpx), olivine (ol) and plagioclase (pl). In applying models with such restrictions, not only must all the relevant phases be present, but additional phases perhaps should also be absent, except for the addition of ilmenite or magnetite, Equation (16) yields poorer *T* estimates for liquids that in addition to cpx+liq+plag are also saturated with orthopyroxene (opx), spinel (sp) and a hydrous phase such as amphibole, or a fluid (fl). Calibration data are liquids saturated with cpx + ol + plag, and are from: Baker and Eggler (1987), Grove et al. (1992), Yang et al. (1996), Grove et al. (1997), and Feig et al. 2006). Test data are also saturated with cpx + ol + plag, and are from: Kennedy et al. (1990), Juster et al. (1989), Dunn and Sen (1994), Grove and Juster (1989), Grove and Bryan (1983), Bender et al. (1978), Baker et al. (1994), Thy et al. (2004), Medard et al. (2004), Morse et al. (2004), Pichavant et al. (2002), Mahood and Baker (1986), Meen (1990), Grove et al. (1982), Tormey et al. (1987), Almeev et al. (2007), Stolper (1980), Sisson and Grove (1993a,b), Di Carlo et al. (2006).

Downloaded from http://pubs.geoscienceworld.org/msa/rimg/article-pdf/69/1/61/2948053/61_Putirka.pdf
by University of California Berkeley Library user
on 16 March 2024

model, i.e., $K_D(\text{Fe-Mg})^{ol\text{-}liq} = 0.30$, is still valid for basaltic systems generally, at $P < 2$-3 GPa (1504 experiments yield $K_D(\text{Fe-Mg})^{ol\text{-}liq} = 0.299 \pm 0.053$).

J. Michael Rhodes (Dungan et al. 1978; Rhodes et al. 1979a) developed a highly elegant graphical means to apply such a test for equilibrium between olivine and a potential liquid by comparing $100{\cdot}\text{Mg\#}^{liq}$ vs. $100{\cdot}\text{Mg\#}^{ol}$ (where *ol* = olivine, and the $\text{Mg\#}^{ol} = \text{Fo} = \text{Mg}^{ol}/(\text{Mg}^{ol}+\text{Fe}^{ol})$; though technically calculated on the basis of cations, it is numerically equivalent to calculate Fo from $X_{\text{MgO}}{}^{ol}/(X_{\text{Mg}}{}^{ol} + X_{\text{FeO}}{}^{ol})$ as in Table 1). The Rhodes's diagram (Fig. 3) simultaneously tests for equilibrium while also displaying various forms of open system behavior to explain disequilibrium.

Thermometers. Hakli and Wright (1967) were probably the first to calibrate an olivine-liquid thermometer, in their case based on Ni partitioning. Their effort was updated by Leeman and Lindstrom (1978) and subsequently expanded to other phases (e.g., Petry et al. 1997; Canil 1999; Righter 2006). Unfortunately, the numbers of experiments reporting NiO are few. Tests using 67 experimental data with NiO analyses show that the model of Arndt (1977):

$$T(^\circ\text{C}) = \frac{10430}{\ln D_{\text{NiO}}^{ol\text{-}liq} + 4.79} - 273.15 \tag{18}$$

yields the least systematic error, but a disappointing SEE of ±108 °C—and recalibration is of little help.

Most recent interest in olivine thermometry has revolved about the partitioning of Mg between olivine and liquid, the first such calibration of which was by Roeder and Emslie (1970). Though apparently less appreciated than their calibration of $K_D(\text{Fe-Mg})^{ol\text{-}liq}$, their Figure 7 presents a highly elegant graphical thermometer that is still quite useful (see Putirka 2005a).

A recent review by Putirka et al. (2007) shows tests of olivine-liquid thermometers based on Mg partitioning. Of published models, that by Beattie (1993) is by far the superior. His equation, re-written here by combining terms, is:

$$T(^\circ\text{C}) = \frac{13603 + 4.943\times10^{-7}\left(P(\text{GPa})\times10^{9} - 10^{-5}\right)}{6.26 + 2\ln D_{\text{Mg}}^{ol/liq} + 2\ln[1.5(C_{NM}^{L})] + 2\ln[3(C_{\text{SiO}_2}^{L})] - NF} - 273.15 \tag{19}$$

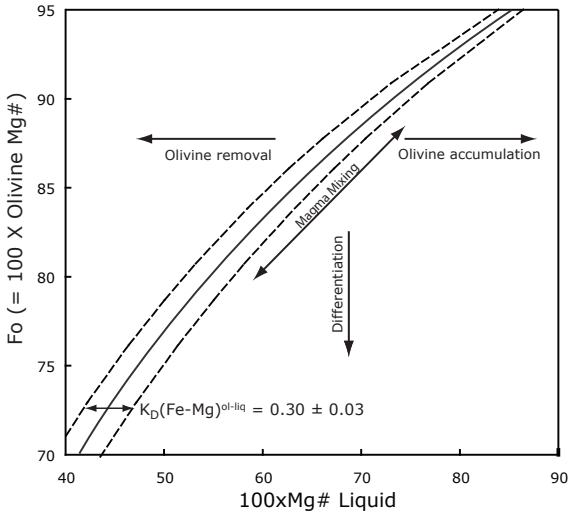

Figure 3. The Rhodes diagram yields tests of olivine-liquid equilibrium. If olivines are in equilibrium with coexisting whole rock or glass compositions, then the putative liquid-olivine pair should lie along the solid line, within some established error bound, here given as $K_D(\text{Fe-Mg})^{ol\text{-}liq} = 0.30 \pm 0.03$. An additional utility of this diagram is that deviations from equilibrium can be used to explain disequilibrium, as shown by arrows. For example, if the maximum forsterite (Fo) content of a suite of olivines from a given rock were in equilibrium with the whole rock, the vertical trend would (as indicated) be consistent with (though not uniquely attributable to) closed system differentiation.

Downloaded from http://pubs.geoscienceworld.org/msa/rimg/article-pdf/69/1/61/2948053/61_Putirka.pdf
by University of California Berkeley Library user
on 16 March 2024

where $= X^{ol}_{MgO}/X^{liq}_{MgO}$; other components are calculated as in Table 1. Interestingly, the Beattie (1993) model works just as well when $D^{ol/liq}_{Mg}$ is calculated from the liquid composition, so like the "glass" thermometers above, Equation (19) can be used absent an olivine composition (where the thermometer retrieves the T at which a liquid would become saturated with olivine at a given P). For this calculation, Beattie's (1993) expression for $D^{ol/liq}_{Mg}$ (ignoring terms for Ni and Co content in his Table 1) must be substituted into Equation (19):

$$D^{ol/liq}_{Mg} = \frac{0.666 - \left(-0.049X^{liq}_{MnO} + 0.027X^{liq}_{FeO}\right)}{X^{liq}_{MgO} + 0.259X^{liq}_{MnO} + 0.299X^{liq}_{FeO}} \tag{20}$$

The combination of Equations (19) and (20) provide remarkably accurate predictions for olivine equilibration temperatures, and if one is interested only in anhydrous systems, at $T < 1650$ °C, no new calibrations are needed. The Beattie (1993) model yields systematic error at very high temperatures and pressures, and Herzberg and O'Hara (2002) provide a correction to eliminate such error: $T(°C) = T(°C)^{B93}_{1bar} + 54P(GPa) - 2P(GPa)^2$, where $T(°C)^{B93}_{1bar}$ is the temperature from Beattie (1993), as in Equation (19), but calculated for the case that $P = 1$ bar.

The Beattie (1993) thermometer also overestimates T for experiments conducted on hydrous bulk compositions. To rectify this issue, and to integrate the pressure sensitivity noted by Herzberg and O'Hara (2002) into the thermodynamic regression equations, Putirka et al. (2007) presented several new equations, the best thermometers of which are Putirka et al.'s (2007) Equations (2) and (4), as reproduced here:

$$\ln D^{ol/liq}_{Mg} = -2.158 + 55.09\frac{P(GPa)}{T(°C)} - 6.213\times10^{-2}\left[H_2O^{liq}\right] + \frac{4430}{T(°C)} + 5.115\times10^{-2}\left[Na_2O^{liq} + K_2O^{liq}\right] \tag{21}$$

$$T(°C) = \{15294.6 + 1318.8P(GPa) + 2.4834[P(GPa)]^2\} / \{8.048 + 2.8352\ln D^{ol/liq}_{Mg} + 2.097\ln[1.5(C^{L}_{NM})] + 2.575\ln[3(C^{liq}_{SiO_2})] - 1.41NF + 0.222H_2O^{liq} + 0.5P(GPa)\} \tag{22}$$

In Equation (21) all compositional terms, such as Na_2O^{liq} and H_2O^{liq} are in wt%, except for $D^{ol/liq}_{Mg}$, which is a cation fraction ratio: $D^{ol/liq}_{Mg} = X^{ol}_{MgO} / X^{liq}_{MgO}$. All other components are calculated from cation fractions on an anhydrous basis, using the notation of Beattie (1993) (Table 1). Incidentally, tests conducted by Putirka et al. (2007) of the Sisson and Grove (1993b) thermometers showed that they did not perform well overall, with systematic errors for various systems, including those that are mafic or alkalic. However, their second equation: $\log_{10}[X^{ol}_{Mg} / (X^{liq}_{MgO}(X^{liq}_{SiO_2})^{0.5})] = 4129/T(K) - 2.082 + 0.0146[P(bar) - 1]/T(K)$, yields very good predictions for T for the CO_2-bearing experiments of Dasgupta et al. (2007) (regression of T^{meas} vs. T^{pred} yields $R^2 = 0.92$; SEE = 27 °C; $n = 21$), greatly outperforming models by Beattie (1993) and Putirka et al. (2007) for these special compositions. The Sisson and Grove (1993b) expression should thus be considered for peridotitic systems containing 2-25 wt% CO_2.

Generally, though, Equations (19) and (22) are by far the most precise (Fig. 4 and Putirka et al. (2007)). Equation (19) provides the best estimates for anhydrous conditions, and (22) the best estimates when water is present (H_2O ranges from 0-18.6% for the test data set). However, although these thermometers are calibrated using different experimental data, they yield similar errors using test data. This suggests that differences in their respective estimates reflect calibration error. In such a case, there is no disadvantage to using both equations and averaging the results, perhaps including the Sisson and Grove (1993b) model in the average, depending upon the extent to which the models are appropriate for the system in question.

Downloaded from http://pubs.geoscienceworld.org/msa/rimg/article-pdf/69/1/61/2948053/61_Putirka.pdf
by University of California Berkeley Library user
on 16 March 2024

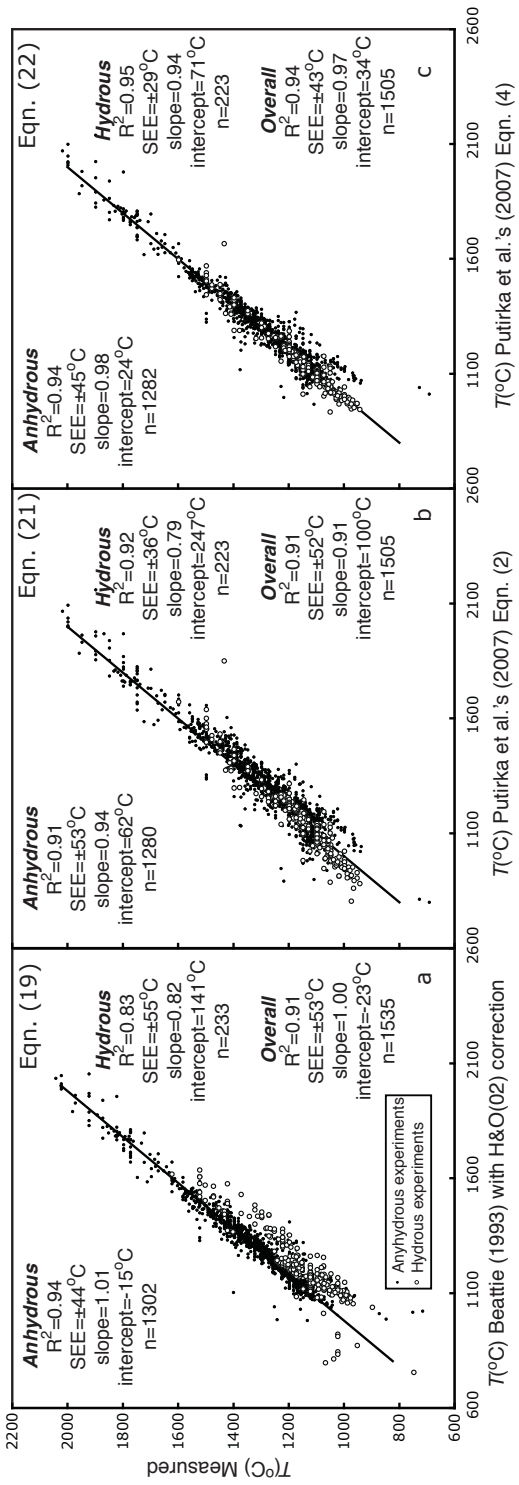

Figure 4. Tests of olivine-liquid thermometers based on the partitioning of Mg. In (a), the Beattie (1993) thermometer (Eqn. 19), using the Herzberg and O'Hara (2002) pressure correction; in (b), Putirka et al.'s (2007) Equation (2) (Eqn. 21); in (c), Putirka et al.'s (2007) Equation (4) (Eqn. 22). For anhydrous conditions, the Beattie (1993) model is best. If water is present, Putirka et al.'s (2007) Equation (4) is best. Data are as in Figures 2a-c.

Downloaded from http://pubs.geoscienceworld.org/msa/rimg/article-pdf/69/1/61/2948053/61_Putirka.pdf
by University of California Berkeley Library user
on 16 March 2024

Plagioclase- and alkali feldspar-liquid thermobarometers

Kudo and Weill (1970) presented the first plagioclase-liquid geothermometer. Given the common occurrence of plagioclase, it is unsurprising that plagioclase thermometry has since received much attention (e.g., Mathez 1973; Drake 1976; Loomis 1979; Glazner 1984; Ariskin and Barmina 1990; Marsh et al. 1990). Putirka's (2005b) review of plagioclase thermometers showed that the calibration of Sugawara (2001), and the MELTS/pMELTS models of Ghiorso et al. (2002) provided the most accurate predictors of T for existing models, but that these models fell short at low T (<1100 °C) and for hydrous systems. That review showed that improvements in T estimation could be obtained from a model that is simpler:

$$\frac{10^4}{T(\mathrm{K})} = 6.12 + 0.257\ln\left(\frac{X^{pl}_{An}}{X^{liq}_{\mathrm{CaO}}\left(X^{liq}_{\mathrm{AlO_{1.5}}}\right)^2\left(X^{liq}_{\mathrm{SiO_2}}\right)^2}\right) - 3.166\left(X^{liq}_{\mathrm{CaO}}\right) \quad (23)$$
$$-3.137\left(\frac{X^{liq}_{\mathrm{AlO_{1.5}}}}{X^{liq}_{\mathrm{AlO_{1.5}}} + X^{liq}_{\mathrm{SiO_2}}}\right) + 1.216\left(X^{pl}_{Ab}\right)^2$$
$$-2.475\times10^{-2}\left(P(\mathrm{kbar})\right) + 0.2166\left(H_2O^{liq}\right)$$

Here, $X^{pl}_{An} = X^{pl}_{\mathrm{CaO}} / \left(X^{pl}_{\mathrm{CaO}} + X^{pl}_{\mathrm{NaO_{0.5}}} X^{pl}_{\mathrm{KO_{0.5}}}\right)$ and $X^{pl}_{Ab} = X^{pl}_{\mathrm{NaO_{0.5}}} / \left(X^{pl}_{\mathrm{CaO}} + X^{pl}_{\mathrm{NaO_{0.5}}} X^{pl}_{\mathrm{KO_{0.5}}}\right)$, where mineral components (all X^i_j) are calculated as cation fractions; *liq* = liquid and *pl* = plagioclase. All liquid components except H_2O^{liq} are cation fractions, calculated on an anhydrous basis without renormalization of weight percent values (Table 1); H_2O^{liq} is the wt% of H_2O in the liquid phase. Equation (23) has performed well in other tests (Blundy et al. 2006), and new tests using data from the LEPR indicate high precision (Fig. 5a), but a global regression yields a ~6 °C improvement in the SEE (Fig. 5b):

$$\frac{10^4}{T(\mathrm{K})} = 6.4706 + 0.3128\ln\left(\frac{X^{pl}_{An}}{X^{liq}_{\mathrm{CaO}}\left(X^{liq}_{\mathrm{AlO_{1.5}}}\right)^2\left(X^{liq}_{\mathrm{SiO_2}}\right)^2}\right) - 8.103\left(X^{liq}_{\mathrm{SiO_2}}\right) \quad (24a)$$
$$+4.872\left(X^{liq}_{\mathrm{KO_{0.5}}}\right) + 1.5346\left(X^{pl}_{Ab}\right)^2 + 8.661\left(X^{liq}_{\mathrm{SiO_2}}\right)^2$$
$$-3.341\times10^{-2}\left(P(\mathrm{kbar})\right) + 0.18047\left(\mathrm{H_2O}^{liq}\right)$$

For alkali feldspars, T can be recovered from two new models based on albite-liquid equilibrium:

$$\frac{10^4}{T(\mathrm{K})} = 17.3 - 1.03\ln\left(\frac{X^{afs}_{Ab}}{X^{liq}_{\mathrm{NaO_{0.5}}} X^{liq}_{\mathrm{AlO_{1.5}}}\left(X^{liq}_{\mathrm{SiO_2}}\right)^3}\right) - 200\left(X^{liq}_{\mathrm{CaO}}\right) \quad (24b)$$
$$-2.42\left(X^{liq}_{\mathrm{NaO_{0.5}}}\right) - 29.8\left(X^{liq}_{\mathrm{KO_{.05}}}\right) + 13500\left(X^{liq}_{\mathrm{CaO}} - 0.0037\right)^2$$
$$-550\left(X^{liq}_{\mathrm{KO_{.05}}} - 0.056\right)\left(X^{liq}_{\mathrm{NaO_{.05}}} - 0.089\right) - 0.078P(\mathrm{kbar})$$

$$\frac{10^4}{T(\mathrm{K})} = 14.6 + 0.055\left(\mathrm{H_2O(wt\%)}\right) - 0.06P(\mathrm{kbar}) - 99.6\left(X^{liq}_{\mathrm{NaO_{0.5}}} X^{liq}_{\mathrm{AlO_{1.5}}}\right) \quad (24c)$$
$$-2313\left(X^{liq}_{\mathrm{CaO}} X^{liq}_{\mathrm{AlO_{1.5}}}\right) + 395\left(X^{liq}_{\mathrm{KO_{0.5}}} X^{liq}_{\mathrm{AlO_{1.5}}}\right) - 151\left(X^{liq}_{\mathrm{KO_{0.5}}} X^{liq}_{\mathrm{SiO_2}}\right)$$
$$+15037\left(X^{liq}_{\mathrm{CaO}}\right)^2$$

Downloaded from http://pubs.geoscienceworld.org/msa/rimg/article-pdf/69/1/61/2948053/61_Putirka.pdf
by University of California Berkeley Library user
on 16 March 2024

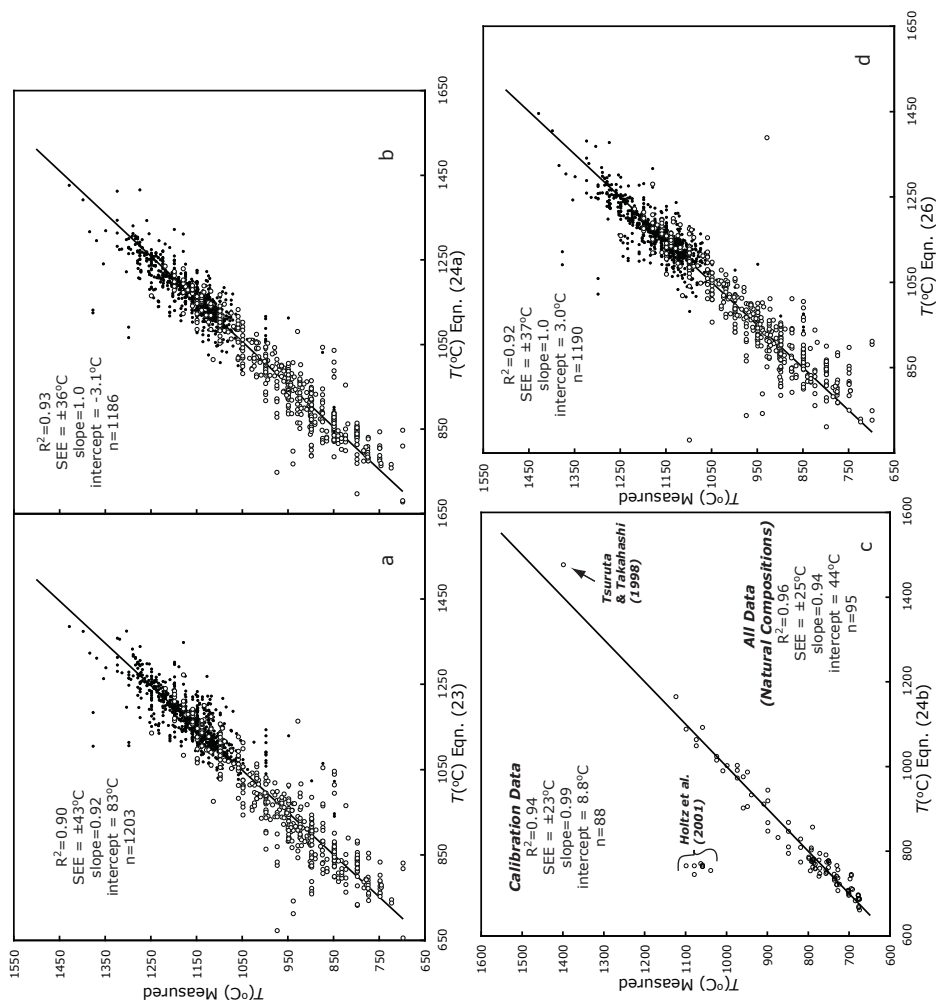

Figure 5. The plagioclase-liquid thermometer from (a) Putirka (2005b) (Eqn. 23), captures much of the variation of data from the Library of Experimental Phase Relations (LEPR); a global regression (b; Eqn. 24a) reduces error slightly; data are the subset of experiments in Figures 2a-c that are plagioclase saturated, plus data from Blundy (1997), Gerke and Kilinc (1992), Grove and Raudsepp (1978), Helz (1976), Holtz et al. (2005), Housh and Luhr (1991), Johnston (1986), Kawamoto et al. (1996), Koester et al. (2002), Martel et al. (1999), Liu et al. (1998, 2000), Miniti and Rutherford (2000), Panjasawatwong et al. (1995), Patino-Douce (1995), Patino-Douce and Beard (1995), Petermann and Hirschmann (2000), Petermann and Lundstrom (2006), Prouteau and Scaillet (2003), Rutherford et al. (1985), Scaillet and Evans (1999), Skjerlie and Patino-Douce (2002), Springer and Seck (1997), Whitaker et al. (2007). In (c), a thermometer based on alkali feldspar-liquid equilibrium (Eqn. 24b) reproduces T for experiments on natural compositions. This model was calibrated using experiments performed at $T < 1050$ °C from Gerke and Kilinc (1992), Koester et al. (2002), Patino-Douce (2005), Patino-Douce and Beard (1995), Patino-Douce and Harris (1998), Scaillet and MacDonald (2003). Test data are from these same studies, but performed at $T > 1050$ °C, with additional data from Holtz et al. (2001) and Tsuruta and Takahashi (1998). In (d), the temperature at which a liquid should become saturated with plagioclase (Eqn. (26)). If this plagioclase saturation temperature is in agreement with that calculated using Equations (23) or (24a), then an approach to equilibrium is indicated,

Downloaded from http://pubs.geoscienceworld.org/msa/rimg/article-pdf/69/1/61/2948053/61_Putirka.pdf
by University of California Berkeley Library user
on 16 March 2024

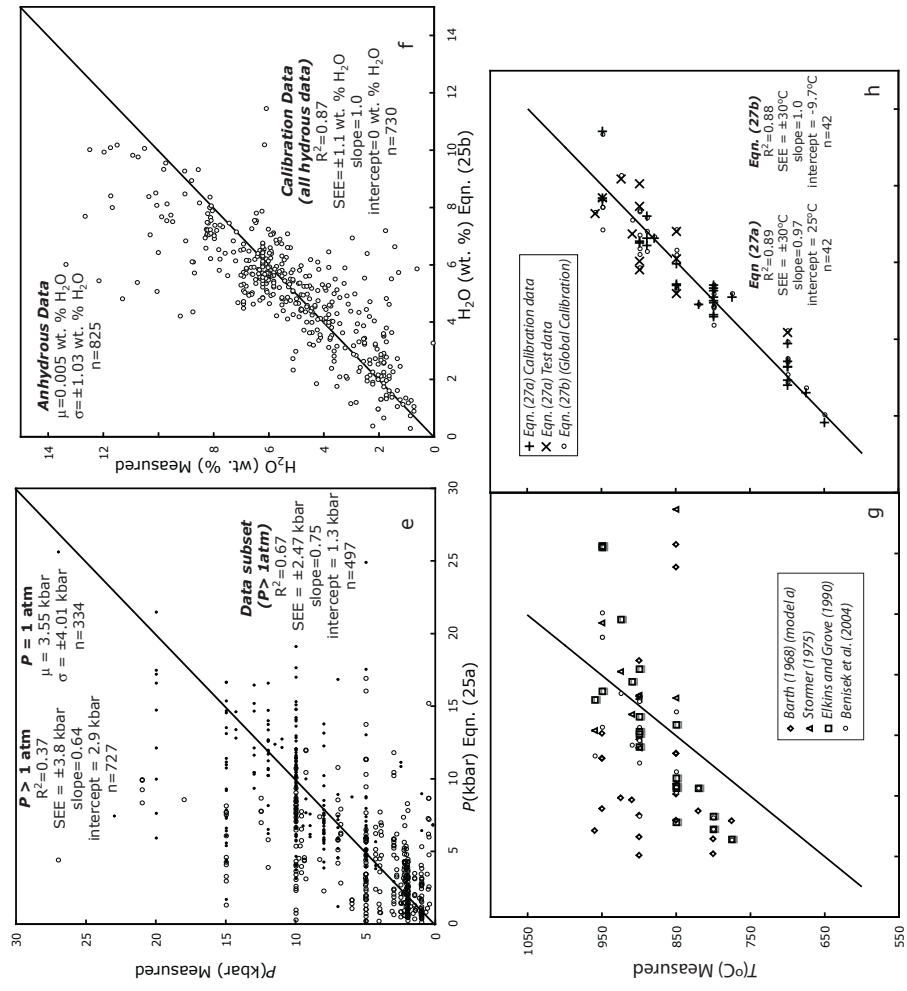

and calculated temperatures may be valid. In (e), the barometer of Putirka (2005b) yields mixed results. The model can predict P to within ± 3 kbar for just under half of all data, but fails to capture P variations for the LEPR data set as a whole; the barometer appears to be work well for a subset consisting of about 2/3 of data obtained at $P > 1$ atm, from: Vander Auwera and Longhi (1994), Vander Auwera et al. (1998), Baker and Eggler (1987), Bartels et al. (1991), Bender et al. (1978), Draper and Johnston (1992), Falloon et al. (1997, 1999), Fram and Longhi (1992), Grove et al. (1992), Housh and Luhr (1991), Kinzler and Grove (1992), Meen (1987), Panjasawatwong et al. (1995), Blatter and Carmichael (2001), Feig et al. (2006), Gardner et al. (1995), Holtz et al. (2005), Martel et al. (1999), Moore and Carmichael (1998), Patino-Douce and Beard (1995), Rutherford et al. (1985), Scaillet and Evans (1999), Sisson and Grove (1993a,b), Takagi et al. (2005), Whitaker et al. (2007). In (f), a new hygrometer (based on equation (H) of Putirka (2005b)) may be useful for systems with $H_2O < 9$ wt%; 1σ model error is <±1 wt%. In (g), existing two-feldspar models are tested using experimental data not used for their calibration; newer, more complex thermodynamic models, share the same systematic error as with Barth (1962, his model a). In (h), a new two-feldspar thermometer, calibrated and tested using the simpler approach of Barth (1951, 1962) with empirical compositional corrections so as to reduce model error.

Downloaded from http://pubs.geoscienceworld.org/msa/rimg/article-pdf/69/1/61/2948053/61_Putirka.pdf
by University of California Berkeley Library user
on 16 March 2024

In Equation (24b), all components are calculated as for (24a); afs = alkali feldspar. The thermometer is calibrated at $T < 1050$ °C, with a calibration error of ±23 °C. The model does not perform well for experimental data for the synthetic system of Holtz et al. (2005) and efforts to include these data result in strong systematic error at $T > 1050$ °C. Although nearly all experiments are hydrous, inclusion of an H_2O^{liq} term similarly yields problems when extrapolating to $T > 1050$ °C, and incorporation of the high T data does not solve this problem. Equation (24c) yields the saturation T for alkali feldspar and is independent of an alkali feldspar composition.

As a possible test for equilibrium, the Ab-An exchange ($K_D(\text{An-Ab})^{\text{afs-}liq} = X_{Ab}^{afs} X_{\text{AlO}_{1.5}}^{liq} X_{\text{CaO}}^{liq} / X_{An}^{afs} X_{\text{NaO}_{0.5}}^{liq} X_{\text{SiO}_2}^{liq}$) is nearly invariant with respect to T-P-H_2O, (but with a large standard deviation) yielding a mean of 0.27±0.18 for 60 experimental data. (The equilibrium constant for Or-Ab exchange is too dependent on T-P-H_2O to be useful in this regard).

Test results for the plagioclase barometer of Putirka (2005b),

$$P(\text{kbar}) = -42.2 + 4.94\times10^{-2}T(\text{K}) + 1.16\times10^{-2}T(\text{K})\ln\left(\frac{X_{Ab}^{pl}X_{\text{AlO}_{1.5}}^{liq}X_{\text{CaO}}^{liq}}{X_{An}^{pl}X_{\text{NaO}_{0.5}}^{liq}X_{\text{SiO}_2}^{liq}}\right) \quad (25a)$$
$$-382.3\left(X_{\text{SiO}_2}^{liq}\right)^2 + 514.2\left(X_{\text{SiO}_2}^{liq}\right)^3 - 19.6\ln\left(X_{Ab}^{pl}\right) - 139.8\left(X_{\text{CaO}}^{liq}\right)$$
$$+287.2\left(X_{\text{NaO}_{0.5}}^{liq}\right) + 163.9\left(X_{\text{KO}_{0.5}}^{liq}\right)$$

are not encouraging (Fig. 5). In the original model, data from Sack et al. (1987) and Sugawara (2001) were excluded due to the potential for Na loss from liquids when using an open furnace design (see Tormey et al. 1987). However, Na loss should not be an issue for experiments conducted in sealed glass tubes, internally heated pressure vessels or in piston-cylinder apparatus. Equation (25) predicts P to within <3 kbar for new data (not used by Putirka 2005b) from Falloon et al. (1997), Scaillet and Evans (1999), Feig et al. (2006) (1-2 kbar experiments), Holtz et al. (2005), Takagi et al. (2005), Almeev et al. (2007), and Whitaker et al. (2007). However, Equation (25) yields poor results for experiments from Meen (1990), Jurewicz et al. (1993), Patino-Douce and Beard (1995), Kawamoto et al. (1996), Patino-Douce and Harris (1998), Koester et al. (2002), Pichavant et al. (2002), Skjerlie et al. (2002), Prouteau et al. (2001), Medard et al. (2004), and Villiger et al. (2004). Worse still, no global correlation appears capable of rectifying these deficiencies, nor explaining why the model can perform well for some data subsets but not for others. Indeed, with some irony, the equilibrium constant for An-Ab exchange, might be more useful as a test for equilibrium, because although it clearly varies with T, P and H_2O (e.g., Hamada and Fuji 2007), the values are normally distributed, and when divided over two temperature intervals yield $K_D(\text{An-Ab})^{pl\text{-}liq} = X_{Ab}^{pl}X_{\text{AlO}_{1.5}}^{liq}X_{\text{CaO}}^{liq} / X_{An}^{pl}X_{\text{NaO}_{0.5}}^{liq}X_{\text{SiO}_2}^{liq} = 0.10\pm0.05$ at $T <$ 1050 °C ($n = 390$; mostly hydrous), and 0.27±0.11 for $T \geq 1050$ °C ($n = 908$). New experiments, designed for the purpose of testing or developing a plagioclase-liquid barometer are needed. At best, the plagioclase barometer cannot be recommended for any other than natural compositions very similar to experimentally studied compositions where the model performs well.

While the status of plagioclase-liquid barometry is firmly in doubt, plagioclase-liquid equilibrium might be useful as a hygrometer, at least if T is well known. Equation (H) of Putirka (2005b) tends to over-predict water contents for the LEPR-derived data set, but a global calibration yields:

$$H_2O(\text{wt\%}) = 25.95 - 0.0032T(^\circ\text{C})\ln\left(\frac{X_{An}^{pl}}{X_{\text{CaO}}^{liq}\left(X_{\text{AlO}_{1.5}}^{liq}\right)^2\left(X_{\text{SiO}_2}^{liq}\right)^2}\right) \quad (25b)$$
$$-18.9\left(X_{\text{KO}_{0.5}}^{liq}\right) + 14.5\left(X_{\text{MgO}}^{liq}\right) - 40.3\left(X_{\text{CaO}}^{liq}\right) + 5.7\left(X_{An}^{pl}\right)^2 + 0.108P(\text{kbar})$$

Downloaded from http://pubs.geoscienceworld.org/msa/rimg/article-pdf/69/1/61/2948053/61_Putirka.pdf
by University of California Berkeley Library user
on 16 March 2024

Equation (25b) yields water contents to within ±1.1 wt% H_2O for 730 hydrous experimental data, and recovers a mean H_2O content of 0.04±1.0 wt% for 825 anhydrous compositions not used for regression analysis (Fig. 5). Of course, Equation (25b) is something of a rearrangement of Equation (24), so as expected, estimates of water content are highly sensitive to T: just a ±38 °C error in T (~1.3σ) translates to a ±1.0 wt% error in H_2O.

As a test for plagioclase-liquid equilibrium, T from Equations (23) or (24a) can be compared to the T required for a liquid to reach plagioclase saturation. The Putirka (2005b) model predicts T to within ±48 °C for the global LEPR data set; a global regression of this data yields a 10 °C improvement in precision (Fig. 5c):

$$\frac{10^4}{T(\mathrm{K})} = 10.86 - 9.7654\left(X_{\mathrm{SiO_2}}^{liq}\right) + 4.241\left(X_{\mathrm{CaO}}^{liq}\right) - 55.56\left(X_{\mathrm{CaO}}^{liq} X_{\mathrm{AlO_{1.5}}}^{liq}\right) \quad (26)$$
$$+37.50\left(X_{\mathrm{KO_{0.5}}}^{liq} X_{\mathrm{AlO_{1.5}}}^{liq}\right) + 11.206\left(X_{\mathrm{SiO_2}}^{liq}\right)^3$$
$$-3.151\times10^{-2}\left(P(\mathrm{kbar})\right) + 0.1709\left(\mathrm{H_2O}^{liq}\right)$$

Equation (26) yields the temperature at which plagioclase should crystallize from a silicate liquid at a given P.

Two-feldspar thermometers

Thomas W. Barth, with some fairness, could be said to be the father of modern geothermobarometry. Barth (1934) first suggested that the relative solution of albite (Ab; $NaAlSi_3O_8$) into plagioclase and alkali feldspar could be formulated as an analytic geothermometer, and he followed his own suggestion with several calibrations (Barth 1951, 1962, 1968). Stormer (1975) presented the first major revision of the two-feldspar thermometer. In Barth's (1951) original formulation, he assumed that albite solutions followed Henry's Law, i.e., that the activity of a component in a dilute solution varies linearly with composition. Stormer (1975) illustrated some "serious deficiencies" in the Barth (1962) model, at least insofar as when one desires to predict the activity of albite. Intervening years have seen the development of additional thermodynamic models, exhibiting increasing complexity (e.g., Whitney and Stormer 1977; Powell and Powell 1977; Fuhrman and Lindsley 1988; Elkins and Grove 1990; Benisek et al. 2004). These efforts, though, have not demonstrated that more complex expressions yield better thermometers. Ever since 1934, calibration efforts have been hampered by a lack of experimental data, and there are probably more published pages devoted to feldspar thermodynamic modeling than there are experimental observations; in the latest model (Benisek et al. 2004), the number of adjustable parameters (21) is more than half the total of modern experimental observations.

Here, tests and new calibrations are performed using 41 experimental data from Elkins and Grove (1990), Gerke and Kilinc (1992), Patino-Douce and Beard (1995), Patino-Douce and Harris (1998), Koester et al. (2002), Patino-Douce (2005) and Auzanneau et al. (2006). As a departure, compositions of experiments are not "adjusted" as was done by Furhman and Lindsley (1988) and Elkins and Grove (1990). In those studies, experimental input data were modified so as to minimize the residuals on parameter estimates in least squares analysis. A problem, though, is that there is no clear path by which to "adjust" the compositions of natural samples, or other experimental data that might be used for test purposes. The issue is not trivial because T estimates are highly sensitive to even small changes in X_{Ab}, X_{An} and X_{Or}. In the event, it is unclear that such adjustments are required to produce a reliable thermometer.

In spite of nearly four decades of thermodynamic modeling, our most complex efforts barely improve upon Barth's (1962) simple partitioning model (his Equation a). Indeed, Barth's (1951) original approach, though seemingly lost among more recent thermodynamic models,

Downloaded from http://pubs.geoscienceworld.org/msa/rimg/article-pdf/69/1/61/2948053/61_Putirka.pdf
by University of California Berkeley Library user
on 16 March 2024

provides a remarkably precise (new) thermometer, when just a few empirical corrections are added:

$$\frac{10^4}{T(^\circ\text{C})} = 9.8 - 0.098P(\text{kbar}) - 2.46\ln\left(\frac{X_{Ab}^{afs}}{X_{Ab}^{plag}}\right) - 14.2\left(X_{\text{Si}}^{afs}\right) + 423\left(X_{\text{Ca}}^{afs}\right) \quad (27a)$$
$$-2.42\ln\left(X_{An}^{afs}\right) - 11.4\left(X_{An}^{plag}X_{Ab}^{pl}\right)$$

$$T(^\circ\text{C}) = \frac{-442 - 3.72P(\text{kbar})}{-0.11 + 0.1\ln\left(\frac{X_{Ab}^{afs}}{X_{Ab}^{pl}}\right) - 3.27\left(X_{An}^{afs}\right) + 0.098\ln\left(X_{An}^{afs}\right) + 0.52\left(X_{An}^{plag}X_{Ab}^{pl}\right)} \quad (27b)$$

The term $X_{\text{Si}}^{\text{afs}}$ is the cation fraction of Si in alkali feldspar, which is calculated in the same way as $X_{SiO_2}^{liq}$. Equation (27a) was calibrated from 30 of the 41 experimental data, using all data from Elkins and Grove (1990) except A″1, the sole observation from Patino-Douce (2005), all data from Patino-Douce and Harris (1998) except APD-624, samples APD570, APD571 and APD547 from Patino-Douce and Beard (1995), and sample 13-89-3 from Gerke and Kilinc (1992). Remaining data and data from Koester et al. (2002) and Auzanneau et al. (2006) were reserved for test purposes. Equation (27a) recovers T for the calibration data to ±23 °C, and ±44 °C for the test data. Equation (27b) represents a global calibration from all 41 experimental observations and recovers T to ±30 °C; these models, though much simpler than recent models, also lack the systematic error of recent efforts.

Orthopyroxene and orthopyroxene-liquid thermobarometers

Tests for equilibrium. As with olivine, the Rhodes' diagram can be used to test for equilibrium for orthopyroxene: 785 experimental data yield $K_{\text{D}}(\text{Fe-Mg})^{opx\text{-}liq} = 0.29\pm0.06$ (where *opx* = orthopyroxene). The value is independent of P or T, but decreases slightly with increased silica contents, where $K_{\text{D}}(\text{Fe-Mg})^{opx\text{-}liq} = 0.4805 - 0.3733X_{\text{Si}}^{liq}$ (X_{Si}^{liq} is the cation fraction of SiO_2 in the equilibrium liquid).

Calculation of orthopyroxene components. All liquid components are based on cation fractions, as illustrated in Table 1. All orthopyroxene components are based on the numbers of cations calculated on a 6-oxygen basis (Table 2). The usefulness of this procedure is that it leads easily to stoichiometric components, and the sum of such cations (ideally 4.0) yields a test for the quality of orthopyroxene analyses. Before investigating geothermobarometers, it is important to understand how certain components are partitioned into orthopyroxene. For example, how is Al charge balanced in orthopyroxene? As a Ca-Tschermak component, $CaAl_2SiO_6$? Or as $FmAl_2SiO_6$ (where Fm = Fe+Mg)? Various such components likely exist, but to write equilibria involving orthopyroxene there is some advantage to understanding which, if any, are dominant. Longhi (1976) and Thompson (1982) show how mixing trajectories can be used to make such identifications. Experimental orthopyroxenes are shown in Figure 6, with end member components calculated using Thompson's (1982) linear algebra approach and the end members: Fm_6O_6, $Ca_2Si_2O_6$, $Na_4Si_2O_6$, Ti_3O_6, Si_3O_6, Al_4O_6 and Cr_4O_6, which are projected onto the triangle Si_3O_6 - Al_4O_6 - Fm_6O_6 (Fig. 6). This projection shows that the dominant mechanism by which Al is incorporated into orthopyroxene is as $FmAl_2SiO_6$. The algorithm used to calculate orthopyroxene for thermobarometry is based on a normative scheme similar to that use for clinopyroxene (Table 2).

Thermometers and barometers. Beattie (1993) appears to present the only thermometer based on orthopyroxene-liquid equilibria. This model works well for some compositions, but over-predicts T for hydrous and low-T, nominally anhydrous compositions (Fig. 7). Two new thermometers rectify these problems:

Downloaded from http://pubs.geoscienceworld.org/msa/rimg/article-pdf/69/1/61/2948053/61_Putirka.pdf
by University of California Berkeley Library user
on 16 March 2024

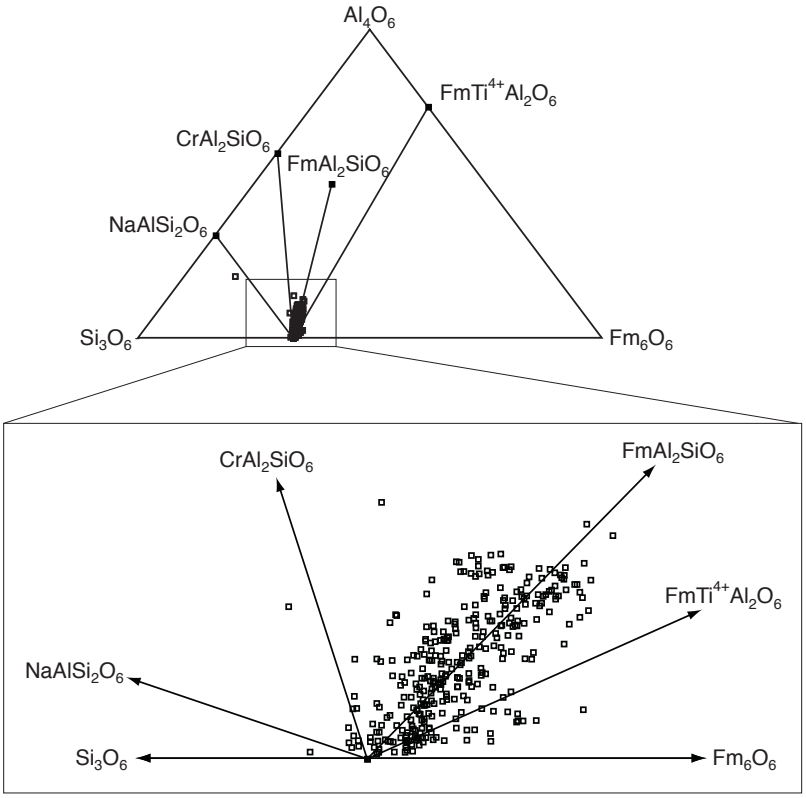

Figure 6. Experimental orthopyroxene compositions are re-cast as various oxide end members using Thompson's (1982) algebraic approach: Fm_6O_6, $Ca_2Si_2O_6$, $Na_4Si_2O_6$, Ti_3O_6, Si_3O_6, Al_4O_6 and Cr_4O_6. These end-member components are projected onto the triangle Si_3O_6 - Al_4O_6 - Fm_6O_6 (upper figure) (Fm = Fe+Mg); the data are concentrated at the base of this triangle, of which a magnified region is shown (lower figure). The projection shows that the dominant mixing vector for Al is toward the component $FmAl_2SiO_6$.

$$\frac{10^4}{T(^\circ\mathrm{C})} = 4.07 - 0.329[P(\mathrm{GPa})] + 0.12[\mathrm{H_2O}^{liq}] \tag{28a}$$
$$+0.567\ln\left[\frac{X^{opx}_{\mathrm{Fm_2Si_2O_6}}}{\left(X^{liq}_{\mathrm{SiO_2}}\right)^2\left(X^{liq}_{\mathrm{FeO}} + X^{liq}_{\mathrm{MnO}} + X^{liq}_{\mathrm{MgO}}\right)^2}\right]$$
$$-3.06[X^{liq}_{\mathrm{MgO}}] - 6.17[X^{liq}_{\mathrm{KO_{0.5}}}] + 1.89[Mg\#^{liq}] + 2.57[X^{opx}_{\mathrm{Fe}}]$$

$$T(^\circ\mathrm{C}) = \frac{5573.8 + 587.9P(\mathrm{GPa}) - 61[P(\mathrm{GPa})]^2}{5.3 - 0.633\ln\left(Mg\#^{liq}\right) - 3.97\left(C^{L}_{NM}\right) + 0.06NF + 24.7\left(X^{liq}_{\mathrm{CaO}}\right)^2 + 0.081\mathrm{H_2O}^{liq} + 0.156P(\mathrm{GPa})} \tag{28b}$$

For Equation (28a), all components are calculated as in Tables 1 and 2. The term $X^{opx}_{Fm_2Si_2O_6}$ is the mole fraction of $Fm_2Si_2O_6$ (or enstatite + ferrosilite, EnFs) as calculated in Table 2, where Fm = Fe + Mn + Mg; terms such as X^{opx}_{Fe} are the number of cations of the indicated element (in this case Fe) in opx, when calculated on a 6 oxygen basis (Table 2). Equation (28b) uses only liquid components to calculate the T at which a liquid should become saturated with orthopyroxene. Equation (28a) was calibrated and tested using only those experimental data

Downloaded from http://pubs.geoscienceworld.org/msa/rimg/article-pdf/69/1/61/2948053/61_Putirka.pdf
by University of California Berkeley Library user
on 16 March 2024

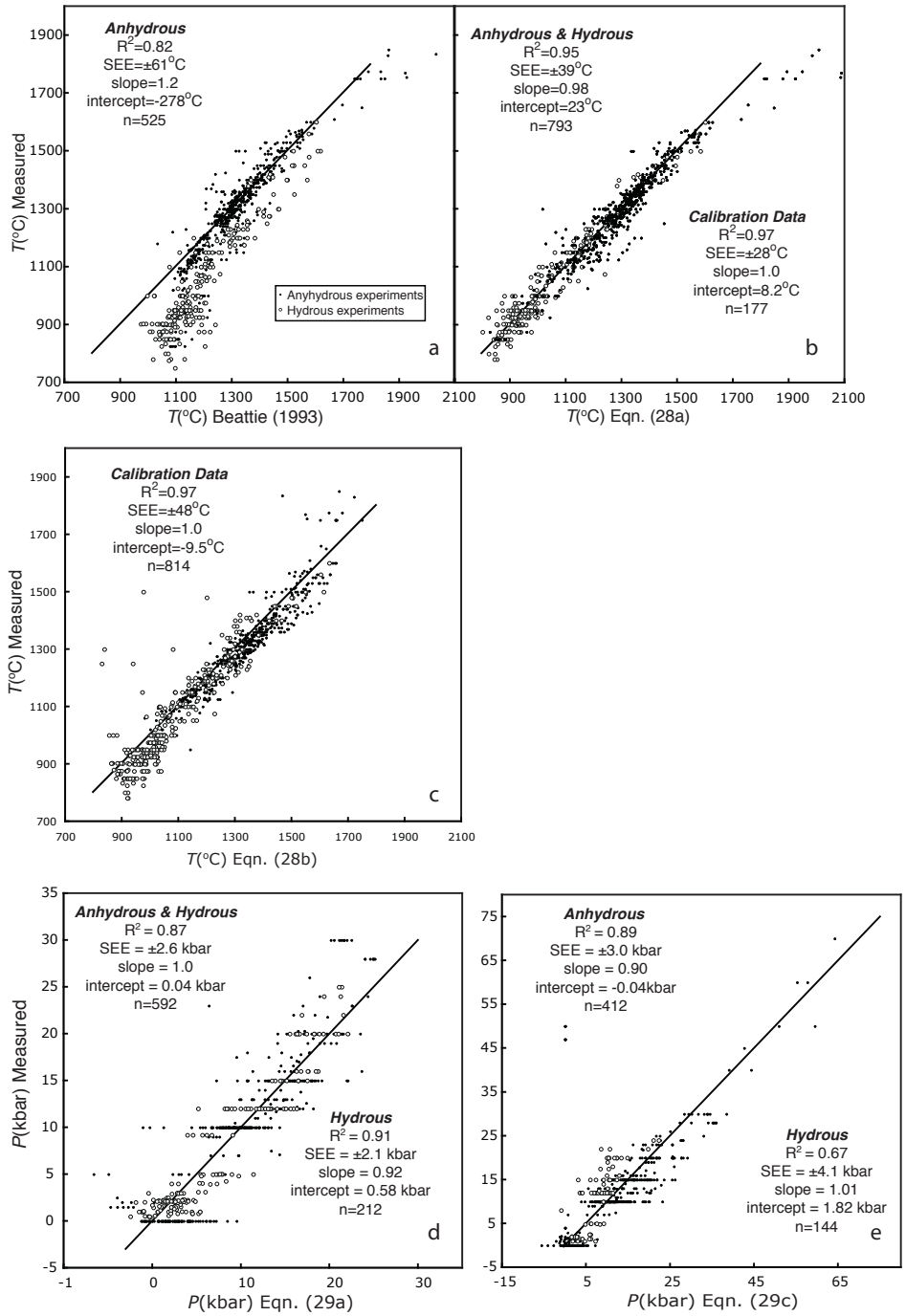

Figure 7. *caption on facing page*

Downloaded from http://pubs.geoscienceworld.org/msa/rimg/article-pdf/69/1/61/2948053/61_Putirka.pdf
by University of California Berkeley Library user
on 16 March 2024

whose orthopyroxenes had cations sums in the range 3.97-4.03. The expression recovers T for the calibration data to ±26 °C (slope and intercept are 0.996 and 5.17 °C; $R^2 = 0.98$; $n = 148$), and to ±41 °C for the test data (slope and intercept are 0.985 and 15.3 °C; $R^2 = 0.95$; $n = 770$). The range of applicability for (28a) is: T = 750-1600 °C; P = 0.0001-11.0 GPa; SiO_2 = 33-77 wt%; H_2O = 0-14.2 wt%. Equation (28b) has a similar range of applicability, and is the result of a global non-linear regression.

Wood (1974) was one of the first to calibrate the Al content in orthopyroxene as a barometer. His Al-in-orthopyroxene model was restricted to rocks in equilibrium with garnet. However, orthopyroxene barometry need not be restricted to such equilibria. The $FmAl_2SiO_6$ component increases slightly with increased P between 1 atm and 0.5 GPa. And as with clinopyroxene, equilibria involving a jadeite-like component $NaAlSi_2O_6$ (or Jd) shows a steep slope when plotted against P/T. Barometers calibrated using $NaAlSi_2O_6$ or $FmAl_2SiO_6$ yield errors of ca. ±2.5-3.0 GPa, and potentially useful expressions include:

$$P(\text{kbar}) = -13.97 + 0.0129T(^\circ\text{C}) + 0.001416T(^\circ\text{C})\ \ln\left[\frac{X^{opx}_{NaAlSi_2O_6}}{X^{liq}_{NaO_{0.5}} X^{liq}_{AlO_{1.5}} \left(X^{liq}_{SiO_2}\right)^2}\right] \qquad (29a)$$
$$-19.64(X^{liq}_{SiO_2}) + 47.49(X^{liq}_{MgO}) + 6.99(X^{opx}_{Fe})$$
$$+37.37\left(X^{opx}_{FmAl_2SiO_6}\right) + 0.748(H_2O^{liq}) + 79.67(X^{liq}_{NaO_{0.5}} + X^{liq}_{KO_{0.5}})$$

$$P(\text{kbar}) = 1.788 + 0.0375T(^\circ\text{C}) + 1.295\times10^{-3}T(^\circ\text{C})\ln\left[\frac{X^{opx}_{FmAl_2SiO_6}}{X^{liq}_{FmO}\left(X^{liq}_{AlO_{1.5}}\right)^2 X^{liq}_{SiO_2}}\right] \qquad (29b)$$
$$-33.42\left(X^{liq}_{AlO_{1.5}}\right) + 9.795\left(Mg\#^{liq}\right) + 36.08\left(X^{liq}_{NaO_{0.5}} + X^{liq}_{KO_{0.5}}\right) + 0.784\left(H_2O^{liq}\right)$$
$$-26.2\left(X^{opx}_{Si}\right) + 14.21\left(X^{opx}_{Fe}\right)$$

$$P(\text{kbar}) = 2064 + 0.321T(^\circ\text{C}) - 343.4\ln T(^\circ\text{C}) + 31.52\left(X^{opx}_{Al}\right) - 12.28\left(X^{opx}_{Ca}\right) \qquad (29c)$$
$$-290\left(X^{opx}_{Cr}\right) + 1.54\ln\left(X^{opx}_{Cr}\right) - 177.2\left(X^{opx}_{Al} - 0.1715\right)^2$$
$$-372\left(X^{opx}_{Al} - 0.1715\right)\left(X^{opx}_{Ca} - 0.0736\right)$$

The term X_{Al}^{opx} is the total number of Al atoms in orthopyroxene when cations are calculated on a 6 oxygen basis (equal to Al(IV) + Al(VI)). Equations (29a,b) derive from global calibrations of 592 experiments. Equation (29a) yields $R^2 = 0.83$ and SEE = ±2.6 kbar; both models underestimate P at $P > 30$ kbar. However, P for 1 atm data, even though included in the regression, yield a mean of 2.2±2.3 kbar, and their exclusion from the regression does not improve accuracy at $P > 0.001$ kbar. Remarkably, though, P is more accurately recovered for hydrous data,

Figure 7. (on facing page) Orthopyroxene-liquid thermometers of (a) Beattie (1993) and (b) and (c) this study are tested using orthopyroxene saturated experiments from data in Figures 2a-c, and from Barnes (1986), Keshav et al. (2004), Schmidt et al. (2004), Hammer et al. (2002), Holtz et al. (2005), Martel et al. (1999), Naney (1983), Prouteau and Scaillet (2003), Springer and Seck (1997). In (d) and (e) are tests of potential orthopyroxene barometers, based on global regressions of experimental data. For (d) the new barometer is based on Jd-liq equilibrium and was calibrated using data from Baker and Eggler (1987), Bartels et al. (1991), Elkins-Tanton et al. (2000, 2003), Falloon and Danyushevsky (2000), Falloon et al. (2001), Gaetani and Grove (1998), Grove and Juster (1989), Holbig and Grove (2007), Kinzler and Grove (1992), Kinzler (1997), Moore and Carmichael (1998), Ratajeski et al. (2005), and Wagner and Grove (1997, 1998). Equation (29c) (e) was derived from a global regression, using only orthopyroxene components as independent variables.

Downloaded from http://pubs.geoscienceworld.org/msa/rimg/article-pdf/69/1/61/2948053/61_Putirka.pdf
by University of California Berkeley Library user
on 16 March 2024

yielding a respectable $R^2 = 0.91$ and SEE ±2.1 kbar—perhaps reflecting more rapid orthopyroxene equilibration when H_2O is present. Because it is sometimes useful to calculate *P* when an equilibrium liquid is unavailable (see Nimis 1995), Equation (29c) was calibrated, using data from Longhi and Pan (1988), Grove and Juster (1989), Bartels et al. (1991), Kinzler and Grove (1992) Kinzler (1997), Wagner and Grove (1998), Walter (1998), Falloon et al. (1997, 1999), Blatter and Carmichael (2001), Gaetani and Grove (1998). The model recovers pressure for the calibration data with a $R^2 = 0.93$ and an SEE of ±2.5 kbar. Equation (29c) exhibits much less systematic error to 70 kbar for anhydrous data, but at the cost of systematic error for hydrous data; predicted pressures for a global dataset ($n = 556$) yield $R^2 = 0.84$ and an SEE of ±3.6 kbar; statistics for hydrous and anhydrous data are shown in Figure 7.

Clinopyroxene and clinopyroxene-liquid thermobarometers

Davis and Boyd (1966) introduced the first pyroxene thermometer, a formulation that requires equilibrium between clino- and orthopyroxene. The two-pyroxene approach has since received much attention, but few volcanic rocks precipitate both ortho- and clino-pyroxene phenocrysts, which limits its usefulness to volcanic systems. For this reason, thermometers and barometers were eventually developed using clinopyroxene compositions alone (Nimis 1995; Nimis and Ulmer 1998; Nimis and Taylor 2000), or clinopyroxene-liquid equilibria (Putirka et al. 1996, 2003).

Calculation of clinopyroxene components. For the models that follow, all liquid components are cation fractions, calculated on an anhydrous basis, without renormalization of wt% values (Table 1). For both the Nimis and Putirka et al. models, clinopyroxene components are based on the numbers of cations on a 6 oxygen basis. As with orthopyroxene, a "good" clinopyroxene analysis has a cation sum very close to 4. Indeed, Nimis (1995) uses cation fractions that are normalized to 4 (which can be achieved by simply multiplying cation fractions by 4). In Putirka et al. (1996, 2003, and below), cation fractions are never renormalized, and the sum is used to check for the validity of a given clinopyroxene analysis. Clinopyroxene components, such as jadeite (Jd), diopside + hedenbergite, (DiHd), and enstatite + ferrosilite (EnFs) are calculated using a normative procedure of Putirka et al. (2003); Nimis (1995) makes direct use of clinopyroxene cations calculated on a 6-oxygen basis (Table 3).

Thermometers and barometers. The highest precision and least systematic error for existing clinopyroxene barometers is Putirka et al. (1996) for anhydrous systems and Putirka et al. (2003) for those that are hydrous (Fig. 8). The Nimis (1995) model contains stronger systematic error, for both anhydrous and hydrous systems (see below). However, the Nimis (1995) model is better than Nimis (1999) (even though Nimis (1999) included corrections for thermal expansion) and Putirka et al. (1996, 2003) in recovering *P* for 1 atm data. For Putirka et al. (1996, 2003), except for 1 atm experiments from Grove and Juster (1989), most all other 1 atm experiments yield high *P* estimates, ca. 2-3 kbar (Fig. 8). And, as with other equilibria, the problem is not solved by adding 1 atm data to regression models. The problems of open furnace experiments have been discussed relative to plagioclase and are relevant here: volatile losses of Na (Tormey et al. 1987) can lead to systematically high *P* estimates (Putirka et al. 1996, 2003). However, although the problem is apparently obviated by the Nimis (1995) approach, which depends only upon clinopyroxene compositions, the Nimis (1995) model also yields anomalously low *P* estimates for high-*P* experiments. For example, the Putirka et al. (2003) barometer yields a mean value μ of 9.5 kbar for 184 experiments equilibrated at 10 kbar, compared to μ = 6.4 kbar for Nimis (1995); for 99 experiments equilibrated at 15 kbar, Putirka et al. (2003) yields μ = 14.5 kbar, compared to μ = 11.7 kbar for Nimis (1995). This is not to say that the Nimis (1995) model is not useful, but rather that all silicate-based barometers have inherent error and should be used with this understanding.

To better describe hydrous samples, new barometers based on Equation (1) were calibrated using H_2O^{liq} (in wt%) as a variable:

Downloaded from http://pubs.geoscienceworld.org/msa/rimg/article-pdf/69/1/61/2948053/61_Putirka.pdf
by University of California Berkeley Library user
on 16 March 2024

Downloaded from http://pubs.geoscienceworld.org/msa/rimg/article-pdf/69/1/61/2948053/61_Putirka.pdf
by University of California Berkeley Library user
on 16 March 2024

Table 3. Pyroxene calculations example part II. Calculation of clinopyroxene components.

	SiO_2	TiO_2	Al_2O_3	FeO	MnO	MgO	CaO	Na_2O	K_2O	Cr_2O_3
1) Cpx, wt%	52.5	0.33	1.58	9.89	0.24	13.29	22.5	0.37	0	0.05
2) mol. wt	60.08	79.9	101.96	71.85	70.94	40.3	56.08	61.98	94.2	152.0
3) mol. prop.	0.8738	0.0041	0.0155	0.1376	0.0034	0.3298	0.4012	0.0060	0.0000	0.0003
4) # of O	1.7477	0.0083	0.0465	0.1376	0.0034	0.3298	0.4012	0.0060	0.0000	0.0010
5) oxy sum	2.6814									
6) ORF	6/(oxy sum) =	2.2376								
	Cations on the basis of 6 oxygens									
	X^{cpx}_{Si}	X^{cpx}_{Ti}	X^{cpx}_{Al}	X^{cpx}_{Fe}	X^{cpx}_{Mn}	X^{cpx}_{Mg}	X^{cpx}_{Ca}	X^{cpx}_{Na}	X^{cpx}_{K}	X^{cpx}_{Cr}
7) cat/6 Oxy	1.9553	0.0092	0.0694	0.3080	0.0076	0.7379	0.8978	0.0267	0.0000	0.0015
8) cation sum	4.0134									
				Clinopyroxene Components						
	$X^{cpx}_{Al(IV)}$	$X^{cpx}_{Al(VI)}$	$X^{cpx}_{Fe(3+)}$	X^{cpx}_{Jd}	X^{cpx}_{CaTs}	X^{cpx}_{CaTi}	X^{cpx}_{CrCaTs}	X^{cpx}_{DiHd}	X^{cpx}_{EnFs}	total
9)	0.0447	0.0247	0.0268	0.0247	0.0000	0.0223	0.0007	0.8747	0.0856	1.0081

To obtain row 7), the basis for calculations by Nimis (1995), first divide row 1) by row 2) to obtain row 3). To get row 4), multiply row 3) by the numbers of oxygens that occur in each formula unit. Row 5) shows the sum of row 4), and the Oxygen Renormalization Factor (ORF) in row 6), is equal to the number of oxygens per mineral formula unit, divided by the sum shown in 5); in our case, we calculate pyroxenes on the basis of six oxygens, yielding ORF = 2.2376. To obtain the numbers of cations on a six oxygen basis, as in row 7), multiply each entry in row 3) by the ORF and the number of cations in each formula unit (see Table 2). Row 8) shows the sum of cations per six oxygens (per formula unit). For a "good" pyroxene analysis, this value should be, as for orthopyroxenes, close to 4, thus providing a test of the quality of a pyroxene analysis. Clinopyroxene components in 9) are calculated from the cations in 7), using the following algorithm: $X^{cpx}_{Al(IV)} = 2 - X^{cpx}_{Si}$; $X^{cpx}_{Al(VI)} = X^{cpx}_{Al} - X^{cpx}_{Al(IV)}$; $X^{cpx}_{Fe(3+)} = X^{cpx}_{Na} + X^{cpx}_{Al(IV)} - X^{cpx}_{Al(VI)} - 2\,X^{cpx}_{Ti} - X^{cpx}_{Cr}$ (Papike te al. 1974); $X^{cpx}_{Jd} = X^{cpx}_{Al(VI)}$ or X^{cpx}_{Na}, whichever is less; if excess $X^{cpx}_{Al(VI)}$ remains after forming X^{cpx}_{Jd}, X^{cpx}_{CaTs} ($CaAl^{IV}Al^{VI}SiO_6$) = $X^{cpx}_{Al(VI)} - X^{cpx}_{Jd}$; if $X^{cpx}_{Al(IV)} > X^{cpx}_{CaTs}$, X^{cpx}_{CaTi} ($CaTiAl_2O_6$) = $[X^{cpx}_{Al(IV)} - X^{cpx}_{CaTs}]/2$; X^{cpx}_{CrCaTs} ($CaCr_2SiO_6$) = $X^{cpx}_{Cr}/2$; X^{cpx}_{DiHd} ($CaFmSi_2O_6$) = $X^{cpx}_{Ca} - X^{cpx}_{CaTi} - X^{cpx}_{CaTs} - X^{cpx}_{CrCaTs}$; X^{cpx}_{EnFs} ($Fm_2Si_2O_6$) = $[X^{cpx}_{Fe} + X^{cpx}_{Mg} - X^{cpx}_{DiHd}]/2$. The sum of the cpx components in 9) should be close to 1.0.

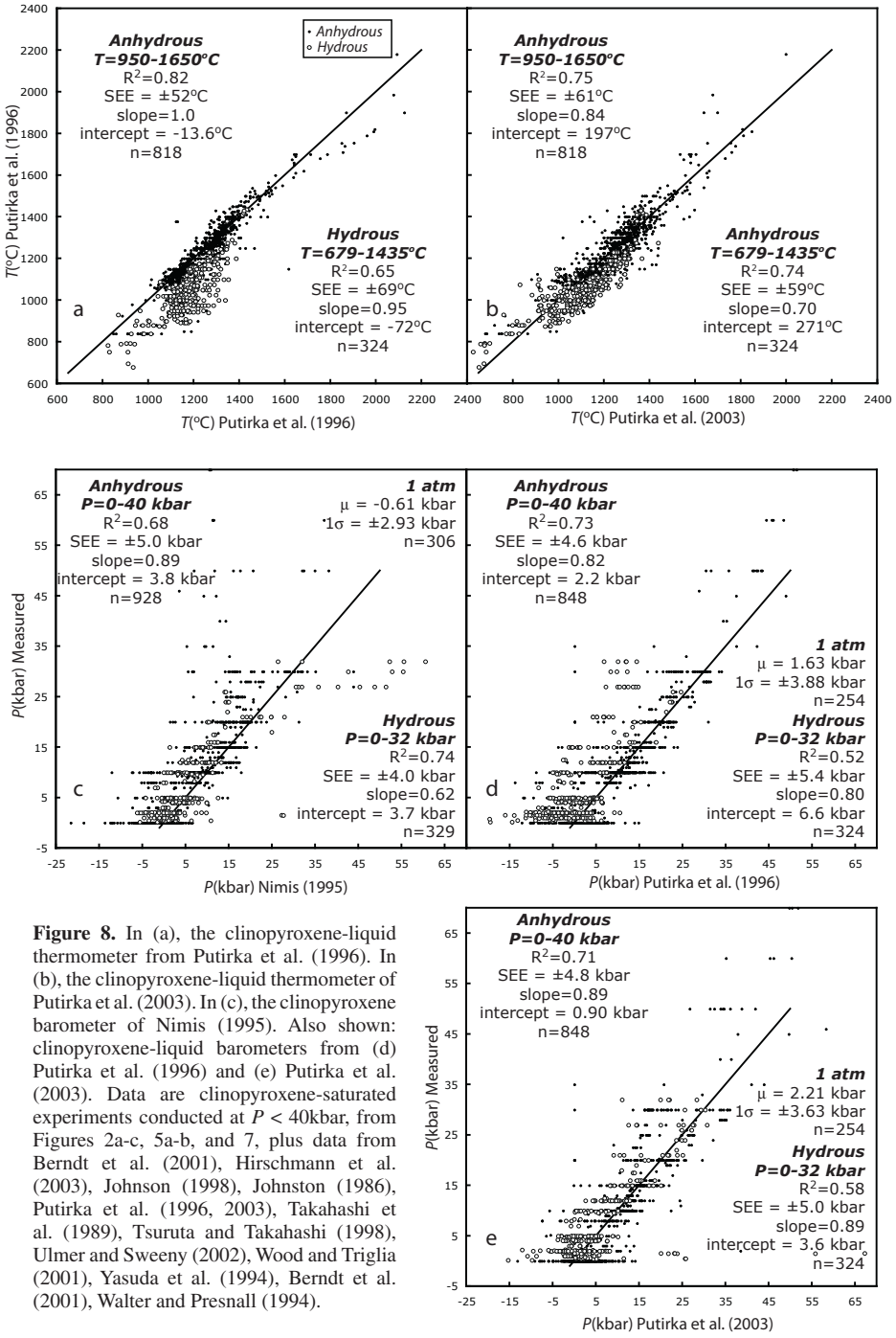

Figure 8. In (a), the clinopyroxene-liquid thermometer from Putirka et al. (1996). In (b), the clinopyroxene-liquid thermometer of Putirka et al. (2003). In (c), the clinopyroxene barometer of Nimis (1995). Also shown: clinopyroxene-liquid barometers from (d) Putirka et al. (1996) and (e) Putirka et al. (2003). Data are clinopyroxene-saturated experiments conducted at $P < 40$kbar, from Figures 2a-c, 5a-b, and 7, plus data from Berndt et al. (2001), Hirschmann et al. (2003), Johnson (1998), Johnston (1986), Putirka et al. (1996, 2003), Takahashi et al. (1989), Tsuruta and Takahashi (1998), Ulmer and Sweeny (2002), Wood and Triglia (2001), Yasuda et al. (1994), Berndt et al. (2001), Walter and Presnall (1994).

Downloaded from http://pubs.geoscienceworld.org/msa/rimg/article-pdf/69/1/61/2948053/61_Putirka.pdf
by University of California Berkeley Library user
on 16 March 2024

$$P(\text{kbar}) = -48.7 + 271\frac{T(\text{K})}{10^4} + 32\frac{T(\text{K})}{10^4}\ln\left[\frac{X^{cpx}_{\text{NaAlSi}_2\text{O}_6}}{X^{liq}_{\text{NaO}_{0.5}} X^{liq}_{\text{AlO}_{1.5}} \left(X^{liq}_{\text{SiO}_2}\right)^2}\right] \quad (30)$$
$$-8.2\ln(X^{liq}_{\text{FeO}}) + 4.6\ln(X^{liq}_{\text{MgO}}) - 0.96\ln(X^{liq}_{\text{KO}_{0.5}}) - 2.2\ln\left(X^{cpx}_{DiHd}\right)$$
$$-31(Mg\#^{liq}) + 56(X^{liq}_{\text{NaO}_{0.5}} + X^{liq}_{\text{KO}_{0.5}}) + 0.76\left(\text{H}_2\text{O}^{liq}\right)$$

$$P(\text{kbar}) = -40.73 + 358\frac{T(\text{K})}{10^4} + 21.69\frac{T(\text{K})}{10^4}\ln\left[\frac{X^{cpx}_{\text{NaAlSi}_2\text{O}_6}}{X^{liq}_{\text{NaO}_{0.5}} X^{liq}_{\text{AlO}_{1.5}} \left(X^{liq}_{\text{SiO}_2}\right)^2}\right] \quad (31)$$
$$-105.7(X^{liq}_{\text{CaO}}) - 165.5(X^{liq}_{\text{NaO}_{0.5}} + X^{liq}_{\text{KO}_{0.5}})^2 - 50.15\left(X^{liq}_{\text{SiO}_2}\right)\left(X^{liq}_{\text{FeO}} + X^{liq}_{\text{MgO}}\right)$$
$$-3.178\ln\left(X^{cpx}_{DiHd}\right) - 2.205\ln(X^{cpx}_{EnFs}) + 0.864\ln(X^{cpx}_{\text{Al}}) + 0.3962\left(\text{H}_2\text{O}^{liq}\right)$$

The term $X_{\text{Al}}{}^{cpx}$ is the total number of Al atoms in clinopyroxene when the formula is calculated on a 6 oxygen basis (equal to $X_{\text{Al(IV)}}{}^{cpx} + X_{\text{Al(VI)}}{}^{cpx}$). Equation (30) was calibrated using Grove and Juster (1989), Kinzler and Grove (1992), Walter and Presnall (1994), Sisson and Grove (1993a,b), Putirka et al. (1996), Scaillet and MacDonald (2003), and Patino-Douce (2005). Equation (31) was calibrated from a global regression of clinopyroxene-saturated experiments, excluding experiments performed at 1 atm (except Grove and Juster 1989) and $P > 40$ kbar (Fig. 9). A new model based on the Nimis (1995) approach was also recalibrated using experiments performed from 0.001-80 kbar:

$$P(\text{kbar}) = 3205 + 0.384T(\text{K}) - 518\ln T(\text{K}) - 5.62\left(X^{cpx}_{\text{Mg}}\right) + 83.2\left(X^{cpx}_{\text{Na}}\right) \quad (32a)$$
$$+68.2\left(X^{cpx}_{DiHd}\right) + 2.52\ln\left(X^{cpx}_{\text{Al(VI)}}\right) - 51.1\left(X^{cpx}_{DiHd}\right)^2 + 34.8\left(X^{cpx}_{EnFs}\right)^2$$

$$P(\text{kbar}) = 1458 + 0.197T(\text{K}) - 241\ln T(\text{K}) + 0.453\left(\text{H}_2\text{O}^{liq}\right) \quad (32b)$$
$$+55.5\left(X^{cpx}_{\text{Al(VI)}}\right) + 8.05\left(X^{cpx}_{\text{Fe}}\right) - 277\left(X^{cpx}_{\text{K}}\right) + 18\left(X^{cpx}_{Jd}\right) + 44.1\left(X^{cpx}_{DiHd}\right)$$
$$+2.2\ln\left(X^{cpx}_{Jd}\right) - 17.7\left(X^{cpx}_{\text{Al}}\right)^2 + 97.3\left(X^{cpx}_{\text{Fe(M2)}}\right)^2$$
$$+30.7\left(X^{cpx}_{\text{Mg(M2)}}\right)^2 - 27.6\left(X^{cpx}_{DiHd}\right)^2$$

Equation (32a) depends only upon the composition of clinopyroxene, and improves the precision of the Nimis (1995) model, but it preserves the systematic error with respect to hydrous experiments. Equation (32b) removes this systematic error, but at the cost of requiring an estimate of the H_2O content of the liquid in equilibrium with the clinopyroxene; it also requires use of additional calculations for the fractions of Fe and Mg occupying M1 and M2 sites, which can be found in Nimis (1995).

Equation (32c) represents a new barometer based on the partitioning of Al between clinopyroxene and liquid.

$$P(\text{kbar}) = -57.9 + 0.0475T(\text{K}) - 40.6(X^{liq}_{\text{FeO}}) - 47.7(X^{cpx}_{CaTs}) \quad (32c)$$
$$+0.676(\text{H}_2\text{O}^{liq}) - 153(X^{liq}_{\text{CaO}_{0.5}} X^{liq}_{\text{SiO}_2}) + 6.89\left(\frac{X^{cpx}_{\text{Al}}}{X^{liq}_{\text{AlO}_{1.5}}}\right)$$

Here, the last term represents the ratio of the total number of Al atoms in clinopyroxene when calculated on a 6 oxygen basis ($X_{\text{Al}}{}^{cpx} = X_{\text{Al(IV)}}{}^{cpx} + X_{\text{Al(VI)}}{}^{cpx}$; see Table 3), and the cation

Downloaded from http://pubs.geoscienceworld.org/msa/rimg/article-pdf/69/1/61/2948053/61_Putirka.pdf
by University of California Berkeley Library user
on 16 March 2024

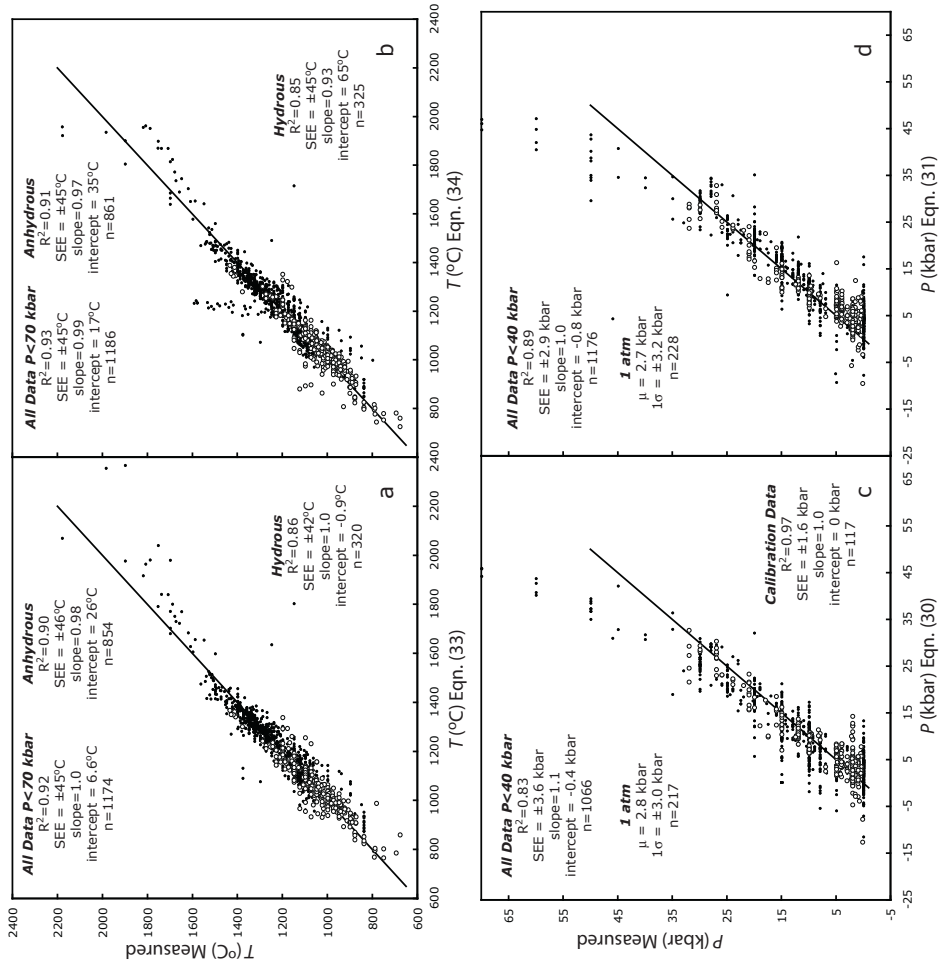

Figure 9. New clinopyroxene-liquid thermometers and barometers based on global calibrations. In (a), clinopyroxene-liquid thermometer based on Jd-DiHd exchange (Eqn. 33). In (b), clinopyroxene saturation thermometer (Eqn. 34). In (c), a barometer based on Jd-liq equilibrium, using calibration data as noted in text (Eqn. 30). In (d), a barometer as in (c) but based on a global calibration (Eqn. 31). In (e), a clinopyroxene-only thermometer of Nimis and Taylor (2000) and in (f) a new calibration for a clinopyroxene-only thermometer, using the Nimis and Taylor (2000) activity model (Eqn. 32d). In (g), a clinopyroxene-only barometer (Eqn. (32a)) and in (h) a similar calibration (32b), but incorporating an H_2O^{liq} term to rectify systematic error for hydrous data. Data are as in Figure 8.

Downloaded from http://pubs.geoscienceworld.org/msa/rimg/article-pdf/69/1/61/2948053/61_Putirka.pdf
by University of California Berkeley Library user
on 16 March 2024

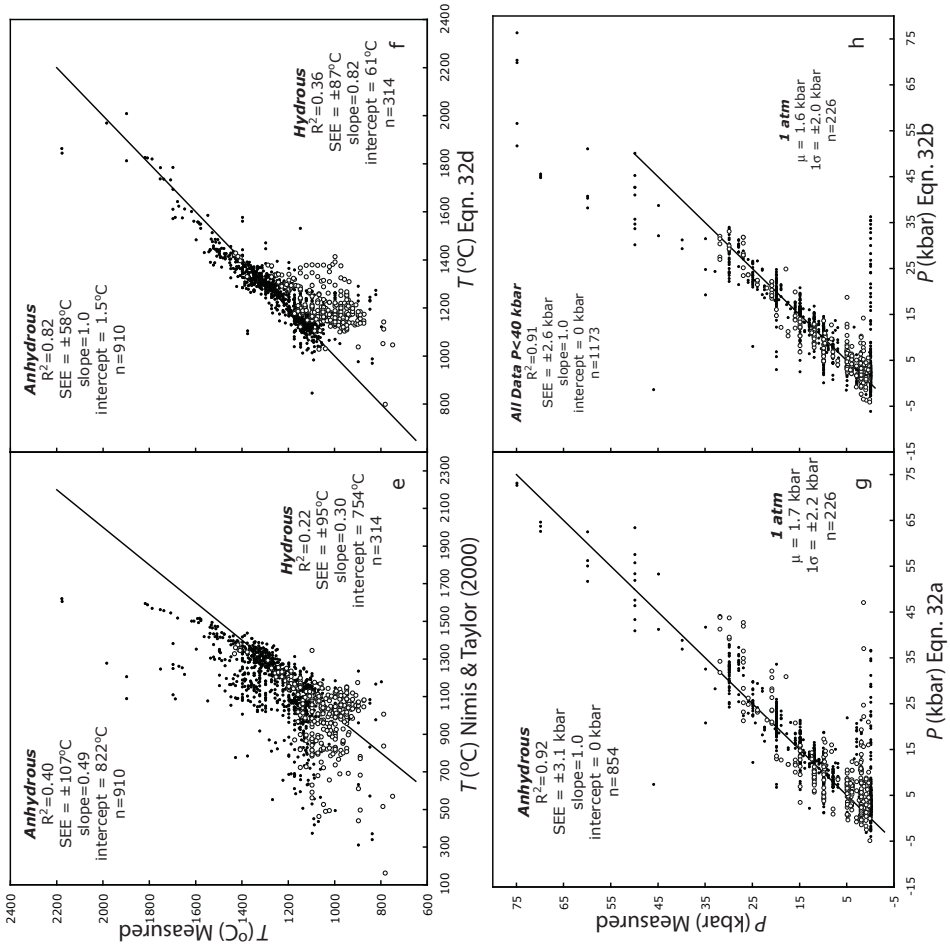

Downloaded from http://pubs.geoscienceworld.org/msa/rimg/article-pdf/69/1/61/2948053/61_Putirka.pdf
by University of California Berkeley Library user
on 16 March 2024

fraction of Al in liquid (see Table 1). This barometer was calibrated using data from Putirka et al. (1996), Kinzler and Grove (1992), Sisson and Grove (1993a,b) and Walter and Presnall (1994); regression statistics are: $R^2 = 0.95$, SEE = ±1.5 kbar, $n = 99$. A test using all available data ($n = 1303$) yield $R^2 = 0.82$ and SEE = ±5 kbar.

Nimis and Taylor (2000) have calibrated a clinopyroxene-only thermometer from a limited data set (Fig. 9e). Using their activity model, a new and more precise thermometer is (Fig. 9f):

$$T(\mathrm{K}) = \frac{93100 + 544P(\mathrm{kbar})}{61.1 + 36.6\left(X_{\mathrm{Ti}}^{cpx}\right) + 10.9\left(X_{\mathrm{Fe}}^{cpx}\right) - 0.95\left(X_{\mathrm{Al}}^{cpx} + X_{\mathrm{Cr}}^{cpx} - X_{\mathrm{Na}}^{cpx} - X_{\mathrm{K}}^{cpx}\right) + 0.395\left[\ln\left(a_{En}^{cpx}\right)\right]^2} \quad (32d)$$

Here, all cation fractions are on the basis of 6 oxygens (as in Eqns. 32a,b), the term $X_{\mathrm{Al}}{}^{cpx}$ refers to total Al ($X_{\mathrm{Al}}{}^{cpx} = X_{\mathrm{Al(IV)}}{}^{cpx} + X_{\mathrm{Al(VI)}}{}^{cpx}$) and the activity of enstatite in clinopyroxene, a_{En}^{cpx}, is as in Nimis and Taylor (2000): $a_{En}^{cpx} = (1 - X_{\mathrm{Ca}}^{cpx} - X_{\mathrm{Na}}^{cpx} - X_{\mathrm{K}}^{cpx}) \cdot (1 - 0.5(X_{\mathrm{Al}}^{cpx} + X_{\mathrm{Cr}}^{cpx} + X_{\mathrm{Na}}^{cpx} + X_{\mathrm{K}}^{cpx}))$.

The Jd-DiHd exchange thermometers (Putirka et al. 1996, 2003) reproduce T to ±52-60 °C. Global calibrations using experiments conducted at $P < 70$ kbar reduce these uncertainties by about 10-20 °C (Fig. 9):

$$\frac{10^4}{T(\mathrm{K})} = 7.53 - 0.14\ln\left(\frac{X_{Jd}^{cpx} X_{\mathrm{CaO}}^{liq} X_{Fm}^{liq}}{X_{DiHd}^{cpx} X_{Na}^{liq} X_{Al}^{liq}}\right) + 0.07\left(\mathrm{H_2O}^{liq}\right) - 14.9\left(X_{\mathrm{CaO}}^{liq} X_{\mathrm{SiO_2}}^{liq}\right) \quad (33)$$
$$-0.08\ln\left(X_{\mathrm{TiO_2}}^{liq}\right) - 3.62\left(X_{\mathrm{NaO_{0.5}}}^{liq} + X_{\mathrm{KO_{0.5}}}^{liq}\right) - 1.1\left(Mg\#^{liq}\right)$$
$$-0.18\ln\left(X_{EnFs}^{cpx}\right) - 0.027P(\mathrm{kbar})$$

$$\frac{10^4}{T(\mathrm{K})} = 6.39 + 0.076\left(\mathrm{H_2O}^{liq}\right) - 5.55\left(X_{\mathrm{CaO}}^{liq} X_{\mathrm{SiO_2}}^{liq}\right) - 0.386\ln\left(X_{\mathrm{MgO}}^{liq}\right) \quad (34)$$
$$-0.046P(\mathrm{kbar}) + 2.2\times10^{-4}\left[P(\mathrm{kbar})\right]^2$$

Equation (34) yields the temperature at which a liquid will become saturated with clinopyroxene at a given pressure, and so can be used as a test of temperatures derived from expressions such as Equation (33).

Tests for equilibrium. Some petrologists (e.g., Klügel and Klein 2005) test for equilibrium on the basis of Fe-Mg exchange coefficients. The danger is that Fe-Mg exchange equilibrium does not necessitate, for example, Na-Al, or Ca-Na exchange equilibrium, etc., and so Rhodes et al. (1979a) and Putirka (1999a, 2005b) suggest that equilibrium values for mineral compositions also be calculated, and compared to observed mineral compositions. Among experimental and natural data, however, deviations in observed and calculated values for $K_{\mathrm{D}}(\mathrm{Fe\text{-}Mg})^{cpx\text{-}liq}$ are highly correlated with deviations between observed and calculated values for DiHd, EnFs, etc., so tests based on Fe-Mg exchange may be sufficient. The Fe-Mg exchange coefficient derived from 1,245 experimental observations yields $K_{\mathrm{D}}(\mathrm{Fe\text{-}Mg})^{cpx\text{-}liq}$ = 0.28±0.08 (with a range from 0.04-0.68, with a roughly normal distribution). This value is not perfectly invariant, and the equation

$$\ln K_D(Fe - Mg)^{cpx-liq} = -0.107 - \frac{1719}{T(\mathrm{K})} \quad (35)$$

accounts for a slight temperature dependency, where $K_{\mathrm{D}}(\mathrm{Fe\text{-}Mg})^{cpx\text{-}liq}$ is recovered with a not so stunning $R^2 = 0.12$ and an SEE of 0.08.

Two-pyroxene thermometers and barometers

Sen et al. (2005) illustrate how sub-solidus equilibria can be crucial to understanding volcanic systems. Thus, since the introduction of the two-pyroxene geothermometer by Davis

Downloaded from http://pubs.geoscienceworld.org/msa/rimg/article-pdf/69/1/61/2948053/61_Putirka.pdf
by University of California Berkeley Library user
on 16 March 2024

and Boyd (1966), much attention has been given to estimating *T* utilizing some form of enstatite-diopside partitioning (e.g., Wood and Banno 1973; Herzberg and Chapman 1976; Wells 1977; Lindsley 1983; Lindsley and Anderson 1983; Mercier et al. 1984; Sen 1985; Sen and Jones 1989; Brey and Köhler 1990).

As with other systems, it is important to test for equilibrium. Using Fe-Mg exchange, 311 experiments yield $K_D(\mathrm{Fe-Mg})^{cpx-opx} = (X^{cpx}_{\mathrm{Fe}} / X^{cpx}_{\mathrm{Mg}}) / (X^{opx}_{\mathrm{Fe}} / X^{opx}_{\mathrm{Mg}}) = 1.09 \pm 0.14$. For calibration and test purposes we exclude data that lie at the outskirts of 3σ.

Of existing thermometers, the Brey and Köhler (1990) model *T*(BKN) is the most precise (Fig. 10a). A new global regression, based on the partitioning of enstatite + ferrosilite (= $Fm_2Si_2O_6$ = EnFs; FmO = FeO + MgO + MnO) between clinopyroxene and orthopyroxene increases precision for the available experimental data (Fig. 10b):

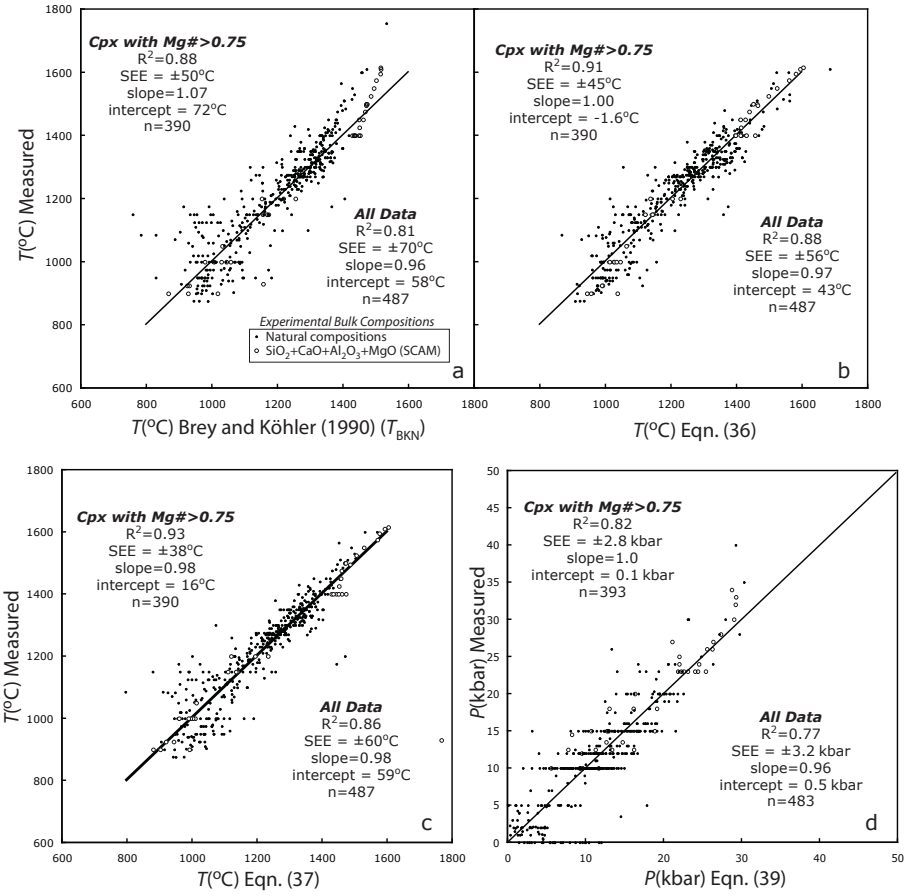

Figure 10. The Brey and Kohler (1990) two-pyroxene thermometer (a) performs reasonably well when predicting *T* for experimental data saturated with two pyroxenes from Figure 2a-c, plus data from Green and Ringwood (1967), Klemme and O'Neill (2000), Gudfinnsson and Presnall (1996), Milholland and Presnall (1998), and Sen (1985). A global regression (Eqn. 36) (b) provides somewhat greater precision, but precision is improved further if the calibration data base is restricted to include only Mg-rich systems, in this case defined as those cpx-opx pairs where $Mg\#^{cpx}$>0.75. In (d), a barometer, based on the Mercier et al. (1984) approach is also calibrated using only high Mg# compositions.

Downloaded from http://pubs.geoscienceworld.org/msa/rimg/article-pdf/69/1/61/2948053/61_Putirka.pdf
by University of California Berkeley Library user
on 16 March 2024

$$\frac{10^4}{T(^\circ\text{C})} = 11.2 - 1.96\ln\left(\frac{X^{cpx}_{EnFs}}{X^{opx}_{EnFs}}\right) - 3.3\left(X^{cpx}_{\text{Ca}}\right) - 25.8\left(X^{cpx}_{\text{CrCaTs}}\right) \quad (36)$$
$$+33.2\left(X^{opx}_{\text{Mn}}\right) - 23.6\left(X^{opx}_{\text{Na}}\right) - 2.08\left(X^{opx}_{En}\right) - 8.33\left(X^{opx}_{Di}\right) - 0.05P(\text{kbar})$$

where the EnFs components in clino- and orthopyroxene are calculated as in Tables 2 and 3 (EnFs = $Fm_2Si_2O_6$ for orthopyroxene), and where $X^{opx}_{En} = [(X^{opx}_{\text{Mg}})/(X^{opx}_{\text{Mg}} + X^{opx}_{\text{Fe}} + X^{opx}_{\text{Mn}})](X^{opx}_{\text{Fm}_2\text{Si}_2\text{O}_6})$, and $X^{opx}_{Di} = [(X^{opx}_{\text{Mg}})/(X^{opx}_{\text{Mg}} + X^{opx}_{\text{Fe}} + X^{opx}_{\text{Mn}})](X^{opx}_{\text{CaFmSi}_2\text{O}_6})$ (with cation fractions calculated on a 6 oxygen basis). The models perform best for mafic systems where $Mg\#^{cpx} > 0.75$. A separate regression using only experiments with $Mg\#^{cpx} > 0.75$ (Fig. 10c) yields the following expression:

$$\frac{10^4}{T(^\circ\text{C})} = 13.4 - 3.4\ln\left(\frac{X^{cpx}_{EnFs}}{X^{opx}_{EnFs}}\right) + 5.59\ln\left(X^{cpx}_{\text{Mg}}\right) - 8.8\left(Mg\#^{cpx}\right) \quad (37)$$
$$+23.85\left(X^{opx}_{\text{Mn}}\right) + 6.48\left(X^{opx}_{\text{FmAl}_2\text{SiO}_6}\right) - 2.38\left(X^{cpx}_{Di}\right) - 0.044P(\text{kbar})$$

With a similar restriction on Mg#, a new barometer (Fig. 10d) was calibrated from a global regression, utilizing the strategy of Mercier et al. (1984):

$$P(\text{kbar}) = -279.8 + 293\left(X^{opx}_{\text{Al(VI)}}\right) + 455\left(X^{opx}_{\text{Na}}\right) + 229\left(X^{opx}_{\text{Cr}}\right) \quad (38)$$
$$+519\left(X^{opx}_{\text{Fm}_2\text{Si}_2\text{O6}}\right) - 563\left(X^{opx}_{En}\right) + 371\left(X^{opx}_{Di}\right) + 327\left(a^{opx}_{En}\right) + \frac{1.19}{K_f}$$

Equation (38) is T-independent and the term $K_f = X^{opx}_{\text{Ca}}/(1 - X^{cpx}_{\text{Ca}})$ is as in Mercier et al. (1984); $X^{opx}_{En} = (X^{opx}_{\text{Fm}_2\text{Si}_2\text{O}_6})(X^{opx}_{\text{Mg}}/[X^{opx}_{\text{Mg}} + X^{opx}_{\text{Mn}} + X^{opx}_{\text{Fe}}])$ and $X^{opx}_{Di} = (X^{opx}_{\text{CaFmSi}_2\text{O}_6})(X^{opx}_{\text{Mg}}/[X^{opx}_{\text{Mg}} + X^{opx}_{\text{Mn}} + X^{opx}_{\text{Fe}}])$; the activity of enstatite in orthopyroxene, a^{opx}_{En}, is similar to Wood and Banno (1973) (with all cations calculated on the basis of 6 oxygens):

$$a^{opx}_{En} = \left(\frac{0.5X^{opx}_{\text{Mg}}}{X^{opx}_{\text{Ca}} + 0.5X^{opx}_{\text{Mg}} + 0.5X^{opx}_{\text{Fe}^{2+}} + X^{opx}_{\text{Mn}} + X^{opx}_{\text{Na}}}\right)\left(\frac{0.5X^{opx}_{\text{Mg}}}{0.5X^{opx}_{\text{Fe}^{2+}} + X^{opx}_{\text{Fe}^{3+}} + X^{opx}_{\text{Al(VI)}} + X^{opx}_{\text{Ti}} + X^{opx}_{\text{Cr}} + 0.5X^{opx}_{\text{Mg}}}\right)$$

Here, $X^{opx}_{Fe^{2+}} = X^{opx}_{Fe} - X^{opx}_{Fe^{3+}}$ where Fe^{3+} is calculated as in Papike et al. (1974): $Fe^{3+} = \text{Al(IV)} + \text{Na} - \text{Al(VI)} - \text{Cr} - 2\text{Ti}$. Equation (38) recovers P to ±3.7 kbar with $R^2 = 0.68$ ($n = 389$; Fig. 11). Precision is greatly increased when T is used as input:

$$P(\text{kbar}) = -94.25 + 0.045T(^\circ\text{C}) + 187.7\left(X^{opx}_{\text{Al(VI)}}\right) + 246.8\left(X^{opx}_{\text{Fm}_2\text{Si}_2\text{O}_6}\right) \quad (39)$$
$$-212.5\left(X^{opx}_{En}\right) + 127.5\left(a^{opx}_{En}\right) - \frac{1.66}{K_f} - 69.4\left(X^{cpx}_{EnFs}\right) - 133.9\left(a^{cpx}_{Di}\right)$$

where terms are as in Equation (38), and the activity of diopside in clinopyroxene, a^{cpx}_{Di}, is $a^{cpx}_{Di} = (X^{cpx}_{\text{Ca}})/(X^{cpx}_{\text{Ca}} + 0.5X^{cpx}_{\text{Mg}} + 0.5X^{cpx}_{\text{Fe}^{2+}} + X^{cpx}_{\text{Mn}} + X^{cpx}_{\text{Na}})$. Equation (39) recovers P to ±2.8 kbar, with $R^2 = 0.82$ ($n = 393$; Fig. 11).

The silica activity barometer

Carmichael et al. (1970) and Nicholls et al. (1971) were the first to show that because the activity of SiO_2 ($a^{liq}_{SiO_2}$) may be buffered at constant P and T by reactions such as

$$Mg_2SiO_4{}^{ol} + SiO_2{}^{liq} = Mg_2Si_2O_6{}^{opx} \quad (40)$$

that $a^{liq}_{SiO_2}$ could be used as a thermometer or barometer for igneous processes. Because most if not all basalts equilibrate with olivine and orthopyroxene in their mantle source regions, there has been much interest in using $a^{liq}_{SiO_2}$ as a barometer for mantle partial melting (though nothing precludes application to other olivine + orthopyroxene saturated liquids). For example, the

Downloaded from http://pubs.geoscienceworld.org/msa/rimg/article-pdf/69/1/61/2948053/61_Putirka.pdf
by University of California Berkeley Library user
on 16 March 2024

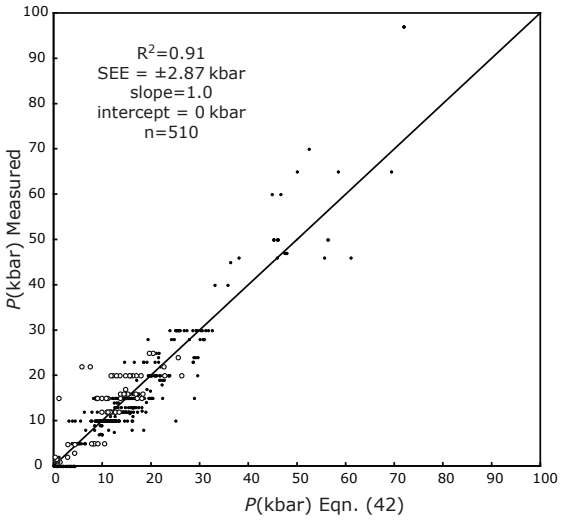

Figure 11. A silica activity barometer, using the activity for SiO_2 in silicate liquids devised by Beattie (1993). The data set is restricted to those liquids that are in equilibrium with both olivine and orthopyroxene (as in Nicholls et al. 1971), which include data from Figure 6, and data from Falloon et al. (1988), and Kushiro (1996).

work of Nicholls et al. (1971) is implicit in the SiO_2-based barometers of Klein and Langmuir (1987), Albarede (1992) and Haase (1996). Langmuir and Hanson (1980) later showed how FeO can be used as a barometer (supported by experiments by Stolper 1980), and Putirka (1999b) used Na/Ti ratios to estimate partial melting depths. But both FeO and Na/Ti are sufficiently sensitive to variations in source region composition and degree of partial melting that they do not readily lend themselves to a simple analytic expression.

The quantitative models of Albarede (1992) and Haase (1996) were calibrated using small data sets, and use wt% SiO_2^{liq} as input, not $a_{SiO_2}^{liq}$; these models capture <35% of the variation in *P* for the larger experimental data set studied here. However, Beattie's (1993) $a_{SiO_2}^{liq}$ is highly correlated with *P*:

$$a_{\mathrm{SiO_2}}^{liq} = \left(3X_{\mathrm{SiO_2}}^{liq}\right)^{-2}\left(1-X_{\mathrm{AlO_{1.5}}}^{liq}\right)^{7/2}\left(1-X_{\mathrm{TiO_2}}^{liq}\right)^{7} \tag{41}$$

When calculated in this way, $a_{SiO_2}^{liq}$ alone describes 80% of the variation in *P* for experimental data when $Mg\#^{liq}$ >0.75, and for 510 experiments with no restrictions on Mg#, $a_{SiO_2}^{liq}$ captures >60% of variation (over the *P-T* range 0.001–70 kbar and 825-2000 °C; SiO_2 ranges from 31.5-70%; data include hydrous compositions). Using the Beattie (1993) $a_{SiO_2}^{liq}$ a new model loosely based on Equations (5) and (41) is:

$$P(\mathrm{kbar}) = 231.5 + 0.186T(^{\circ}\mathrm{C}) + 0.1244T(^{\circ}\mathrm{C})\ln\left(a_{\mathrm{SiO_2}}^{liq}\right) - 528.5\left(a_{\mathrm{SiO_2}}^{liq}\right)^{1/2} \tag{42}$$
$$+103.3\left(X_{\mathrm{TiO_2}}^{liq}\right) + 69.9\left(X_{\mathrm{NaO_{0.5}}}^{liq} + X_{\mathrm{KO_{0.5}}}^{liq}\right) + 77.3\left(\frac{X_{\mathrm{AlO_{1.5}}}^{liq}}{X_{\mathrm{AlO_{1.5}}}^{liq} + X_{\mathrm{SiO_2}}^{liq}}\right)$$

where all compositional terms are cation fractions (Table 1). Equation (42) was calibrated using a "global" database of partial melting experiments (iteratively removing data outside ±3σ) where liquids are in equilibrium with olivine and orthopyroxene (± other phases). Interestingly, calibrations on smaller data sets yield little improvement in the SEE for *P*, and fared poorly when predicting *P* for data not used in the calibration. Equation (42) recovers *P* to ±2.9 kbar, with $R^2 = 0.91$ (Fig. 11).

Downloaded from http://pubs.geoscienceworld.org/msa/rimg/article-pdf/69/1/61/2948053/61_Putirka.pdf
by University of California Berkeley Library user
on 16 March 2024

APPLICATIONS

Magma transport at Hawaii

Thermobarometers can be of immense use for understanding the mechanical controls of magma transport. For example, although it is reasonably well understood that density contrasts, such as at the Moho, may control magma transport (Stolper and Walker 1980), other transport models emphasize the roles of stress states within the lithosphere (ten-Brink and Brocher 1987; Parsons and Thompson 1993) or fracture toughness (Putirka 1997). These views yield contrasting predictions regarding where magmas are stored prior to eruption. Presuming that magmas undergo an episode of cooling and crystallization during storage, thermobarometers provide a test.

To illustrate, Putirka (1997) posited that magmas are stored over a wide depth range at Hawaii, and that the Moho does not provide a necessary barrier to magma transport. New data from the Hawaii Scientific Drilling project, and a re-analysis of some existing data, modify this view. Table 4 shows *P-T* calculations for a Pu'u O'o episode-3 flow (Garcia et al. 1992) using several new and existing models. The thermobarometers are in agreement yielding mean *P-T* estimates of 4.8±0.8 kbar and 1469±16 °C; standard deviations are well within model error. For Pu'u O'o episodes 1-10, depth-time estimates are shown for individual crystals whose mineral-whole rock pairs yield $K_D(\text{Fe-Mg})^{cpx\text{-}liq}$ within ±0.08 of values predicted using (35) (Fig. 12a). As in Putirka (1997), crystallization depths become shallower with time. These magmas appear to have been stored simultaneously over a range of depths, with a top-to-bottom emptying of a rather lengthy and semi-continuous and connected conduit.

However, existing data from Mauna Kea (Frey et al. 1990, 1991) and 291 new clinopyroxene-whole rock pairs from the HSDP-2 (Rhodes and Vollinger 2004; new mineral compositions from this study) alter the story line. Of these data, 120 clinopyroxenes yield $K_D(\text{Fe-Mg})^{cpx\text{-}liq}$ within ±0.08 of values determined from Equation (35). Seventy-five (73%) fall within the depth range for "high density cumulates" determined from seismic studies (Hill and Zucca 1987). This clustering, and a trend to lower *T* just above the Moho, was not evident in the smaller data set examined by Putirka (1997). Moreover, *P-T* estimates from ultramafic xenoliths (Fodor and Galar 1997; Eqns. 38, 39) (Table 5) also exhibit clustering near the Moho, and a trend towards higher (more volcanic-like) *T*. The volcanic phenocryst, seismic, and xenolith data thus all support the conclusions of Fodor and Galar (1997, p.1) that ultramafic xenoliths at Mauna Kea are "gravity settled and *in situ* cumulates from reservoir bottoms." However, both the volcanic phenocryst and xenolith suites also yield depth ranges as great as 35 km. A hybrid model is supported, involving a magma mush column (e.g., Ryan 1988; Marsh 1995) that extends below the Moho, possibly with the mechanical controls advocated by Putirka (1997), with transport inhibited by density contrasts near the Moho (Garcia et al. 1995; 8-14 km).

The conditions of mantle partial melting

The glass and olivine-liquid thermometers, and the silica activity barometer are calibrated to 60-70 kbar, and can be applied to understand mantle melting. For example, Morgan (1971) suggested that volcanism at Hawaii or Yellowstone is driven by plumes—thermal upwellings, which rise though the mantle. Like Hess (1962), Morgan (1971) argued that heat from the core drives mantle convection.

The mantle plume model thus predicts that "hot spots" should be hotter than ambient mantle (which feeds mid-ocean ridge basalt (MORB) volcanism). In other words, they should exhibit an "excess temperature," reflecting their derivation from a source with excess heat. Recent skepticism of the mantle plume model (e.g., Foulger and Natland 2003) has prompted efforts to estimate mantle potential temperatures (T_p) at ocean islands, to test whether hot spots are truly hot (e.g., Putirka 2005a; Putirka et al. 2007; Herzberg et al. 2007; Putirka 2008). T_p represents the *T* the mantle would have if it rose to the surface, adiabatically,

Downloaded from http://pubs.geoscienceworld.org/msa/rimg/article-pdf/69/1/61/2948053/61_Putirka.pdf
by University of California Berkeley Library user
on 16 March 2024

Downloaded from http://pubs.geoscienceworld.org/msa/rimg/article-pdf/69/1/61/2948053/61_Putirka.pdf
by University of California Berkeley Library user
on 16 March 2024

Table 4. Example calculations for clinopyroxene thermobarometers.

	SiO_2	TiO_2	Al_2O_3	FeO	MnO	MgO	CaO	Na_2O	K_2O	Cr_2O_3
Whl-rk (wt%)[1]	50.2	2.83	13.74	11.07	0.17	6.6	10.48	2.49	0.57	0.202
Whl-Rk (cat fr)	0.4795	0.0203	0.1547	0.0884	0.0014	0.0940	0.1072	0.0461	0.0069	0.0015
Cpx (wt%)	52.9	0.7	2.1	7.6	0	17.9	18.7	0.27	0	0.2
Cat per 6 O[2]	1.9337	0.0192	0.0905	0.2323	0.0000	0.9755	0.7323	0.0191	0.0000	0.0058
	$X^{cpx-6ox}_{Al^{IV}}$	$X^{cpx-6ox}_{Al^{VI}}$	Fe^{3+}	$K_D(Fe\text{-}Mg)^{cpx\text{-}liq}$	X^{cpx}_{Jd}	X^{cpx}_{CaTs}	X^{cpx}_{CaTi}	X^{cpx}_{CrCaTs}	X^{cpx}_{DiHd}	X^{cpx}_{EnFs}
	0.0663	0.0242	0.0169	0.253	0.0191	0.0051	0.0306	0.0029	0.6938	0.2570

Putirka et al. (1996)		Putirka et al. (2003)	
Eqn. T2	Eqn. P1		
T(°C)	P(kbar)[3]	T(°C)	P(kbar)
1194	5.3	1214	5.1

New Models (this study)			
Eqn. 30	Eqn. 31	Eqn. 32a	Eqn. 32b
P(kbar)	P(kbar)	P(kbar)	P(kbar)
4.9	6.3	4.0	4.1
Eqn. 32d	Eqn. 33	Eqn. 34	Eqn. (35)
T(°C)	T(°C)	T(°C)	$K_D(Fe\text{-}Mg)^{cpx\text{-}liq}$
1199	1198	1198	0.283

Mean estimates		
	P(kbar)	T(°C)
Mean	4.95	1201
std dev	0.85	7.7

[1]"Whl-Rk" is a whole rock composition, for sample 3-88, Garcia et al. (1992).
[2]Clinopyroxene (cpx) cations (on the basis of 6 oxygens) are calculated as in Table 2.
[3]P calculated from Putirka et al. (1996) solved iteratively using Equation (T2) of Putirka et al. (1996); all other T-sensitive P estimates use T(K) from Putirka et al. (2003).

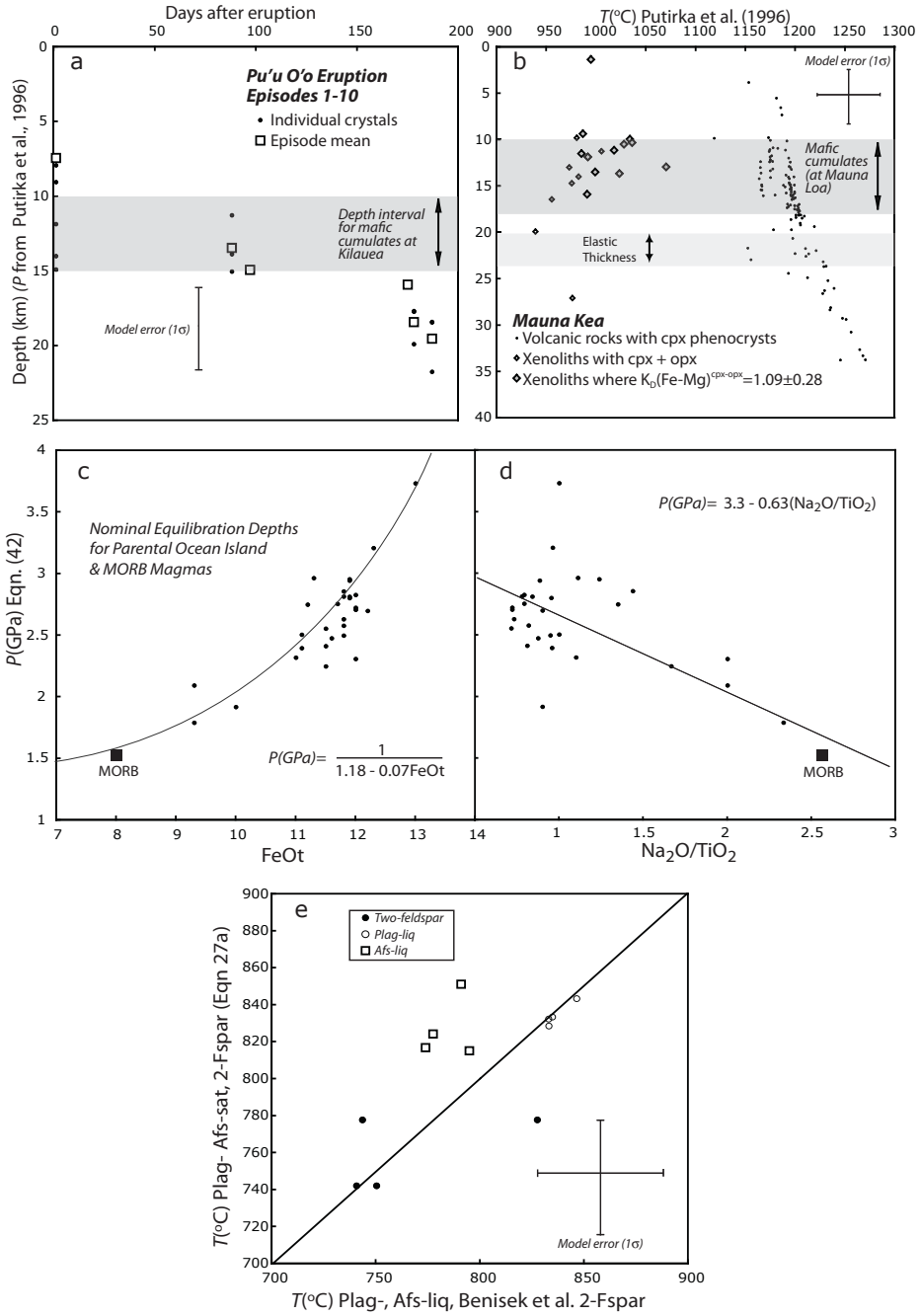

Figure 12. *caption on facing page*

Downloaded from http://pubs.geoscienceworld.org/msa/rimg/article-pdf/69/1/61/2948053/61_Putirka.pdf
by University of California Berkeley Library user
on 16 March 2024

without melting, and so provides a convenient reference for inter-volcano comparisons (see McKenzie and Bickle 1988). Table 6 shows calculations using parental liquid compositions for MORB and Hawaii (from Putirka 2008). For these calculations, Equations (22) and (42) are solved simultaneously to derive *P* and *T*, where *T* represents the temperature of olivine-liquid equilibration and *P* the pressure of olivine+orthopyroxene+liquid equilibration. Additional *T* estimates (Table 6) are derived using this *P* (from Eqns. 22, 42) as input. Mantle equilibration temperatures are converted to T_p by correcting for the heat of fusion, and adiabatic upwelling (Table 6). The thermometers yield highly consistent results.

The difference between T_p at Hawaii and T_p at MORB is the excess temperature, T_{ex}, which reflects some fraction of the excess heat derived from the plume source. The T_{ex} at Hawaii is ~260 °C, and the nominal depth of equilibration there is more than 50% greater than beneath mid-ocean ridges (Table 6). The calculated pressures of equilibration are called "nominal" because the reconstructed "parental liquids" used as input (Putirka 2008) are likely to represent some averaging of a range of melt compositions that exist within a melting column of considerable depth extent (Klein and Langmuir 1987). For 27 other ocean islands (Putirka 2008), average T_{ex} = 160±52 °C and average equilibration pressures and depths are 2.6±0.4 GPa and 85±11 km.

Computed inter-island variations in *P* may be real. Pressures calculated from $a^{liq}_{SiO_2}$ are correlated with other *P*-sensitive components. For example, a positive correlation between *P* (based on $a^{liq}_{SiO_2}$) and FeOt is expected (Fig. 12c) because increased *P* means that greater amounts of olivine (and FeOt) enter the liquid (Langmuir and Hanson 1980; Stolper 1980; Klein and Langmuir 1987). And a negative correlation is expected for Na_2O/TiO_2 (Fig. 12d), because the distribution coefficient for Na in clinopyroxene increases relative to that for Ti, with increased *P* (Putirka 1999b).

Temperature estimates in felsic volcanic systems

Unfortunately, few published studies on felsic volcanic rocks report both alkali feldspar, plagioclase feldspar and glass compositions. But such compositions from the 75 ka Toba tuffs (Beddoe-Stephens et al. 1983) indicate how some of the models presented here might be used to better understand the thermal record of such systems.

Figure 12. (on facing page) In (a) and (b) Hawaiian rock and mineral compositions are used to illustrate the use of several of the thermometers and barometers given in this study. Whole-rock-cpx pairs from the Pu'u O'o eruption of Kilauea (Garcia et al. 1989, 1992), are used in (a) to compare depth and time; the relationship indicates a top-to-bottom emptying of a continuous conduit that extends to >20 km below the Kilauea summit. In (b), depth (*d*)-*T* estimates at Mauna Kea from xenoliths (Fodor and Galar 1997) are compared to *d*-*T* estimates from volcanic rocks with clinopyroxene (cpx) phenocrysts (Frey et al. 1990, 1991; Yang et al. 1996; Rhodes and Vollinger 2004 with mineral compositions from this study). The volcanic and xenolith suites both indicate transport of magmas from as great at 35 km, but also storage and cooling of magma near the base of the volcano, in the depth range of "mafic cumulates" (Hill and Zucca 1987). In (c), depth estimates are calculated using calculated parental magma compositions for MORB and 27 ocean islands from Putirka (2008), and are compared to FeOt and Na_2O/TiO_2 contents for these magmas. There is some circularity for (c) because FeOt contents are used to estimate *P*. But the cross correlations are as expected if variations in SiO_2-FeOt-Na_2O/TiO_2 reflect partial melting depths, driven by differences in partial melting temperatures (see Klein and Langmuir 1987 and Putirka 1999b). In (e), temperatures are calculated for Toba Tuff ignimbrites (Beddoe-Stephens et al. 1983) using the two feldspar (2-Fspar) and plagioclase- and alkali feldspar-liquid equilibria. Glass compositions are melt inclusions in plagioclase and alkali feldspar (Beddoe-Stephens et al. 1983). The match between the two plagioclase models indicates that plagioclase most closely approaches equilibrium with included glass. Alkali feldspar *T* estimates are within 2σ of one another, but only one sample yields temperatures within 1σ. Though the plagioclase (plag) and alkali feldspar (afs) temperatures are within model error, plagioclase may be closer to equilibrium, and perhaps precipitated at a higher *T* than alkali feldspar, and temperatures derived from two-feldspar thermometry may be too low.

Downloaded from http://pubs.geoscienceworld.org/msa/rimg/article-pdf/69/1/61/2948053/61_Putirka.pdf
by University of California Berkeley Library user
on 16 March 2024

Table 5. Examples of two-pyroxene *P-T* calculations.

	SiO_2	TiO_2	Al_2O_3	FeO	MnO	MgO	CaO	Na_2O	K_2O	Cr_2O_3
Cpx (wt%)	52.3	0.7	3	5.1	0.11	16.6	21.5	0.33	0	0.58
Cat per 6 O[1]	1.9122	0.0192	0.1293	0.1559	0.0034	0.9048	0.8422	0.0234	0	0.0168
	$X^{cpx-6ox}_{Al^{IV}}$	$X^{cpx-6ox}_{Al^{VI}}$	Fe^{3+}	X^{cpx}_{Jd}	X^{cpx}_{CaTs}	X^{cpx}_{CaTi}	X^{cpx}_{CrCaTs}	X^{cpx}_{DiHd}	X^{cpx}_{EnFs}	
	0.0878	0.0414	0.0146	0.0234	0.0180	0.0349	0.0084	0.7809	0.1399	
	X^{cpx}_{En}	X^{cpx}_{Di}	a^{cpx}_{Di}							
	0.1189	0.6640	0.6050							
	SiO_2	**TiO_2**	**Al_2O_3**	**FeO**	**MnO**	**MgO**	**CaO**	**Na_2O**	**K_2O**	**Cr_2O_3**
Opx (wt%)	55	0.34	1.5	11.3	0.24	30.7	0.9	0.01	0	0.19
Cat per 6 O[1]	1.944	0.0090	0.0625	0.3340	0.0072	1.617	0.0341	0.0007	0	0.0053
	$X^{cpx-6ox}_{Al^{IV}}$	$X^{cpx-6ox}_{Al^{VI}}$	Fe^{3+}	X^{opx}_{Jd}	$X^{opx}_{FmTiAlSiO_6}$	X^{opx}_{CrCaTs}	$X^{opx}_{FmAl_2SiO_6}$	X^{opx}_{DiHd}	X^{opx}_{EnFs}	
	0.0563	0.00614	0.0275	0.0007	0.0090	0.0053	0.0001	0.0341	0.9576	
	X^{opx}_{En}	X^{opx}_{Di}	a^{opx}_{En}	a^{opx}_{Di}						
	0.7908	0.0281	0.6451	0.0340						

New Models (this study)[2]

$K_D(Fe\text{-}Mg)^{cpx\text{-}opx}$	Eqn. 38 ***P*(kbar)**	Eqn. 39/36 ***P*(kbar)**	Eqn. 36/39 ***T*(°C)**	Eqn. 37/38 ***T*(°C)**
0.835	2.2	3.4	985	964

[1] Clinopyroxene (cpx)-orthopyroxene (opx) pair is from sample C2 of Fodor and Galar (1997) with compositions shown in wt% and as cations on the basis of 6 oxygens.
[2] Equations (39) and (36) are solved simultaneously; Equation (38) is *T*-independent and Equation (36) uses 3.4 kbar as input. All clinopyroxene and orthopyroxene calculations are as in Tables 2-4 and as noted in the text.

Downloaded from http://pubs.geoscienceworld.org/msa/rimg/article-pdf/69/1/61/2948053/61_Putirka.pdf
by University of California Berkeley Library user
on 16 March 2024

Table 6. Examples of liquid, olivine-liquid, and mantle potential temperature calculations.

	SiO_2	TiO_2	Al_2O_3	FeO	MnO	MgO	CaO	Na_2O	K_2O	H_2O
MORB[1]	48.5	0.9	15.9	8	0.1	13.2	11.1	2.3	0	0.11
Hawaii[1]	47.2	1.6	9	11.6	0.2	21.4	7.3	1.4	0.2	0.65

	$D_{Mg}^{ol\text{-}liq}$ (Eqn. 20)	Eqn. 13	Eqn. 14	Eqn. 15	Eqn. 16	Eqn. 19	Eqn. 19 w/H&O[3]	Eqn. 22	Mean T(°C)	Std. dev. T(°C)
MORB[2]	3.39	1342	1343	1359	1375	1390	1381	1374	1366	19
Hawaii[2]	2.12	1557	1575	1547	1513	1614	1579	1557	1563	31

	Eqn. 42 P(kbar)	Depth[5] (km)	T_p^{corr}	T_p	T_{ex}
MORB[4]	15.6	52.5	33	1399	-
Hawaii[4]	27.3	88.8	97	1660	261

[1]Mid-ocean ridge (MORB) and Hawaiian compositions are "parental" magmas, as calculated in Putirka (2008).
[2]All temperatures are calculated in °C.
[3] "Equation (19) w/H&O" uses Equation (19) and the correction for pressure from Herzberg and O'Hara (2002); see text.
[4]T_p is mantle potential temperature (see text); T_p^{corr} is the correction required to convert an olivine equilibration T (i.e., Eqn. 22) to T_p and is given by: $T_p = T^{ol\text{-}liq} + 667F - 1.33P$(kbar), where F (melt fraction) is 0.08 for MORB and 0.20 at Hawaii (see Putirka et al. 2007) and Equation (22) is used as input.
[5]P from Equation (42) is converted to depth (d) using a regression fit based on PREM (Anderson, 1989): d(km)=14.6 + 29P(GPa) − 0.157[P(GPa) − 8.4]^2.

Downloaded from http://pubs.geoscienceworld.org/msa/rimg/article-pdf/69/1/61/2948053/61_Putirka.pdf
by University of California Berkeley Library user
on 16 March 2024

T estimates at Toba based on plagioclase-liquid equilibrium (Eqn. 23) and plagioclase-saturation (Eqn. 26) are nearly identical (Fig. 12e) (Table 7). Although this might reflect the higher precision of the plagioclase-based models, it might also indicate that plagioclase-hosted melt inclusions have more closely approached equilibrium with their host minerals, since all but one alkali feldspar-glass inclusion pair yield mineral-melt and mineral saturation temperatures that are >1σ apart. The one alkali feldspar-glass pair that most closely approaches equilibrium has a *T* estimate slightly less than that for plagioclase, perhaps indicating that plagioclase precipitated at a slightly higher *T* than alkali feldspar. If this is the case, temperatures from two-feldspar thermometry might not be valid, since if alkali-feldspars are not in equilibrium with their included glass, they would seem unlikely to be in equilibrium with neighboring plagioclase feldspars. In that case, *T* estimates from the two-feldspar thermometers may be too low by 40-70 °C. A greater number of samples are clearly needed to interpret these data with confidence, but the Toba examples illustrate how multiple thermometers can be used to better understand the thermal history of silicic systems.

SOURCES OF ERROR RELATIVE TO *P* AND *T*

Geothermometry and geobarometry involve two sources of error. 1) *Model error* measures the precision of a model, the magnitude of which can be identified from regression statistics. This error results from experimental error, and includes the error in reproducing *P* or *T* in the laboratory, lack of attainment of equilibrium during an experiment, and errors related to compositional measurements; the latter two are likely the most important (Putirka et al. 1996). 2) The *error of treatment* is related to the application of a model, and will trend towards greater values as natural systems deviate from experimental conditions; the most serious issue here is probably the pairing of a given mineral with its equilibrium liquid—less an issue for experiments, but problematic for natural magmas when they behave as open systems. It is also important that natural magmas and minerals have compositions and equilibration conditions similar to those studied experimentally. The best guard against error is to compare *P-T* conditions from different equilibria, which need not match precisely (olivine may precipitate before clinopyroxene) but should be correlated.

Model error

Estimates for model error can be derived from regression statistics. Usually, a "standard error of estimate" or SEE (equivalent to the root mean square error, RMSE), is reported for *T* or *P*. Like a standard deviation (1σ) in a normal distribution, the SEE (or RMSE) represents the interval ±E such that there is a 68.26% probability that the true value lies between −E and +E. If the calibration data are small in number and of high quality, the SEE will probably underestimate true model error, since by the nature of regression, coefficients are optimized for a highly specific set of circumstances, which natural samples are unlikely to mimic perfectly. If the calibration data derive from a single laboratory, it is also possible that there is systematic error related to experimental design. A truer test of model error can be derived from "test data," i.e., experimental data not used for regression.

How does one decide which experimental data should be used for test or calibration purposes? Hirschmann et al. (2008) note that many experiments are conducted at too short a time scale to allow diffusional exchange between minerals and liquid. Long-duration experiments, however, provide no assurances of equilibrium since thermal gradients in such can induce compositional gradients (Lesher and Walker 1988). In any case, errors on estimates of *P* (Eqn. 30) and *T* (Eqn. 33) are nearly independent of experimental run duration, as are values for $K_D(\text{Fe-Mg})^{ol\text{-}liq}$, an often-used test of equilibrium (Fig. 13).

Estimates of error. Various thermometers tend to yield comparable calibration errors, on the order of ±25-30 °C, when more than a few hundred experiments are used for regression.

Downloaded from http://pubs.geoscienceworld.org/msa/rimg/article-pdf/69/1/61/2948053/61_Putirka.pdf
by University of California Berkeley Library user
on 16 March 2024

Table 7. Examples of feldspar calculations.

	SiO_2	TiO_2	Al_2O_3	FeO	MnO	MgO	CaO	Na_2O	K_2O	H_2O
Toba, R301 P [1]	73.78	0.08	12.56	1	0.04	0.02	0.89	3.01	4.47	4.0

	An	Ab	Or
Plagioclase[1]	0.372	0.586	0.042
Alkali Feldspar[1]	0.012	0.276	0.712

Two Feldspar Temperatures

Eqn 27a *T*(°C)	Eqn 27b *T*(°C)	B(2004) *T*(°C)[2]
743	818	778

Feldspar-liquid P-T and H_2O Calculations

Eqn. 23 *T*(°C)	Eqn. 24a *T*(°C)	Eqn. 24b *T*(°C)	Eqn. 24c *T*(°C)	Eqn. 26 *T*(°C)	Eqn. 25 *P*(kbar)	Eqn. 25b/23 H_2O[3]	Eqn. 25b/24b H_2O[3]
846	815	794	815	843	4.03	3.2	4.05

[1]Glass and feldspar data are from Beddoe-Stephens et al. (1983).
[2]Two feldspar thermometer of Benisek et al. (2004).
[3]H_2O calculations are in wt%, calculated at a pressure of 1 kbar, and at a *T* calculated from Equations (23) and (24b); when calculated using a pressure of 4 kbar, wt% values for H_2O are 0.5% less.

Downloaded from http://pubs.geoscienceworld.org/msa/rimg/article-pdf/69/1/61/2948053/61_Putirka.pdf
by University of California Berkeley Library user
on 16 March 2024

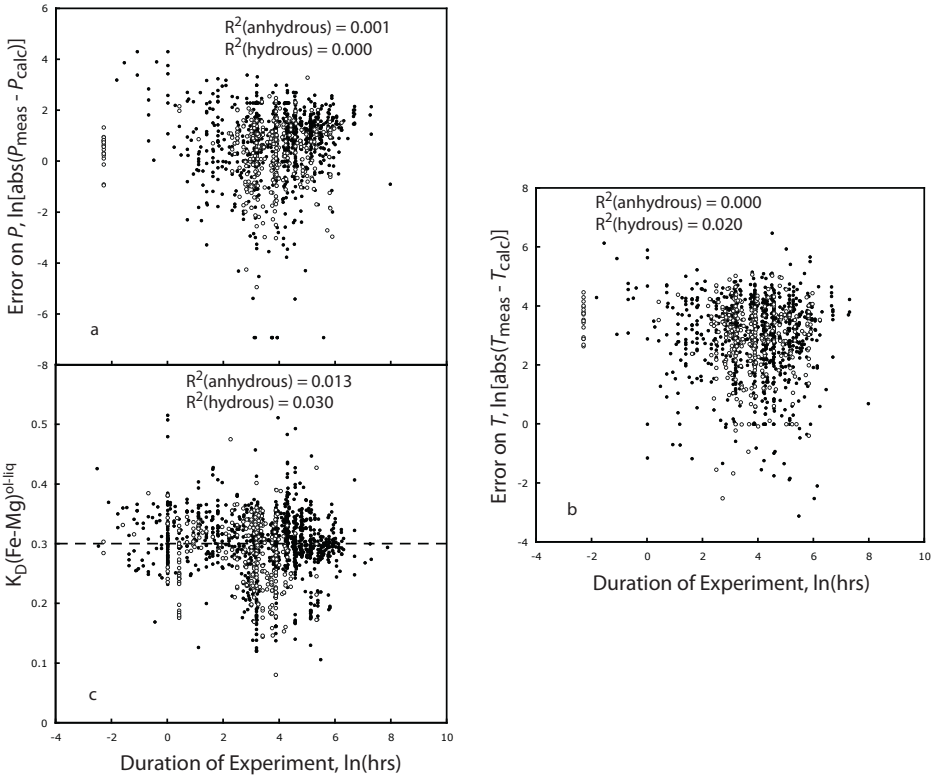

Figure 13. In (a) and (b) model errors are compared to experimental "run" duration, for *P* (Eqn. 30) and *T* (Eqn. 33) respectively. Model error is calculated as the natural log of the absolute value of the difference between predicted and experimentally reported *P* or *T*. In (c), the Fe-Mg exchange coefficient between olivine and liquid, $K_D(\text{Fe-Mg})^{ol\text{-}liq}$, is compared to experimental run duration. R^2 values are shown for hydrous (open symbols) and anhydrous (closed symbols) data. Except for some anhydrous experiments conducted at less than a few hours, increased experimental run durations do not necessarily yield improvement in model precision, or apparently even a closer approach to Fe-Mg exchange equilibrium.

Thus ±25-30 °C probably represents the smallest magnitude for model error that one can expect for any individual *T* estimate derived from a generalized silicate-based thermometer (regardless of whether smaller errors are reported). Similarly, the highest precision to be expected from silicate-based barometers is in the range ±1.5-2.5 kbar.

As noted in prior sections, there is hope that if experimental error is random, then more precise estimates can be derived by averaging individual *P-T* estimates. Because many experiments are conducted at 8, 10, 12 kbar, etc., it is easy to test this idea by calculating *P* for a number of experiments performed at a given pressure (say 10 kbar), then compare the mean of those estimates, and the standard error on that mean, to the measured value. Such calculations indicate that mineral-melt barometers may be as precise as ±0.5-1.0 kbar (a "standard error on the mean") when estimates are averaged for isobaric systems (e.g., Putirka et al. 1996, 2003).

For thermometers the increase in precision is not so clear. For 35 experiments on dry basalts conducted at 1200 °C, Equation (19) (Beattie 1990) yields a mean of 1225±52 °C (the ±52 °C is the standard deviation) with a standard error on the mean of ±9 °C; the mean value thus deviates from the measured value by more than twice the standard error on the mean and

Downloaded from http://pubs.geoscienceworld.org/msa/rimg/article-pdf/69/1/61/2948053/61_Putirka.pdf
by University of California Berkeley Library user
on 16 March 2024

so the latter does not reflect greater accuracy. For the same data, Equation (22) yields the same standard error on the mean (±9 °C) with a mean value of 1213±50 °C; the mean estimate is still more than one standard error from the measured value. Although these standard errors on the means do not represent increased accuracy, the absolute differences between the mean and measured *T* estimates might, in which case averaging several *T* estimates (for isothermal systems), yield error as low as ±13-25 °C.

***P-T* slopes and correlated error.** Mordick and Glazner (2006) note that because the clinopyroxene-liquid barometer is highly dependent on *T*, *P-T* estimates are necessarily correlated. This principle holds for any *T*-sensitive barometer or *P*-sensitive thermometer. Mordick and Glazner (2006) use a Monte Carlo technique to simulate random error and generate a *P-T* error array for clinopyroxene-liquid pairs to illustrate the correlation. Putirka and Condit (2003) adopt the method of Kohn and Spear (1991), using multiple analyses on a single grain to generate a similar array. However determined, a key issue is that the coefficients of any *T*-sensitive barometer or *P*-sensitive thermometer lead to a natural slope in *P-T* space. In the clinopyroxene-liquid example, the slope is not without meaning: the *P-T* arrays generated from Equations (30) or (31) yield the *T* at which a given liquid will become saturated with clinopyroxene at a given *P*—a clinopyroxene saturation surface.

Of potentially great interest is when such *P-T* slopes deviate from natural saturation conditions. For example, Putirka and Condit (2003) interpret near-isobaric extensions from the saturation *P-T* trend to represent episodes of magma stagnation, as magmas isobarically migrate down-*T* toward the ambient geotherm. A near-isothermal slope, in contrast, might indicate partial crystallization during a period of rapid vertical transport (Armienti et al. 2007). To make such interpretations, though, the observed *P-T* slope must deviate significantly from the intrinsic slope of mineral saturation. To make such a test, one could select a single equilibrium mineral-liquid pair to use as input, select an arbitrary range of temperatures, also to be used as input, and then use Equations (30) or (31) to calculate *P* for such conditions. The *P-T* array thus generated will represent the clinopyroxene saturation curve for that particular liquid. The difference between the slopes derived from different input compositions (as in Mordick and Glazner 2006) may thus also be used to derive model error on the *P-T* slope.

Error of treatment

Error of treatment is much more difficult to define than model error, since it depends upon how closely a natural system mimics experimental compositions and conditions. Because of the wide array of compositions that have been experimentally studied, over a very wide range of *P* and *T*, few natural conditions probably require model extrapolation. However, nearly all the models discussed in this chapter presume equilibration between a given mineral-melt or mineral-mineral pair. In natural systems, the pairing of equilibrium phases is not always clear. For example, in a lava flow, what is the liquid? Is it the whole rock? The glass? Some combination thereof? One might expect that the whole rock is the most appropriate "liquid" when considering phenocrysts. But this further presumes that the whole rock acted as a closed system.

The methods of Roeder and Emslie (1970) and Rhodes et al. (1979a) are key to testing for equilibrium. These tests are based on another assumption: two or more naturally occurring phases are equilibrated if their compositions yield exchange coefficients (e.g., $K_D(\text{Fe-Mg})^{ol\text{-}liq}$, $K_D(\text{Fe-Mg})^{ol\text{-}liq}$, $K_D(\text{Fe-Mg})^{cpx\text{-}opx}$), or predicted mineral compositions (Rhodes et al. 1979a; Putirka 1999), that mimic values determined in "equilibrium" (isothermal and isobaric) experiments. Fe-Mg exchange coefficients are commonly used since they appear to be largely independent of *P* or *T*. One strategy to estimate such error, then, is to estimate the standard deviation for *P-T* estimates for crystals that pass some such equilibration filter. If the error is less than model error then it is plausible that the crystals either precipitated from the liquid used as input, or a liquid much like it, which in any case should provide a useful *P-T* estimate. The hope then is that model error approaches true error.

Downloaded from http://pubs.geoscienceworld.org/msa/rimg/article-pdf/69/1/61/2948053/61_Putirka.pdf
by University of California Berkeley Library user
on 16 March 2024

Compositional corrections. If mineral compositions from a single lava flow yield a wide range of *P-T* estimates, then either the conditions of crystallization were not static (and differences in *P* and *T* are real and should not be averaged), or the minerals crystallized from different melts. In the later case, mineral-melt pairs might not yield "equilibrium" values for a particular exchange coefficient, and one could make a correction for open system processing. This correction could involve using the whole rock as a starting composition, then using mass balance equations to add or subtract observed phenocryst phases until a "calculated liquid" composition is derived that yields an equilibrium value for Fe-Mg exchange (between either olivine-liquid or clinopyroxene-liquid; Putirka 1997; Putirka and Condit 2003), or a better match between observed and calculated mineral components (Putirka and Condit 2003). These corrections can result in a very large shift in estimates of *P* and *T* compared to estimates based on observed (i.e., disequilibrium) mineral-whole rock or mineral-glass pairs. The assumption is that error is decreased by such corrections, since the calculated liquid composition is, by design, consistent with tests for equilibrium. But assuredly, error is attached to the calculation. The error must be in proportion to whether the calculated liquid represents an actual liquid composition. To estimate error, one could examine the variance of *P-T* estimates using observed magma compositions that are similar to calculated compositions. And temperatures derived from different equilibria should be better correlated with one another following such corrections.

The effects of disequilibrium. Since our thermometers and barometers are based on an assumption of equilibrium, any form of disequilibrium (such as pairing a given mineral with the wrong liquid) will yield errors. But how large are such errors? And how reliable are our tests for equilibrium? Cooling rate experiments (see review by Hammer 2008), conducted at constant *P*, but with a constantly changing *T*, provide an example of forced disequilibrium. Here, Equation (32c) is tested using cooling rate experiments on a lunar ferro-basalt by Grove and Bence (1979); the experiments were conducted at 1 atm (0.001 kbar) at cooling rates of 0.5 °C/hr to >600 °C/hr.

For these tests, *P* was calculated using the initial experimental *T*, and observed mineral and melt compositions as input. For the 12 experiments conducted at cooling rates of 0.5-10 °C/hr, Equation (32c) yields a *P* range of −1.82 to 1.86 kbar and a mean of −0.5±1.4 kbar—well within model error of 0.001 kbar (Fig. 14a), and with a standard deviation similar to the model error. One lesson is that not all negative values of *P* should be ignored—they may sometimes reflect the error that results when one attempts to predict a value that is effectively zero. Another is that error is apparently random (and so the mean estimate is better than any individual estimate). Still another is that at cooling rates ≤10 °C/hr, near-equilibrium conditions are apparently achieved, since the model recovers the equilibrium *P*. Still another lesson is relative to the use of the initial *T* as input into Equation (32c). If mean *T* or final experimental *T* is used as input, the slow cooling rate experiments do not yield a mean of 1 atm. Apparently, slowly diffusing species, such as Al, record and retain initial *P-T* conditions, and will not rapidly re-equilibrate, at least at lower temperatures. This means that, in practice, clinopyroxene-based barometers might be expected to yield information about the deeper parts of a magmatic system, and will not readily yield shallow *P-T* conditions unless precipitated at such conditions.

Also interesting is that at cooling rates ≥40 °C/hr, the mean of *P* estimates using Equation (32c) increases monotonically, to a value of 4.6 kbar at cooling rates >550 °C/hr (Fig. 14a). Equation (32c) makes use of the clinopyroxene-melt partition coefficient for Al, $D_{Al}^{cpx\text{-}liq}$, and this coefficient also increases with cooling rate, which provides the source for this 4.6 kbar error (Fig. 14b). The interpretation: at low cooling rates, $D_{Al}^{cpx\text{-}liq}$ retains its equilibrium value and so provides the correct *P* (on average); at higher cooling rates, higher values of $D_{Al}^{cpx\text{-}liq}$ are disequilibrium values (see Lofgren et al. 2006). (One intriguing implication is that if *P* and *T* are known, partition coefficients might be used to estimate cooling rates.)

Downloaded from http://pubs.geoscienceworld.org/msa/rimg/article-pdf/69/1/61/2948053/61_Putirka.pdf
by University of California Berkeley Library user
on 16 March 2024

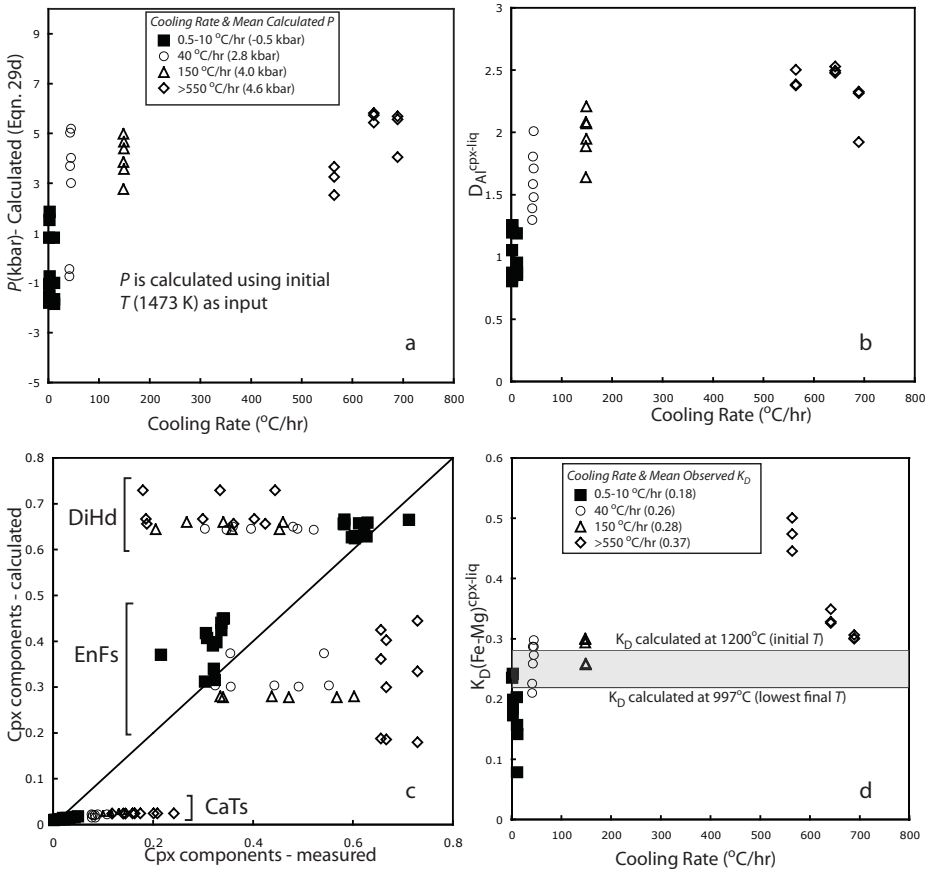

Figure 14. In (a) *P* is calculated using Equation (32c) for 1 atm cooling rate experiments (Grove and Bence 1979); initial experimental *T* (1200 °C) is used as input. Experiments conducted at cooling rates ≤10 °C/hr yield a mean value of −0.5 kbar, effectively equivalent to the actual value of 0.001 (or ca. 0) kbar. (b) As crystallization rates exceed 40 °C/hr, the error on *P* increases, due to the increase in the partition coefficient for Al. (c) The models of Putirka (1999) are used to predict the equilibrium values for the clinopyroxene components DiHd, EnFs and CaTs, using experimental *P, T* and liquid compositions as input. Only experiments conducted at cooling rates ≤10 °C/hr cluster near calculated equilibrium values. The graph is effectively identical if calculated rather than observed *P* (0.001 kbar for all) is used as input. (d) Observed values for $K_D(Fe\text{-}Mg)^{cpx\text{-}liq}$ are compared to cooling rate. The highest cooling rate experiments most strongly deviate from expected equilibrium values, but at lower cooling rates, Fe-Mg is a less effective discriminator for equilibrium as observed values for K_D closely match expected equilibrium values. The gray box shows the range of K_D values obtained from Equation (35) when using the highest *T* (initial *T* = 1200 °C) and the lowest of the final experimental *T* (975 °C) as input.

Can our tests for equilibrium effectively filter these disequilibrium cases (i.e., Roeder and Emslie 1970; Putirka 1999)? Figure 14c shows results for the models of Putirka (1999) when used to predict equilibrium clinopyroxene compositions for DiHd, EnFs, and CaTs (Fig. 14c), using initial *T* and observed *P* (0.001 kbar) as input. At the lower cooling rates, the measured components match closely the predicted equilibrium values, and at higher cooling rates, measured values deviate from equilibrium. So the test appears to be effective (Figure 14c is effectively identical when calculated *P*, instead of the observed 0.001 kbar, is used as input).

Downloaded from http://pubs.geoscienceworld.org/msa/rimg/article-pdf/69/1/61/2948053/61_Putirka.pdf
by University of California Berkeley Library user
on 16 March 2024

Values for $K_D(Fe\text{-}Mg)^{cpx\text{-}liq}$ are also affected by cooling rate (see Hammer 2008), and *P* derived from very high cooling rates could be rejected on the basis of such values. But at cooling rates as high as 150 °C/hr, observed values are close to the equilibrium value (0.28, when using initial *T* as input) and, curiously, low cooling rate experiments yield values that are too low on average, even if the final experimental *T* is used as input into Equation (35). Thus Fe-Mg exchange appears to be somewhat less effective a discriminator than DiHd, EnFs or CaTs, which may reflect the more rapid diffusion of Fe and Mg compared to Al and Ca. Various tests for equilibrium, at least in combination, should thus be successful at filtering erroneous results (Fig. 14), but further tests of this sort should help greatly to better delimit error.

CONCLUSIONS

A great number of igneous thermometers and barometers have been calibrated since T. W. Barth's early efforts to calibrate a two-feldspar thermometer. In light of a rather expansive experimental database (e.g., Hirschmann et al. 2008) we can now confidently calculate *T*, and in some cases *P*, for nearly any volcanic or other igneous system, using relatively simple models. The geologic limits of such methods are few. Nearly all the models presented here apply to rocks equilibrated between 700-1700 °C, 1 bar- to 40 or 70 kbar, with water contents ranging from 0-10 wt%. Liquid compositions range from basalt to rhyolite, from picrite to phonolite, from tephrite to trachyte, and everything in between. Thermometers and barometers can be used to calculate *T* and *P* to a precision of ±30 °C and ±1.5 kbar, respectively, for individual mineral-melt or mineral-mineral pairs. Cooling rate (disequilibrium) experiments further indicate that existing tests for equilibrium (i.e., Roeder and Emslie 1970; Rhodes et al. 1979b; Putirka 1999) are useful as filters against non-equilibrium mineral-melt pairs.

A natural question is: Can precision be increased? More clever activity models offer a seemingly slim hope; only the activity models of Wood and Banno (1973), Beattie (1993) and Nimis and Taylor (2000) prove their worth in this regard, yielding thermometric errors of ~25-30 °C. New experiments would aid the cases of the two-feldspar and two-pyroxene models, and clarify the potential for plagioclase barometry. But absent the development of experimental techniques that circumvent or subdue the obstacle of diffusion, increased precision might instead be accomplished by the calibration of models targeted to a narrow range of rock types, or geologic problems (using a narrow set of $P\text{-}T\text{-}X_i^j$ conditions). This should obviate the need for some of the compositional corrections that are required for thermometers and barometers intended for broad application.

To increase accuracy, model tests could also be conducted using natural samples, where *P-T* conditions are known. For example, Rosalind Helz (pers. comm.) reports that at Hawaii, sequential skylight sampling shows the growth of new silicate phases, as lavas flow and cool downstream. Geobarometers tend to yield 1 bar estimates in such cases (Putirka 2005b), even when they do not yield 1 atm estimates for all 1atm experimental studies; additional tests of this sort can provide compelling tests of accuracy and error for experimentally derived calibrations. Undoubtedly, similar or more clever tests could be devised using well characterized systems, such as at Mt. Etna, Mt. St. Helens, or Long Valley, etc., especially where new isotopic methods (Cooper and Reid 2008) indicate the presence of long-lived systems, yielding "long duration" (near-equilibrium?) experiments, mitigated, of course, by the potential problems of open system behavior.

ACKNOWLEDGMENTS

Thanks to Alex Speer for all is his aid in organizing various aspects of the short course and volume, and to Jodi Rosso for her many editorial efforts and endless patience in answering

Downloaded from http://pubs.geoscienceworld.org/msa/rimg/article-pdf/69/1/61/2948053/61_Putirka.pdf
by University of California Berkeley Library user
on 16 March 2024

questions. Thanks to my co-authors in this volume for their willingness to contribute. Finally, this chapter greatly benefited by thoughtful reviews and comments by Lawford Anderson, Cin-Ty Lee and Frank Tepley. This work was supported by NSF-EAR grants 0337345, 0421272 and 0313688.

REFERENCES

Agee CB, Walker D (1990) Aluminum partitioning between olivine and ultrabasic silicate liquid to 6 GPa. Contrib Mineral Petrol 105:243-254

Agee CB, Draper DS (2004) Experimental constraints on the origin of Martian meteorites and the composition of the Martian mantle. Earth Planet Sci Lett 224:415-429

Albarede F (1992) How deep to common basaltic magmas form and differentiate? J Geophys Res 97:10997-11009

Almeev RA, Holtz F, Koepke J, Parat F, Botcharnikov RE (2007) The effect of H_2O on olivine crystallization in MORB: experimental calibration at 200 MPa. Am Mineral 92:670-674

Anderson DL (1989) Theory of the Earth. Blackwell, Brookline Village, MA

Anderson JL, Barth AP, Wooden JL, Mazdab F (2008) Thermometers and thermobarometers in granitic systems. Rev Mineral Geochem 69:121-142

Ariskin AA (1999) Phase equilibria modeling in igneous petrology: use of COMAGMAT model for simulation fractionation of ferro-basaltic magmas and the genesis of high-alumina basalt. J Volcanol Geotherm Res 90:115-162

Ariskin AA, Barmina GS (1990) Equilibria thermometry between plagioclases and basalt or andesite magmas. Geochem Int 27:129-134

Armienti P, Tonarini S, Innocenti F, D'Orazio M (2007) Mount Etna pyroxene as tracer of petrogenetic processes and dynamics of the feeding system. *In:* Cenozoic Volcanism in the Mediterranean Area. Beccaluva L, Bianchini G, Wilson M (eds), Geol Soc Am Spec Paper 418:265-276

Arndt NT (1977) Partitioning of nickel between olivine and ultrabasic komatiite liquids. Carn Inst Wash Year Book 76:553-557

Auzanneau E, Vielzeuf D, Schmidt MW (2006) Experimental evidence of decompression melting during exhumation of subducted continental crust. Contrib Mineral Petrol 152:125-148

Bacon C, Carmichael ISE (1973) Stages in the P-T path of ascending basalt magma: an example from San Quintin, Baja California. Contrib Mineral Petrol 41:1-22

Baker RB, Eggler DH (1987) Compositions of anhydrous and hydrous melts coexisting with plagioclase, augite, and olivine or low-Ca pyroxene from 1 atm to 8 kbar: Application to the Aleutian volcanic center of Atka. Am Mineral 72:12-28

Baker MB, Grove TL, Price R (1994) Primitive basalts and andesites from the Mt. Shasta region, N. California: products of varying melt fraction and water content. Contrib Mineral Petrol 118:111-129

Barclay J, Carmichael ISE (2004) A hornblende basalt from western Mexico: water saturated phase relations constrain a pressure-temperature window of eruptibility. J Petrol 45:485-506

Barnes SJ (1986) The distribution of chromium among orthopyroxene, spinel and silicateliquid at atmospheric pressure. Geochim Cosmochim Acta 50:1889-1909

Bartels KS, Kinzler RJ, Grove TL (1991) High pressure phase relations of primitive high-alumina basalts from Medicine Lake volcano, northern California. Contrib Mineral Petrol 108:253-270.

Barth TW (1934) Temperatures in lavas and magmas and a new geologic thermometer. Naturen 6:187-192

Barth TW (1951) The feldspar geologic thermometers. Neues Jahrb Mineral 82:143-154

Barth TW (1962) The feldspar geologic thermometers. Norsk Geol Tidsskr 42:330-339

Barth TW (1968) Additional data for the two-feldspar geothermometer. Lithos1:21-22

Beattie P (1993) Olivine-melt and orthopyroxene-melt equilibria. Contrib Mineral Petrol 115:103-111

Becquerel AC (1826) Procédé a l'aide duquel on peut mesurer d'intensité d'un courant électrique. Ann Chim Phys 31:371

Beddoe-Stephens B, Aspden JA, Shepherd TJ (1983) Glass inclusions and melt compositions of the Toba tuffs, northern Sumatra. Contrib Mineral Petrol 83:278-287

Bender JF, Langmuir CH, Hanson GN (1984) Petrogenesis of basalt glasses from the Tamayo Region, East Pacific Rise. J Petrol 25:213-254

Benisek A, Kroll H, Cemic L (2004) New developments in two-feldspar thermometry. Am Mineral 89:1496-1504

Berndt J, Holtz F, Koepke J (2001) Experimental constraints on storage conditions in the chemically zoned phonolitic magma chamber of the Laacher See volcano. Contrib Mineral Petrol 140:469-486

Blatter DL, Carmichael ISE (2001) Hydrous phase equilibria of a Mexican high-silica andesite: A candidate for a mantle origin? Geochim Cosmochim Acta 65:4043-4065

Downloaded from http://pubs.geoscienceworld.org/msa/rimg/article-pdf/69/1/61/2948053/61_Putirka.pdf
by University of California Berkeley Library user
on 16 March 2024

Blundy J, Cashman K (2008) Petrologic reconstruction of magmatic system variables and processes. Rev Mineral Geochem 69:179-239
Blundy J, Cashman K, Humphreys M (2006) Magma heating by decompression-driven crystallization beneath andesite volcanoes. Nature 443:76-80
Bottinga Y, Weill DF (1972) The viscosity of magmatic silicate liquid, a model for calculation. Am J Sci 272:438-475
Bowen NL (1913) The melting phenomena of the plagioclase feldspars. Am J Sci 35:577-599
Bowen NL (1914) The ternary system: diopside-forsterite-silica. Am J Sci 38:270-264
Bowen NL (1915) The later stages of the evolution of the igneous rocks. J Geology Supp 8, 23:1-91
Bowen NL, Tuttle OF (1950) The system $NaAlSi_3O_8$-$KAlSi_3O_8$-H_2O. J Geol 489-511
Box GEP, Draper, NR (1987) Empirical Model-Building and Response Surfaces. Wiley, New York
Brey GP, Kohler T (1990) Geothermobarometry in four-phase lherzolites II. New thermobarometers, and practical assessment of existing thermobarometers. J Petrol 31:1353-1378
Buddington AF, Fahey J, Vlisdis A (1955) Thermometric and petrogenetic significance of titaniferous magnetite. Am J Sci 253:497-532
Buddington AF, Lindsley DH (1964) Iron-titanium oxide minerals and synthetic equivalents. J Petrol 5:210-357
Bulatov VK, Girnis AV, Brey GP (2002) Experimental melting of a modally heterogeneous mantle. Mineral Petrol 75:131-152
Canil D (1999) The Ni-in-garnet geothermometer: calibration at natural abundances. Contrib Mineral Petrol 136:240-246
Carmichael ISE, Nicholls J, Smith AL (1970) Silica activity in igneous rocks. Am Mineral 55:246-263
Carmichael I.S.E., Turner FJ, Verhoogen J (1974) Igneous Petrology. McGraw-Hill Book Company, New York
Castellan GW (1971) Physical Chemistry, 2nd ed. Addison-Wesley, Reading, Massachusetts
Chen HK, Delano JW, Lindsley DH (1982) Chemistry and phase relations of VLT volcanic glasses from Apollo 14 and Apollo 17. Proc Lunar Planet Sci Conf 13:A171-A181
Cooper KM, Reid MR (2008) Uranium-series crystal ages. Rev Mineral Geochem 69:479-554
Dann JC, Holzheid AH, Grove TL, McSween HY (2001) Phase equilibria of the Shergotty meteorite: Constraints on pre-eruptive water contents of Martian magmas and fractional crystallization under hydrous conditions. Meteorit Planet Sci 36:793-806
Dasgupta R, Hirschmann MM, Smith N (2007) Partial melting experiments of peridotite + CO_2 at 3 GPa and genesis of alkalic ocean island basalts. J Petrol 48:2093-2124
Daubeny C (1835) Some account of the eruption of Vesuvius, which occurred in the month of August 1834, extracted from the manuscript notes of the Cavaliere Monticelli, foreign member of the Geological Society; together with a statement of the products of the eruption and of the condition of the volcano subsequently to it. Philos Trans R Soc London 125:153-159
Davis BTC, Boyd DR (1966) The join $Mg_2Si_2O_6$-$CaMgSi_2O_6$ at 30 kilobars pressure and its application to pyroxenes from kimberlites. J Geophys Res 71:3567-3576
Day AL, Allen ET (1905) The isomorphism and thermal properties of the feldspars. Am J Sci 14:93-131
Delano JW (1977) Experimental melting relations of 63545, 76015, and 76055. Proc Lunar Planet Sci Conf 8:2097-2123
Di Carlo I, Pichavant M, Rotolo SG, Scaillet B (2006) Experimental crystallization of a high-K arc basalt: the golden pumice, Stromboli Volcano (Italy). J Petrol 47:1317-1343
Doelter C (1902) Die chemische Zusammensetzung und die Genesis der Monzonigesteine. Tscher Mineral Petrograph Mitteilung 21:191-225
Drake MJ (1976) Plagioclase-melt equilibria. Geochim Cosmochim Acta 40:457-465
Draper DS, Green TH (1997) P-T phase relations of silicic, alkaline, aluminous mantle-xenolith glasses under anhydrous and C-O-H fluid-saturated conditions. J Petrol 38:1187-1224
Draper DS, Green TH (1999) P-T phase relations of silicic, alkaline, aluminous liquids: new results and applications to mantle melting and metasomatism. Earth Planet Sci Lett 170:255-268
Draper DS, Johnston AD (1992) Anhydrous PT phase relations of an Aleutian high-MgO basalt; an investigation of the role of olivine-liquid reaction in the generation of arc high-alumina basalts. Contrib Mineral Petrol 112:501-519
Dungan MA, Long PE, Rhodes JM (1978) Magma mixing at mid-ocean ridges: evidence from legs 45 and 45-DSDP. Geophys Res Lett 5:423-425
Dunn T, Sen C (1994) Mineral/matrix partition coefficient for orthopyroxene, plagioclase, and olivine in basaltic to andesitic systems: a combined analytical and experimental study. Geochim Cosmochim Acta 58:717-733
Elkins-Tanton LT, Draper DS, Agee CB, Jewell J, Thorpe A, Hess PC (2007) The last lavas erupted during the main phase of the Siberian flood volcanic province: results from experimental petrology. Contrib Mineral Petrol 153:191-209

Downloaded from http://pubs.geoscienceworld.org/msa/rimg/article-pdf/69/1/61/2948053/61_Putirka.pdf
by University of California Berkeley Library user
on 16 March 2024

Elkins LT, Fernandes VA, Delano JW, Grove TL (2000) Origin of lunar ultramafic green glasses: Constraints from phase equilibrium studies. Geochim Cosmochim Acta 64:2339-2350

Elkins LT, Grove TL (1990) Ternary feldspar experiments and thermodynamic models. Am Mineral 75:544-559

Elkins-Tanton, LT, Chatterjee N, Grove TL (2003) Experimental and petrological constraints on lunar differentiation from the Apollo 15 green picritic glasses. Meteorit Planet Sci 38:515-527

Essene EJ (1982) Geologic thermometry and barometry. Rev Mineral 10:153-206

Elthon D, Scarfe CM (1984) High-pressure phase equilibria of a high-magnesia basalt and the genesis of primary oceanic basalts. Am Mineral 69:1-15

Esperança S, Holloway JR (1987) On the origin of some mica-lamprophyres; experimental evidence from a mafic minette. Contrib Mineral Petrol 95:207-216

Falloon, TJ, Danyushevsky LV (2000) Melting of refractory mantle at 1.5, 2 and 2.5 GPa under anhydrous and H_20-undersaturated conditions: implications for the petrogenesis of high-Ca boninites and the influence of subduction components on mantle melting. J Petrol 41:257-283

Falloon TJ, Danyushevsky LV, Green DH (2001) Peridotite melting at 1 GPa; reversal experiments on partial melt compositions produced by peridotite-basalt sandwich experiments. J Petrol 42:2363-2390

Falloon TJ, Green DH (1987) Anhydrous partial melting of MORB pyrolite and other peridotite compositions at 10 kbar; implications for the origin of primitive MORB glasses. Mineral Petrol 37:181-219

Falloon TJ, Green DH, Danyushevsky LV, Faul UH (1999) Peridotite melting at 1.0 and 1.5 GPa: an experimental evaluation of techniques using diamond aggregates and mineral mixes for determination of near-solidus melts. J Petrol 40:1343-1375

Falloon TJ, Green DH, Hatton CJ, Harris KL (1988) Anhydrous partial melting of a fertile and depleted peridotite from 2 to 30 Kb and application to basalt petrogenesis. J Petrol 29:1257-1282

Falloon TJ, Green DH, O-Neill H-St, Hibberson WO (1997) Experimental tests of low degree peridotite partial melt compositions; implications for the nature of anhydrous near-solidus peridotite melts at 1 GPa. Earth Planet Sci Lett 152:149-162

Feig ST, Koepke J, Snow JE (2006) Effect of water on tholeiitic basalt phase equilibria: an experimental study under oxidizing conditions. Contrib Mineral Petrol 152:611-638

Fodor RV, Galar P (1997) A view into the subsurface of Mauna Kea Volcano, Hawaii: crystallization processes interpreted through the petrology and petrography of gabbroic and ultramafic xenoliths. J Petrol 38:581-624

Foulger GR, Natland JH (2003) Is "hotspot" volcanism a consequence of plate tectonics? Science 300:921-922

Fram MS, Longhi J (1992) Phase equilibria of dikes associated with Proterozoic anorthosite complexes. Am Mineral 77:605-616

Frey FA, Garcia MO, Wise WS, Kennedy A, Gurriet P, Albarede F (1991) The evolution of Mauna Kea volcano, Hawaii: petrogenesis of tholeiitic and alkalic basalts. J Geophys Res 96:14347-14375

Frey FA, Wise WS, Garcia MO, West H, Kwon S-T, Kennedy A (1990) Evolution of Mauna Kea volcano, Hawaii: petrologic and geochemical constraints on postshield volcanism. J Geophys Res 95:1271-1300

Fuhrman ML, Lindsley DH (1988) Ternary-feldspar modeling and thermometry. Am Mineral 73:201-215

Fujii T, Bougault H (1983) Melting relations of a magnesian abyssal tholeiite and the origin of MORBs. Earth Planet Sci Lett 62:283-295

Gaetani GA, Grove T (1998) The influence of melting of mantle peridotite. Contrib Mineral Petrol 131:323-346

Garcia MO, Ho RA, Rhodes JM, Wolfe EW (1989) Petrologic constraints on rift-zone processes: results from episode 1 of the Pu'u O'o eruption of Kilauea volcano, Hawaii. Bull Volcanol 52:81-96

Garcia MO, Hulsebosch TP, Rhodes JM (1995) Olivine-rich submarine basalts from the southwest rift zone of Mauna Loa Volcano: implications for magmatic processes and geochemical evolution. *In:* Mauna Loa Revealed: Structure, Composition, History, and Hazards. Rhodes JM, Lockwood JP (eds) AGU Geophysical Monograph 92:219-239

Garcia MO, Rhodes JM, Wolfe EW, Ulrich GE, Ho RA (1992) Petrology of lavas from episodes 2-47 of the Pu'u O'o eruption of Kilauea Volcano, Hawaii: evolution of magmatic processes. Bull Volcanol 55:1-16

Gardner JE, Rutherford M, Carey S, Sigurdsson H (1995) Experimental constraints on pre-eruptive water contents and changing magma storage prior to explosive eruptions of Mount St Helens volcano. Bull Volcanol 57:1-17

Gee LL, Sack RO (1988) Experimental petrology of melilite nephelinites. J Petrol 29:1233-1255

Gerke TL, Kilinc AI (1992) Enrichment of SiO_2 in rhyolites by fractional crystallization: an experimental study of peraluminous granitic rocks from the St. Francois Mountains, Missouri, USA. Lithos 29:273-283

Ghiorso MS (1987) Modeling magmatic systems: thermodynamic relations. Rev Mineral 17:443-465

Ghiorso MS, Hirschmann MM, Reiners PW, Kress VC III (2002) The pMELTS: a revision of MELTS for improved calculation of phase relations and major element partitioning related to partial melting of the mantle to 3 GPa. Geochem Geophys Geosyst 3:1-36, 10.1029/2001GC000217

Downloaded from http://pubs.geoscienceworld.org/msa/rimg/article-pdf/69/1/61/2948053/61_Putirka.pdf
by University of California Berkeley Library user
on 16 March 2024

Glazner AF (1984) Activities of olivine and plagioclase components in silicate melts and their application to geothermometry. Contrib Mineral Petrol 88:260-268
Green DH, Ringwood AE (1967) The genesis of basaltic magmas. Contrib Mineral Petrol 15:103-190
Grove TL, Beaty DW (1980) Classification, experimental petrology and possible volcanic histories of the Apollo 11 high-K basalts. Proc Lunar Planet Sci Conf 11:149-177
Grove TL, Bence AE (1979) Crystallization kinetics in a multiply saturated basalt magma: an experimental study of Luna 24 ferrobasalt. Proc Lunar Planet Sci Conf 10:439-478
Grove TL, Bryan WB (1983) Fractionation of pyroxene-phyric MORB at low pressure: an experimental study. Contrib Mineral Petrol 84:293-309
Grove TL, Donnelly-Nolan, JM Housh T (1997) Magmatic processes that generated the rhyolite of Glass Mountain, Medicine lake volcano, N. California. Contrib Mineral Petrol 127:205-223
Grove TL, Elkins-Tanton LT, Parman SW, Chatterjee N, Müntener O, Gaetani GA (2003) Fractional crystallization and mantle-melting controls on calk-alkaline differentiation trends. Contrib Mineral Petrol 145:515-533
Grove TL, Gerlach DC, Sando TW (1982) Origin of calc-alkaline series lavas at Medicine Lake Volcano by fractionation, assimilation and mixing. Contrib Mineral Petrol 80:160-182
Grove TL, Juster TC (1989) Experimental investigations of low-Ca pyroxene stability and olivine-pyroxene-liquid equilibria at 1-atm in natural basaltic and andesitic liquids. Contrib Mineral Petrol 103:287-305
Grove TL, Kinzler RJ, Bryan WB (1990) Natural and experimental phase relations of lavas from Serocki Volcano. Proc Ocean Drill Prog 106/109:9-17
Grove TL, Kinzler RJ, Bryan WB (1992) Fractionation of mid-ocean ridge basalt (MORB). *In:* Mantle Flow and Melt Generation at Mid-Ocean Ridges. Phipps Morgan J, Blackman, DK, Sinton JM (eds) AGU Geophysical Monograph Series 7:281-310
Grove TL, Raudsepp M (1978) Effects of kinetics on the crystallization of quartz normative basalt 15597: an experimental study. Proc Lunar Planet Sci Conf 9:585-599
Gudfinnsson GH, Presnall DC (1996) Melting relations of model lherzolite in the system CaO-MgO-Al_2O_3-SiO_2 at 2.4-3.4 GPa and the generation of komatiites. J Geophys Res 101:27701-27709
Haase KM (1996) The relationships between the age of the lithosphere and the composition of oceanic magmas: constraints on partial melting, mantle sources and the thermal structure of the plates. Earth Planet Sci Lett 144:75-92
Hakli TA, Wright TL (1967) The fractionation of nickel between olivine and augite as a geothermometer. Geochim Cosmochim Acta 31:877-884
Hamada M, Fuji T (2007) H_2O-rich island arc low-K tholeiite magma inferred from Ca-rich plagioclase-melt inclusion equilibria. Geochem J 41:437-461
Hall J (1798) Experiments on whinstone and lava. Proc R Soc Edinburgh 5:43-74
Hammer JE (2008) Experimental studies of the kinetics and energetic of magma crystallization. Rev Mineral Geochem 69:9-59
Hammer JE, Rutherford MJ, Hildreth W (2002) Magma storage prior to the 1912 eruption at Novarupta, Alaska. Contrib Mineral Petrol 144:144-162
Hansteen TH, Klügel A (2008) Fluid inclusion thermobarometry as a tracer for magmatic processes. Rev Mineral Geochem 69:143-177
Helz RT (1976) Phase relations of basalts in their melting ranges at P_{H2O} = 5kb. Part II. Melt compositions. J Petrol 17:139-193
Helz RT, Thornber CR (1987) Geothermometry of Kilauea Iki lava lake, Hawaii. Bull Volcanol 49:651-668
Herzberg C, Asimow PD, Arndt N, Niu Y, Lesher CM, Fitton JG, Cheadle MJ, Saunders AD (2007) Temperature in ambient mantle and plumes: constraints form basalts, picrites and komatiites. Geochem Geoophys Geosyst 8:10.1029/2006GC001390
Herzberg CT, Chapman NA (1976) Clinopyroxene geothermometry of spinel-lherzolites. Am Mineral 61:626-637
Herzberg C, O'Hara MJ (1998) Phase equilibrium constraints on the origin of basalts, picrites and komatiites. Earth Sci Rev 44:39-79
Herzberg C, O'Hara MJ (2002) Plume-associated ultramafic magmas off Phanerozoic age. J Petrol 43:1857-1883
Hess H (1962) History of the ocean basins. *In:* Petrologic Studies: A Volume in Honor of A.F. Buddington. Engle AE, James HL, Leonard BF (eds) GSA Special Volume,p 599-620
Hesse M, Grove TL (2003) Absarokites from the western Mexican Volcanic Belt: constraints on mantle wedge conditions. Contrib Mineral Petrol 146:10-27
Hill DP, Zucca JJ (1987) Geophysical constraints on the structure of Kilauea and Mauna Loa volcanoes and some implications for seismomagmatic processes. USGS Surv Prof Paper 1350:903-917
Hirschmann MM, Ghiorso MS, Davis FA, Gordon SM, Mukherjee S, Grove TL, Krawczynski M, Medard E, Till CB (2008) Library of experimental phase relations: a database and web portal for experimental magmatic phase equilibria data. Geochem Geophys Geosyst 9, Q03011, doi:10.1029/2007GC001894

Downloaded from http://pubs.geoscienceworld.org/msa/rimg/article-pdf/69/1/61/2948053/61_Putirka.pdf
by University of California Berkeley Library user
on 16 March 2024

Holbig ES, Grove TL (2008) Mantle melting beneath the Tibetan Plateau: Experimental constraints on ultrapotassic magmatism. J Geophys Res doi:10.1029/2007JB005149

Holtz F, Becker A, Freise M, Johannes W (2001) The water-undersaturated and dry Qz-Ab-Or system revisited. Experimental results at very low water activities and geological implications. Contrib Mineral Petrol 141:347-357

Holtz F, Sato H, Lewis J, Behrens H, Nakada S (2005) Experimental Petrology of the 1991-19995 Unzen Dacite, Japan. Part I: Phase relations, phase composition, and pre-eruptive conditions. J Petrol 46:319-337

Housh TB, Luhr JF (1991) Plagioclase-melt equilibria in hydrous systems. Am Mineral 76:477-492

Jaggar TA (1917) Thermal gradient of Kilauea lava lake. Wash Acad Sci 7:397-405

Jefferys WH, Berger JO (1992) Ockham's razor and Bayesian analysis. Am J Sci 80:64-72

Johnson KTM (1998) Experimental determination of partition coefficients for rare earth and high-field-strength elements between clinopyroxene, garnet, and basaltic melt at high pressures. Contrib Mineral Petrol 133:60-68

Johnston AD (1986) Anhydrous P-T phase relations of near-primary high-alumina basalt from the South Sandwich Islands. Contrib Mineral Petrol 92:368-382

JMP, Statistics and Graphics Guide (2002), Version 5, SAS Institute, Cary, NC, USA

Joly J (1891) On the determination of the melting points of minerals, Part 1. Uses of the meldometer. Proc R Irish Acad 2:38

Jurewicz AJG, Mittlefehldt DW, Jones JH (1993) Experimental partial melting of the Allende (CV) and Murchison (CM) chondrites and the origin of asteroidal basalts. Geochim Cosmochim Acta 57:2123-2139

Juster CT, Grove TL, Perfit MR (1989) Experimental constraints on the generation of FeTi basalts, andesite, and rhyodacites at the Galapagos Spreading Center, 85°W and 95°W. J Geophys Res 94:9251-9274

Kawamoto T, Hervig RL, Holloway JR (1996) Experimental evidence for a hydrous transition zone in the early Earth's mantle. Earth Planet Sci Lett 142:587-592

Kelemen PB, Joyce DB, Webster JD, Holloway JR (1990) Reaction between ultramafic rock and fractionating basaltic magma II. Experimental investigation of reaction between olivine tholeiite and harzburgite at 1150-1050 °C and 5kb. J Petrol 31:99-134

Kennedy AK, Grove TL, Johnson RW (1990) Experimental and major element constraints on the evolution of lavas from Lihir Island, Papua New Guinea. Contrib Mineral Petrol 104:722-734.

Keshav S, Gudfinnsson GH, Sen G, Fei Y (2004) High-pressure melting experiments on garnet clinopyroxenite and the alkalic to tholeiitic transition in ocean-island basalts. Earth Planet Sci Lett 223:365-379

Kinzler RJ, Grove TL (1985) Crystallization and differentiation of Archean komatiite lavas from northeast Ontario: phase equilibrium and kinetic studies. Am Mineral 70:40-51

Kinzler RJ (1997) Melting of mantle peridotite at pressures approaching the spinel to garnet transition: Application to mid-ocean ridge basalt petrogenesis. J Geophys Res 102:853-874

Kinzler RJ, Grove TL (1992) Primary magmas of mid-ocean ridge basalts 1. Experiments and methods. J Geophys Res 97:6885-6906

Kjarsgaard BA (1998) Phase relations of a carbonated high-CaO nephelinite at 0.2 and 0.5 GPa. J Petrol 39:061-2075

Klein EM, Langmuir CH (1987) Global correlations of ocean ridge basalt chemistry with axial depth and crustal thickness. J Geophys Res 92:8089-8115

Klemme S, O'Neil HSC (2000) The near-solidus transition from garnet lherzolite to spinel lherzolite. Contrib Mineral Petrol 138:237-248

Klügel A, Klein F (2005) Complex storage and ascent at embryonic submarine volcanoes from the Madeira Archipelago. Geology 34:337-340

Koester E, Pawley AR, Fernandes LA, Porcher CC, Soliani Jr E (2002) Experimental melting of cordierite gneiss and the petrogenesis of syntranscurrent peraluminous granites in southern Brazil. J Petrol 43:1595-1616

Kogi R, Müntener O, Ulmer P, Ottolini L (2005) Piston-cylinder experiments on H_2O undersaturated Fe-bearing systems: an experimental setup approaching fO_2 conditions of natural calc-alkaline magmas. Am Mineral 90:708-717

Kogiso T, Hirose K, Takahashi E (1998) Melting experiments on homogeneous mixtures of peridotite and basalt; application to the genesis of ocean island basalts. Earth Planet Sci Lett 162:45-61

Kogiso T, Hirschmann MM (2001) Experimental study of clinopyroxenite partial melting and the origin of ultra-calcic melt inclusions. Contrib Mineral Petrol 142:347-360

Kohn MT, Spear FJ (1991) Error propagation for barometers: 2. Applications to rocks. Am Mineral 76:138-147

Kudo AM, Weill DF (1970) An igneous plagioclase thermometer. Contrib Mineral Petrol 25:52-65

Kushiro I (1996) Partial melting of a fertile mantle peridotite at high pressures: an experimental study using aggregates of diamond. *In:* Earth Processes: Reading the Isotopic Code. Baso A, Hart S (eds) AGU Geophysical Monograph 95:109-122

Downloaded from http://pubs.geoscienceworld.org/msa/rimg/article-pdf/69/1/61/2948053/61_Putirka.pdf
by University of California Berkeley Library user
on 16 March 2024

Kushiro I, Mysen B (2002) A possible effect of melt structure on the Mg-Fe^{2+} partitioning between olivine and melt. Geochim Cosmochim Acta 66:2267-2272
Kushiro I, Walter MJ (1998) Mg-Fe partitioning between olivine and mafic-ultramafic Melts. Geophys Res Lett 25:2337-2340
Langmuir CH, Hanson GN (1980) An evaluation of major element heterogeneity in the mantle sources of basalts. Phil Trans R Soc Lond A 297:383-407
Laporte D, Toplis MJ, Seyler M, Devidal J-L (2004) A new experimental technique for extracting liquids from peridotite at very low degrees of melting: application to partial melting of depleted peridotite. Contrib Mineral Petrol 146:463-484
Leeman WP, Lindstrom DJ (1978) Partitioning of Ni^{2+} between basaltic and synthetic melts and olivines – an experimental study. Geochim Cosmochim Acta 42:801-816
Lesher CE, Walker D (1988) Cumulate maturation and melt migration in a temperature gradient. J Geophys Res 93:10295-10311
Lindsley DH (1983) Pyroxene thermometry. Am Mineral 68:477-493
Lindsley DH, Anderson DJ (1983) A two-pyroxene thermometer. J Geophys Res 88:A887-A906
Liu TC, Chen BR, Chen CH (1998) Anhydrous melting experiment of a Wannienta basalt in the Kuanyinshan area, northern Taiwan, at atmospheric pressure. Terr Atm Ocean Sci 9:165-182
Liu TC, Chen BR, Chen, CH (2000) Melting experiment of a Wannienta basalt in the Kuanyinshan area, northern Taiwan, at pressures up to 2.0 GPa. J Asian Earth Sci 18:519-531
Lofgren GE, Huss GR, Wasserburg GJ (1006) An experimental study of trace-element partitioning between Ti-Al-clinopyroxene and melt: equilibrium and kinetic effects including sector zoning. Am Mineral 91:1596-1606
Longhi J (1976) Iron, Magnesium, and Silica in Plagioclase. Ph.D. Thesis, Harvard University, 296 pp
Longhi J (1995) Liquidus equilibria of some primary lunar and terrestrial melts in the garnet stability field. Geochim Cosmochim Acta 59:2375-2386
Longhi J (2002) Some phase equilibrium systematics of lherzolite melting: I. Geochem Geophys Geosys 3:doi:10.1029/2001GC000204
Longhi J, Pan V (1988) A reconnaissance study of phase boundaries in low-alkali basaltic liquids. J Petrol 29:115-147
Longhi J, Pan V (1989) The parent magmas of the SNC meteorites. Proc Lunar Planet Sci Conf 19:451-464
Loomis TP (1979) An empirical model for plagioclase equilibrium in hydrous melts. Geochim Cosmochim Acta 43:1753-1759
Maaloe S (2004) The PT-phase relations of an MgO-rich Hawaiian tholeiite: the compositions of primary Hawaiian tholeiites. Contrib Mineral Petrol 148:236-246
Mahood GA, Baker DR (1986) Experimental constraints on depths of fractionation of mildly alkalic basalts and associated felsic rocks: Pantelleria, Strait of Sicily. Contrib Mineral Petrol 93:251-264
Marsh BD (1995) Solidification fronts and magmatic evolution. Mineral Mag 60:5-40
Marsh BD, Fournelle J, Myers JD, Chou I-M. (1990) On plagioclase thermometry in island-arc rocks: experiments and theory. *In:* Fluid-Mineral interactions: A Tribute to H.P. Eugster. Spencer RJ, Chou I-M (eds) Geochemical Society Special Publication 2:65-83
Martel C, Pichavant M, Holtz F, Scaillet B, Bourdier J, Traineau H (1999) Effects of fO_2 and H_2O on andesite phase relations between 2 and 4 kbar. J Geophys Res 104:29453 29470
Mathez EA (1973) Refinement of the Kudo-Weill plagioclase thermometer and its applications to basaltic rocks. Contrib Mineral Petrol 41:61-72
McKenzie D, Bickle MJ (1988) The volume and composition of melt generated by extension of the lithosphere. J Petrol 29:625-679
McCoy TJ, Lofgren GE (1999) Crystallization of the Zagami shergottite: an experimental study. Earth Planet Sci Lett 173:397-411
McDade P, Blundy JD, Wood BJ (2003) Trace element partitioning on the Tinaquillo lherzolite solidus at 1.5 GPa. Phys Earth Planet Interior 139:129-147
Medard E, Grove TL (2008) The effect of H_2O on the olivine liquidus of basaltic melts: experiments and thermodynamic models. Contrib Mineral Petrol 155:417-432
Medard E, Schmidt MW, Schiano P (2004) Liquidus surfaces of ultracalcic primitive melts: formation conditions and sources. Contrib Mineral Petrol 148:201-215
Meen JK (1987) Formation of shoshonites from calcalkaline basalt magmas: geochemical and experimental constraints from the type locality. Contrib Mineral Petrol 97:333-351
Meen JK (1990) Elevation of potassium content of basaltic magma by fractional crystallization: the effect of pressure. Contrib Mineral Petrol 104:309-331
Mercier J-C, Beoit V, Girardeau J (1984) Equilibrium state of diopside-bearing harzburgites from ophiolites: geobarometric and geodynamic implications. Contrib Mineral Petrol 85:391-403
Mibe K, Fuji T, Yasuda A, Ono S (2005) Mg-Fe partitioning between olivine and ultramafic melts at high pressure. Geochim Cosmochim Acta 70:757-766

Downloaded from http://pubs.geoscienceworld.org/msa/rimg/article-pdf/69/1/61/2948053/61_Putirka.pdf
by University of California Berkeley Library user
on 16 March 2024

Milholland CS, Presnall DC (1998) Liquidus phase relations in the CaO-MgO-Al_2O_3-SiO_2 system at 3.0 GPa: the aluminous pyroxene thermal divide and high pressure fractionation of picritic and komatiitic magmas. J Petrol 39:3-27

Minitti ME, Rutherford MJ (2000) Genesis of the Mars Pathfinder sulfur-free rock from SNC parental liquids. Geochim Cosmochim Acta 64:2535-2547

Montierth C, Johnston AD, Cashman KV (1995) An empirical glass-composition-based geothermometer for Mauna Loa lavas. *In:* Mauna Loa Revealed: Structure, Composition, History, and Hazards. Rhodes JM, Lockwood JP (eds) AGU Geophysical Monograph 92:207-217

Moore G, Carmichael ISE (1998) The hydrous phase equilibria (to 3 kbar) of an andesite and basaltic andesite from western Mexico: constraints on water content and conditions of phenocryst growth. Contrib Mineral Petrol 130:304-319

Mordick BE, Glazner AF (2006) Clinopyroxene thermobarometry of basalts from the Coso and Big Pine volcanic fields, California. Contrib Mineral Petrol doi 10.1007s00410-006-0097-0

Morgan WJ (1971) Convection plumes in the lower mantle. Nature 230:42-43

Morse SA, Brady JB, Sporleder BA (2004) Experimental petrology of the Kiglapait Intrusion; cotectic trace for the lower zone at 5 kbar in graphite. J Petrol 45:2225-2259

Müntener O, Kelemen PB, Grove TL (2001) The role of H_2O during crystallization of primitive arc magmas under uppermost mantle conditions and genesis of igneous pyroxenites: and experimental study. Contrib Mineral Petrol 141:643-658

Musselwhite DS, Dalton HA, Kiefer WS, Treiman AH (2006) Experimental petrology of the basaltic shergottite Yamato-980459: Implications for the thermal structure of the Martian mantle. Meteorit Planet Sci 41:1271-1290

Naney MT (1983) Phase equilibria of rock-forming ferromagnesian silicates in granitic Systems. Am J Sci 283:993-1033

Nicholls J, Carmichael ISE (1972) The equilibration temperature and pressure of various lava types with spine- and garnet-peridotite. Am Mineral 57:941-959

Nicholls J, Carmichael ISE, Stormer JC (1971) Silica activity and P_{total} in igneous rocks. Contrib Mineral Petrol 33:1-20

Nielsen RL, Drake MJ (1979) Pyroxene-melt equilibria. Geochim Cosmochim Acta 43:1259-1272

Nimis P (1995) A clinopyroxene geobarometer for basaltic systems based on crystals-structure modeling. Contrib Mineral Petrol 121:115-125

Nimis P (1999) Clinopyroxene geobarometry of magmatic rocks. Part 2. Structural geobarometers for basic to acid, tholeiitic and mildly alkaline systems. Contrib Mineral Petrol 135:62-74

Nimis P, Taylor WR (2000) Single clinopyroxene thermobarometry for garnet peridotites. Part 1 Calibration and testing of a Cr-in-cpx barometer and an enstatite-in-cpx thermometer. Contrib Mineral Petrol 139:541-554

Nimis P, Ulmer P (1998) Clinopyroxene geobarometry of magmatic rocks. Part 1: an expanded structural geobarometer for anhydrous and hydrous basic and ultrabasic systems. Contrib Mineral Petrol 133:122-135

Nordstrom DK, Munoz JL (1986) Geochemical Thermodynamics. Blackwell, Brookline, Massachusetts

O'Nions RK, Powell R (1977) The thermodynamics of trace element distribution. *In:* Thermodynamics in Geology. Fraser DG (ed) Reidel, Dordrecht-Holland, p 349-363

Panjasawatwong Y, Danyushevsky LV, Crawford AJ, Harris KL (1995) An experimental study of the effects of melt composition on plagioclase-melt equilibria at 5 and 10 kbar: implications for the origin of magmatic high-An plagioclase. Contrib Mineral Petrol 118:420-432.

Papike JJ, Cameron KL, Baldwin K (1974) Amphiboles and pyroxenes: characterization of other than quadrilateral components and estimates of ferric iron from microprobe data. Geol Soc Am Abst Prog 6:1053-1054

Parman SW, Dann JC, Grove TL, deWit MJ (1997) Emplacement conditions of komatiite magmas from the 3.49 Ga Komati Formation, Barberton Greenstone Belt, South Africa. Earth Planet Sci Lett 150:303-323

Parman SW, Grove TL (2004) Harzburgite melting with and without H_2O: experimental data and predictive modeling. J Geophys Res 109:doi:10.1029/2003JB002566

Parsons T, Thompson, GA (1993) Does magmatism influence low-angle normal faulting? Geology 21:247-250

Patino-Douce AE (1995) Experimental generation of hybrid silicic melts by reaction of high-Al basalt with metamorphic rocks. J Geophys Res 100:15623-15639

Patino-Douce AE (2005) Vapor-absent melting of tonalite at 15-32 kbar. J Petrol 46:275-290.

Patino-Douce AE, Beard JS (1995) Dehydration-melting of biotite gneiss and quartz amphibolite from 3 to 15 kbar. J Petrol 36:707-738.

Patino-Douce AE, Harris N (1998) Experimental constraints on Himalayan anatexis. J Petrol 39:689-710

Perret RA (1913) Volcanic research at Kilauea in the summer of 1911. Am J Sci 4:475-483.

Downloaded from http://pubs.geoscienceworld.org/msa/rimg/article-pdf/69/1/61/2948053/61_Putirka.pdf
by University of California Berkeley Library user
on 16 March 2024

Petermann M, Hirschmann MM (2000) Anhydrous partial melting experiments on MORB-like eclogite: Phase relations, phase compositions and mineral-melt partitioning of major elements at 2-3 GPa. J Petrol 44:2173-2201

Petermann M, Lundstrom CC (2006) Phase equilibrium experiments at 0.5 GPa and 1100-1300 °C on a basaltic andesite from Arenal volcano, Costa Rica. J Volcanol 157:222-235

Petry C, Chakraborty S, Palme H (1997) Olivine-melt nickel-iron exchange Thermometer: cosmochemical significance and preliminary experimental results. Meteor Planet Sci 32:106-107

Pichavant M, Martel C, Bourdier J-L, Scaillet B (2002a) Physical conditions, structure, and dynamics of a zoned magma chamber: Mount Pele (Martinique, Lesser Antilles Arc). J Geophys Res 107:1-25

Pichavant M, Mysen BO, MacDonald R (2002b) Source and H_2O content of high-MgO magmas in island arc settings: an experimental study of a primitive calc-alkaline basalt from St. Vincent, Lesser Antilles arc. Geochim Cosmochim Acta 66:2193-2209

Pickering-Witter J, Johnston AD (2000) The effects of variable bulk composition on the melting systematics of fertile peridotitic assemblages. Contrib Mineral Petrol 140:190-211

Powell M, Powell R (1977) Plagioclase-alkali feldspar geothermometry revisited. Mineral Mag 41:253-256

Prouteau G, Scaillet B, Pichavant M, Maury R (2001) Evidence for mantle metasomatism by hydrous silicic melts derived from subducted oceanic crust. Nature 410:197-200

Putirka K (1997) Magma transport at Hawaii: inferences from igneous thermobarometry. Geology 25:69-72

Putirka K (1998) Garnet + liquid equilibrium. Contrib Mineral Petrol 131:273-288

Putirka K (1999a) Clinopyroxene+liquid equilibrium to 100 kbar and 2450 K. Contrib Mineral Petrol 135:151-163

Putirka K (1999b) Melting depths and mantle heterogeneity beneath Hawaii and the East Pacific Rise: Constraints from Na/Ti and REE ratios. J Geophys Res 104:2817-2829.

Putirka K (2005a) Mantle potential temperatures at Hawaii, Iceland, and the mid-ocean ridge system, as inferred from olivine phenocrysts: Evidence for thermally–driven mantle plumes. Geochem Geophys Geosys doi:10.1029/2005GC000915

Putirka K (2005b) Igneous thermometers and barometers based on plagioclase + liquid equilibria: tests of some existing models and new calibrations. Am Mineral 90:336-346

Putirka K (2008) Excess temperatures at ocean islands: implications for mantle layering and convection. Geology 36:283-286

Putirka K, Condit C (2003) A cross section of a magma conduit system at the margins of the Colorado Plateau. Geology 31:701-704

Putirka K, Johnson M, Kinzler R, Walker D (1996) Thermobarometry of mafic igneous rocks based on clinopyroxene-liquid equilibria, 0-30 kbar. Contrib Mineral Petrol 123:92-108

Putirka K, Perfit M, Ryerson FJ, Jackson MG (2007) Ambient and excess mantle temperatures, olivine thermometry, and active vs. passive upwelling. Chem Geol 241:177-206.

Putirka K, Ryerson FJ, Mikaelian H (2003) New igneous thermobarometers for mafic and evolved lava compositions, based on clinopyroxene + liquid equilibria. Am Mineral 88:1542-1554

Ratajeski K, Sisson TW, Glazner AF (2005) Experimental and geochemical evidence for derivation of the El Capitan Granite, California, by partial melting of hydrous gabbroic lower crust. Contrib Mineral Petrol 149:713-734

Rhodes JM, Dungan MA, Blanchard DP, Long PE (1979a) Magma mixing at mid-ocean ridges: evidence form basalts drilled near 22°N on the mid-Atlantic ridge. Tectonophys 55:35-61

Rhodes JM, Lofgren GE, Smith DP (1979b) One atmosphere melting experiments on ilmenite basalt 12008. Proc Lunar Planet Sci Conf 10:407-422

Rhodes JM, Vollinger MJ (2004) Composition of basaltic lavas sampled by phase-2 of the Hawaii Scientific Drilling Project: geochemical stratigraphy and magma series types. Geochem Geophys Geosys 5:doi:10.1029/2002GC00434

Righter K, Leeman WP, Hervig RL (2006) Partitioning of Ni, Co, and V between spinel-structured oxides and silicate melts; importance of spinel composition. Chem Geol 227:1-25

Robinson JAC, Wood BJ, Blundy JD (1998) The beginning of melting of fertile and depleted peridotite at 1.5 GPa. Earth Planet Sci Lett 155:97-111

Roeder PL, Emslie RF (1970) Olivine-liquid equilibrium. Contrib Mineral Petrol 29:275-289

Rutherford MJ, Sigurdsson H, Carey S, Andrew. (1985) The May 18, 1980, eruption of Mount St. Helens; 1, Melt composition and experimental phase equilibria. J Geophys Res 90:2929-2947

Ryan MP (1988) The mechanics and three-dimensional internal structure of active magmatic systems: Kilauea volcano, Hawaii. J Geophys Res 93:4213-4248

Ryan TP (1997) Modern Regression Methods. Wiley, New York

Sack RO, Walker D, Carmichael ISE (1987) Experimental petrology of alkalic lavas: constraints on cotectics of multiple saturation in natural basic liquids. Contrib Mineral Petrol 96:1-23

Salters VJM, Longhi J (1999) Trace element partitioning during the initial stages of melting beneath mid-ocean ridges. Earth Planet Sci Lett 166:15-30

Downloaded from http://pubs.geoscienceworld.org/msa/rimg/article-pdf/69/1/61/2948053/61_Putirka.pdf
by University of California Berkeley Library user
on 16 March 2024

Scaillet B, Evans BW (1999) The 15 June 1991 Eruption of Mount Pinatubo. I. Phase Equilibria and pre-eruption P-T-fO_2-fH_2O conditions of the dacite magma. J Petrol 40:381-411
Scaillet B, MacDonald R (2003) Experimental constraints on the relationships between peralkaline rhyolites of the Kenya rift valley. J Petrol 44:1867-1894
Schmidt MW, Green DH, Hibberson WO (2004) Ultra-calcic magmas generated from Ca-depleted mantle: an experimental study on the origin of ankaramites. J Petrol 45:531-554.
Schwab BE, Johnston AD (2001) Melting systematics of modally variable, compositionally intermediate peridotites and the effects of mineral fertility. J Petrol 42:1789-1811
Scoates JS, Lo Cascio M, Weis, D, Lindsley DH (2006) Experimental constraints on the origin and evolution of mildly alkalic basalts from the Kerguelen Archipelago, Southeast Indian Ocean. Contrib Mineral Petrol 151:582-599
Sen G (1985) Experimental determination of pyroxene compositions in the system CaO-MgO-Al_2O_3-SiO_2 at 900-1200 °C and 10-15 kbar using PbO and H_2O fluxes. Am Mineral 70:678-695
Sen G, Jones R (1989) Experimental equilibration of multicomponent pyroxenes in the spinel peridotite field: implications for practical thermometers and a possible barometer. J Geophys Res 94:17871-17880
Sen G, Keshav S, Bizimis M (2005) Hawaiian mantle xenoliths and magmas: composition and thermal character of the lithosphere. Am Mineral 90:871-887
Shepherd FS, Rankin GA, Wright FE (1909) The binary systems of alumina with silica, lime and magnesia. Am J Sci 28:293-315
Sisson TW, Grove TL (1993a) Experimental investigations of the role of H_2O in calc-alkaline differentiation and subduction zone magmatism. Contrib Mineral Petrol 113:143-166
Sisson TW, Grove TL (1993b) Temperatures and H_2O contents of low-MgO high-alumina basalts. Contrib Mineral Petrol 113:167-184
Skjerlie KP, Patino-Douce AE (2002) The fluid-absent partial melting of a zoisite-bearing quartz eclogite from 1.0 to 3.2 GPa; implications for melting in thickened continental crust and for subduction-zone processes. J Petrol 43:291-314
Sosman RB, Merwin HE (1913) Data on the intrusion temperature of the Palisade diabase. J Wash Acad 3:389-395
Spear FS (1993) Metamorphic Phase Equilibria and Pressure-Temperature-Time Paths. Mineralogical Society of America Monograph, Washington D.C.
Springer W, Seck HA (1997) Partial fusion of basic granulites at 5 to 15 kbar: implications for the origin of TTG magmas. Contrib Mineral Petrol 127:30-45
Stolper E (1977) Experimental petrology of eucritic meteorites Geochim Cosmochim Acta 41:587-611
Stolper E (1980) A Phase Diagram for Mid-Ocean Ridge Basalts: Preliminary Results and Implications for Petrogenesis. Contrib Mineral Petrol 74:13-27
Stolper E, Walker D (1980) Melt density and the average composition of basalt. Contrib Mineral Petrol 74:7-12
Stormer JC (1975) A practical two-feldspar geothermometer. Am Mineral 60:667-674
Sugawara T (2001) Ferric iron partitioning between plagioclase and silicate liquid: thermodynamics and petrological applications. Contrib Mineral Petrol 141:659-686
Takagi D, Sato H, Nakagawa N (2005) Experimental study of a low-alkali tholeiite at 1-5kbar:optimal condition for the crystallization of high-An plagioclase in hydrous arc tholeiite. Contrib Mineral Petrol 149:527-540
Takahashi E (1980) Melting relations of an alkali-olivine basalt to 30 kbar, and their bearing on the origin of alkali basalt magmas. Carneige Institute Washington Year Book 79:271-276
Takahashi E, Nakajima K, Wright TL (1998) Origin of the Columbia River basalts: melting model of a heterogeneous plume head. Earth Planet Sci Lett 162:63-80
Taura H, Yurimoto H, Kurita K, Sueno S (1998) Pressure dependence on partition coefficients for trace elements between olivine and the coexisting melts. Phys Chem Mineral 25:469-484
ten Brink US, Brocher TM (1987) Multichannel seismic evidence for a subcrustal intrusive complex under Oahu and a model for Hawaiian volcanism. J Geophys Res 92:13687-13707
Thompson JB (1967) Thermodynamic properties of simple solutions. *In*: Researches in Geochemistry, Vol 2. Abelson PH (ed) Wiley, New York, p 340-361
Thompson JB (1982) Composition space: an algebraic and geometric approach. Rev Mineral 10:1-31
Thornber CR, Heliker C, Sherrod DR, Kauahikaua JP, Miklius A, Okubo PG, Trusdell FA, Budahn JR, Ridley WI, Meeker GP (2003) Kilauea East Rift Zone magmatism: an episode 54 perspective. J Petrol 44:1525-1559
Thy P (1991) High and low pressure phase equilibria of a mildly alkalic lava from the 965 Surtsey eruption: experimental results. Lithos 26:223-243
Thy P, Lesher CE, Fram MS (2004) Low Pressure experimental constraints on the evolution of basaltic lavas from site 917, southeast Greenland continental margin. Proc Ocean Drill Prog 152:359-372

Downloaded from http://pubs.geoscienceworld.org/msa/rimg/article-pdf/69/1/61/2948053/61_Putirka.pdf
by University of California Berkeley Library user
on 16 March 2024

Toplis MJ (2005) The thermodynamics of iron and magnesium partitioning between olivine and liquid: criteria for assessing and predicting equilibrium in natural and experimental systems. Contrib Mineral Petrol 149:22-39

Tormey DR, Grove TL, Bryan WB (1987) Experimental petrology of normal MORB near the Kane Fracture Zone: 22°-25° N, mid-Atlantic Ridge. Contrib Mineral Petrol 96:121-139

Torrens HS (2006) The geological work of Gregory Watt, his travels with William Maclure in Italy (1801-1802) and Watt's "proto-geological" map of Italy (1804). *In:* The Origins of Geology in Italy. Vai GB, Caldwell WGE (eds) p 179-198

Tsuruta K, Takahashi E (1998) Melting study of the an alkali basalt JB-1 up to 12.5 GPa: behavior of potassium in the deep mantle. Phys Earth Planet Int 107:119-130

Tuttle OF, Bowen NL (1958) The origin of granite in the light of experimental studies in the system $NaAlSi_3O_8$-$KAlSi_3O_8$-SiO_2-H_2O. Geol Soc Am Mem 174

Vander Auwera J, Longhi J (1994) Experimental study of jotunite (hypersthene monzodiorite): constraints on the parent magma composition and crystallization conditions (P, T, fO_2) of the Bjerkreim-Sokndal layered intrusion (Norway). Contrib Mineral Petrol 118:60-78

Vander Auwera J, Longhi J, Duchesne J-C (1998) A liquid line of descent of the jotunite (hypersthene monzodiorite) suite. J Petrol 39:439-468

Villiger S, Ulmer P, Müntener O, Thompson AB (2004) The liquid line of descent of anhydrous, mantle-derived, tholeiitic liquids by fractional and equilibrium crystallization - an experimental study at 1.0 GPa. J Geol 45:2369-2388

Wagner TP, Grove TL (1997) Experimental constraints on the origin of lunar high-Ti ultramafic glasses. Geochim Cosmochim Acta 61:1315-1327

Wagner TP, Grove TL (1998) Melt/harzburgite reaction in the petrogenesis of tholeiitic magma from Kilauea volcano, Hawaii. Contrib Mineral Petrol 131:1-12

Walter MJ (1998) Melting of garnet peridotite and the origin of komatiite and depleted lithosphere of komatiite and depleted lithosphere. J Petrol 39:29-60

Walter MJ, Presnall DC (1994) Melting behavior of simplified lherzolite in the system CaO-MgO-Al_2O_3-SiO_2-Na_2O from 7 to 35 kbar. J Petrol 35:329-359

Wasylenki LE, Baker MB, Kent AJR, Stolper EM (2003) Near-solidus melting of the shallow upper mantle: partial melting experiments on depleted peridotite. J Petrol 44:1163-1191

Wells PRA (1977) Pyroxene thermometry in simple and complex systems. Contrib Mineral Petrol 62:129-139

Whitaker ML, Nekvasil, H, Lindsley DH, Difrancesco NJ (2007) The role of pressure in producing compositional diversity in intraplate basaltic magmas. J Petrol 48:365-393

Whitney JA, Stormer JC (1977) The distribution of $NaAlSi_3O_8$ between coexisting microcline and plagioclase and its effect on geothermometric calculations. Am Mineral 62:687-691

Wood BJ (1974) The solubility of alumina in orthopyroxene coexisting with garnet. Contrib Mineral Petrol 46:1-15

Wood BJ, Banno S (1973) Garnet-orthopyroxene and orthopyroxene-clinopyroxene relationships in simple and complex systems. Contrib Mineral Petrol 42:109-124

Wood BJ, Trigila R (2001) Experimental determination of aluminous clinopyroxene-melt partition coefficients for potassic liquids, with application to the evolution of the Roman province potassic magmas. Chem Geol 172:213-223

Wright FE, Larsen ES (1909) Quartz as a geologic thermometer. Am J Sci 27:421-447

Xirouchakis D, Hirschmann MM, Simpson J (2001) The effect of titanium on the silica content of mantle-derived melts. Geochem Cosmochim Acta 65:2029-2045

Yang HJ, Frey FA, Clague DA, Garcia MO (1996) Mineral chemistry of submarine lavas from Hilo Ridge, Hawaii: implications for magmatic processes within Hawaiian rift zones. Contrib Mineral Petrol 135:355-372

Yasuda A, Fujii T, Kurita K (1994) Melting phase relations of an anhydrous mid-ocean ridge basalt from 3 to 20 GPa: Implications for the behavior of subducted oceanic crust in the mantle. J Geophys Res 99:9401-9414

Yoder HS, Tilley CE (1962) Origin of basalt magmas: an experimental study of natural and synthetic rock systems. J Petrol 3:342-532

Downloaded from http://pubs.geoscienceworld.org/msa/rimg/article-pdf/69/1/61/2948053/61_Putirka.pdf
by University of California Berkeley Library user
on 16 March 2024